MODELLING AND ADAPTIVE CONTROL

OF A ROLL BENDING PROCESS:

WORKPIECE DYNAMICS

by

YEONG JE PARK

B.S., Seoul National University
(1978)

M.S., Korea Advanced Institute of Science and Technology
(1980)

SUBMITTED TO THE DEPARTMENT OF
MECHANICAL ENGINEERING
IN PARTIAL FULFILLMENT OF THE
REQUIREMENTS OF THE DEGREE OF

MECHANICAL ENGINEER

at the

MASSACHUSETTS INSTITUTE OF TECHNOLOGY

June, 1987

© Massachusetts Institute of Technology

Signature of Author _____
Department of Mechanical Engineering
May 28, 1987

Certified by _____
David E. Hardt
Thesis Supervisor

Accepted by _____
Ain A. Sonin
Chairman, Department Graduate Committee

In memory of my mother and grandfather

MODELLING AND ADAPTIVE CONTROL

OF A ROLL BENDING PROCESS:

WORKPIECE DYNAMICS

by

YEONG JE PARK

Submitted to the Department of Mechanical Engineering
on May 28, 1987 in partial fulfillment of the
requirements for the Degree of
Mechanical Engineer

ABSTRACT

The recent closed-loop control scheme for a roll bending system shows good performance at low feedrates, but there is still an instability problem due to the workpiece vibration at high feedrates. The objective of this research is to make a model of the workpiece related to instability of the roll bending system and to design an adaptive control system that will stabilize the system.

A dynamic analysis of the workpiece in a roll bending process is presented to show workpiece vibration, which causes instability of the system. The workpiece is modelled as a cantilever beam composed of a static section and a free section. The maximum moment for roll bending results from the static moment due to the point load and the dynamic moment due to the lateral beam vibration. The first mode frequency is used as the natural frequency of the workpiece dynamics, and the damping ratio was obtained by a test using a dynamic structural analyzer. The natural frequency was shown to be a length-dependent parameter, and the roll bending system is nonminimum phase due to the workpiece dynamics. The simulated responses based on the workpiece model agree with the experimental responses. As the workpiece length continuously increases the system becomes unstable due to the increased vibration and low frequency of the workpiece.

An adaptive control system is required to stabilize the system and to obtain better performances. The typical adaptive controls such as a Self Tuning Control(STC) or MRAC(Model Reference Adaptive Cotrol) are not suitable for this system because of the length-variant frequency and nonminimum phase. Thus, a modified Scheduled Gain Adaptive Control(SGAC) is proposed, using root-locus method and Tustin's approximation

for the discrete-time controller. The simulated responses show that the system can be stabilized regardless of the increased length of the workpiece and that the feedrate can be increased up to 25 inch/sec. A robust MRAC with a new adaptive law is proposed for zero residual tracking errors in nonminimum phase system. The simulation shows that the system behaves satisfactorily up to about 3 seconds with a feedrate of 10 in/sec. The proposed control scheme represents a major improvement in the roll bending system because of the stability at increased feedrates.

Thesis Supervisor: Dr. David E. Hardt
Title: Associate Professor of Mechanical Engineering

ACKNOWLEDGEMENTS

TABLE OF CONTENTS

LIST OF FIGURES

CHAPTER 1

INTRODUCTION

1.1. Previous Research

Roll bending is widely used in the metal forming industry to form continuous curvature shapes from long flat materials. It can provide fast operations for circular shapes and high dimensional accuracies of the workpiece. A pyramid three-roll bending apparatus shown in Figure 1.1 is a typical configuration of roll bending with a movable center roll and a pair of fixed outer rolls. As the workpiece travels through the rolls, the center roll is adjusted to produce a variable bend along the length of the workpiece. In this way each point can be given a specific maximum moment and a corresponding permanent deformation.

Recently the roll bending process is sought to be automated, because the manual reworking of the part to obtain the desired precise shape is time-consuming and expensive. Control of roll bending has been the subject of several investigations, but none has yet addressed the central problem of stability and productivity of the roll bending system because of the workpiece vibration. The recent works by Hardt [1], Allison [2], and Stelson [3] have shown that a material adaptive control scheme can be developed for the brakeforming process which will significantly improve productivity by explicitly

FINAL SHAPE

WORKPIECE
BEFORE BEND

WORKPIECE
MOVEMENT

FIXED
ROLLER

CENTER POSITION
ROLLER
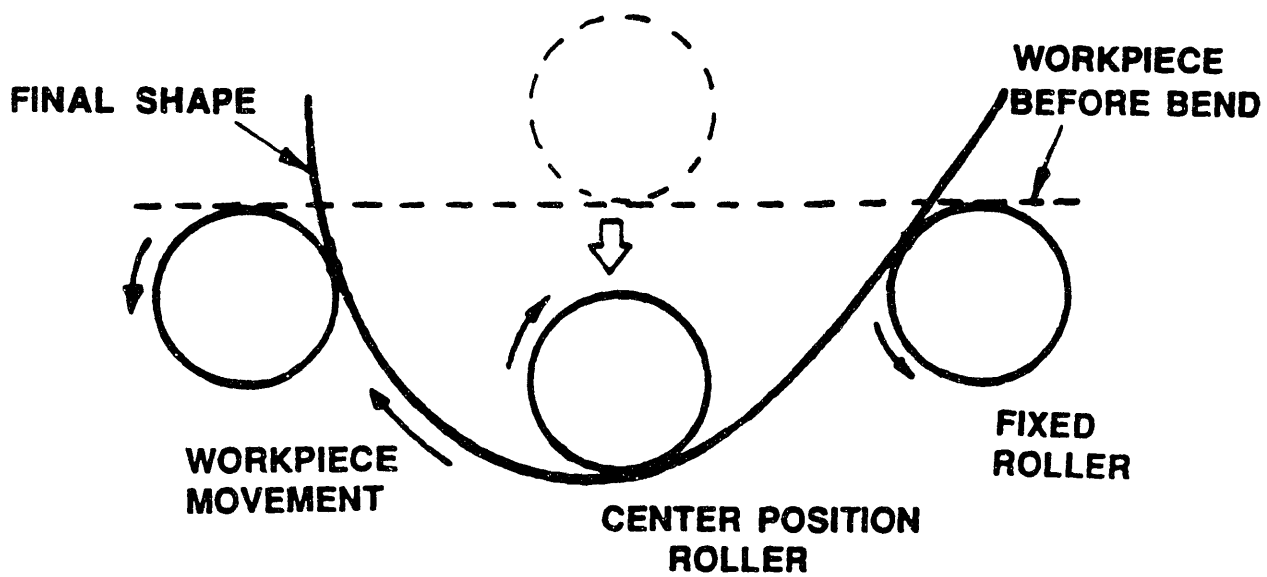
Figure 1.1 A Typical Three-Roll Bending Configuration

accounting for material properties. The roll bending process is a variation of the brakeforming process. Hansen [4] and Cook et al. [5] designed an open loop controller for a roll bending machine and demonstrated that good control of the final shape is possible if the material properties including springback are known beforehand. A closed loop control of the system has been developed by Roberts [6], Hardt [7], and Hale [8] to obtain a desired shape of the workpiece, using a servo and output feedback. The advantage of this control scheme is that no prior knowledge is required for controller implementation. Although the control scheme works well in theory, the process is limited to very low feedrates below 0.7 in/sec due to instability.

An improved control system using velocity feedback, which was developed by Hale [9], showed that a desired shape was formed at low feedrates of about 3.3 in/sec, without knowing workpiece model. But the system was still unstable at high feedrates of about 13 in/sec due to the effect of the unknown workpiece vibration. Therefore it is essential to develop a reliable model of the workpiece dynamics and design a controller that will stabilize the system even at high feedrates for complete automation.

1.2. Thesis Overview

The **static** analysis and closed loop control of roll bending has been developed for automatic roll bending control system, but the model of the workpiece dynamics, which is related to oscillation and instability, is yet unknown. In this research, the dynamic analysis of the workpiece is presented and an adaptive controller is designed for the system stability and productivity.

The mechanics of the roll bending process is presented in Chapter 2. The moment-curvature relationship and curvature-roll position relationship are introduced, showing the springback and nonlinearity as the characteristics of the workpiece.

In Chapter 3, a workpiece model and a dynamic analysis of the roll bending process are presented. The main parameters of workpiece, natural frequency and damping ratio, are obtained by theoretical analysis and a test using a dynamic analyzer. These values determine the positions of poles and zeroes of the workpiece on root-locus, which is used in the analysis of the system and the design of a controller. The transfer function between the center-roll position and the unloaded curvature is obtained, including the workpiece dynamics. The simulated responses are obtained to check the workpiece model with the experimental responses.

In Chapter 4, a Scheduled Gain Adaptive Control (SGAC) system for system stability is proposed. A continuous-time controller for SGAC is designed, based on the root locus method. It is converted to a discrete-time controller for the real time control, by using Tustin's Approximation method.

Chapter 5 provides the Model Reference Adaptive Control (MRAC) applications to the proposed roll bending system. The adaptive part is located around the plant and constructed prior to a controller design. The NLV algorithm is used for the stable MRAC system. A new adaptive law is also used for the robust MRAC with zero residual tracking errors.

Chapter 6 contains the conclusions and some suggestions for future research. The computer programs used for the simulations are presented in the Appendix.

CHAPTER 2

STATIC ANALYSIS AND CLOSED LOOP CONTROL

2.1. Introduction

A number of analyses of the bending mechanics have been developed. The goal of these analyses is to predict the unloaded curvature response of the workpiece with the given initial geometry, constitutive law of the material, and the applied moment. The term "curvature" used in this thesis denotes the curvature of the natural plane unless otherwise specified. In this chapter the static analysis of roll bending mechanics is presented, considering the springback and nonlinearity of the material.

The closed loop control system and the experimental responses of a roll bending process, performed by Hale [9], are also presented in this chapter. In the work presented by Hale [9], only the static model of the workpiece was considered, and the system became unstable at high feedrate due to the workpiece vibration. In this chaper the same control system as the one in [9] is reanalyzed, using the system block diagram. In the next chapter modelling and simulation of the workpiece dynamics will be presented to show the workpiece vibration. The same control method used for the experiments in [9] will be used for the simulation in order to check the workpiece model.

2.2. Moment-Curvature Relationship

A **workpiece** in a three roll bending apparatus can be modeled as a beam under three-point loading, as shown in Figure 2.1. As beam is loaded, initially the material is stressed elastically. If the stress in the loaded beam is below the yield stress, the beam will recover its original shape by springback when the beam is unloaded. However, if the beam is loaded past the elastic limit, the beam is plastically deformed and will be permanently deformed when unloaded. The relationship between the stress state of workpiece and the resulting curvature can be seen in the moment-curvature relationship, which can be derived from the stress-strain relationship.

As the workpiece moves through the rolls, the bending moment of a point fixed in the workpiece increases progressively as it approaches the center roll. If no more moment is generated between the center and fixed outer rolls, the workpiece has the maximum bending moment at the center roll contact point. Once the workpiece passes the center roll, the moment decreases to zero at the outer roll contact point. During the roll bending process, the pinch roll is allowed to rotate about the center of the drive roll. In this way, the pinch roll seeks the point of zero rate-of-change or maximum moment location. Although not strictly correct, it is assumed that the moment varies linearly with arc-length of the workpiece, as shown in Figure

2.2. **The center** roll contact position on the workpiece is not necessarily mid-point between the outer rolls because of the floating roll arrangement.

The moment-curvature diagram for a typical loading and unloading of an initially flat workpiece is shown in Figure 2.3. In the elastic region below the yielding moment, the workpiece deforms linearly to the original shape when unloaded. However, if it is loaded beyond the proportional limit, both the elastic and plastic deformation occurs. As the moment begins to decrease, the workpiece will unload elastically along the line almost parallel to the initial elastic line, until the moment vanishes. At that point, the workpiece has a permanent or unloaded curvature K_u. The workpiece springback ΔK is defined as the difference between the maximum loaded curvature and the final unloaded curvature:

$$\Delta K = K_L - K_u \tag{2.1}$$

where K_L is the maximum loaded curvature and K_u is the unloaded curvature. The springback can also be expressed in terms of the moment. Since the unloading path is a linear function of the moment, the springback can be defined by:

$$\Delta K(s) = M(s) / (dM/dK) \tag{2.2}$$
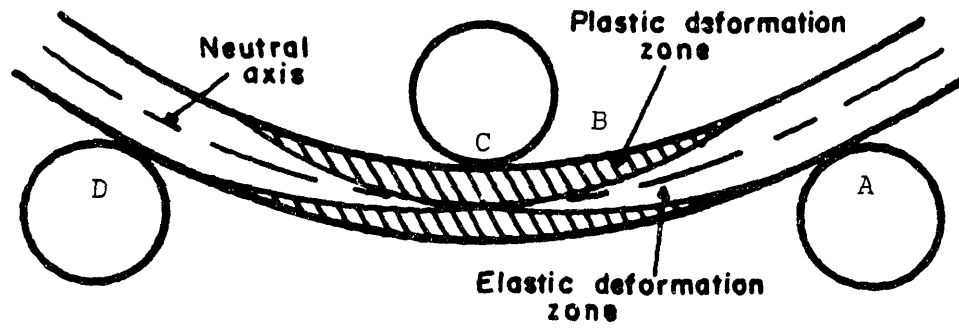
Figure 2.1   Stress State in a Loaded Beam
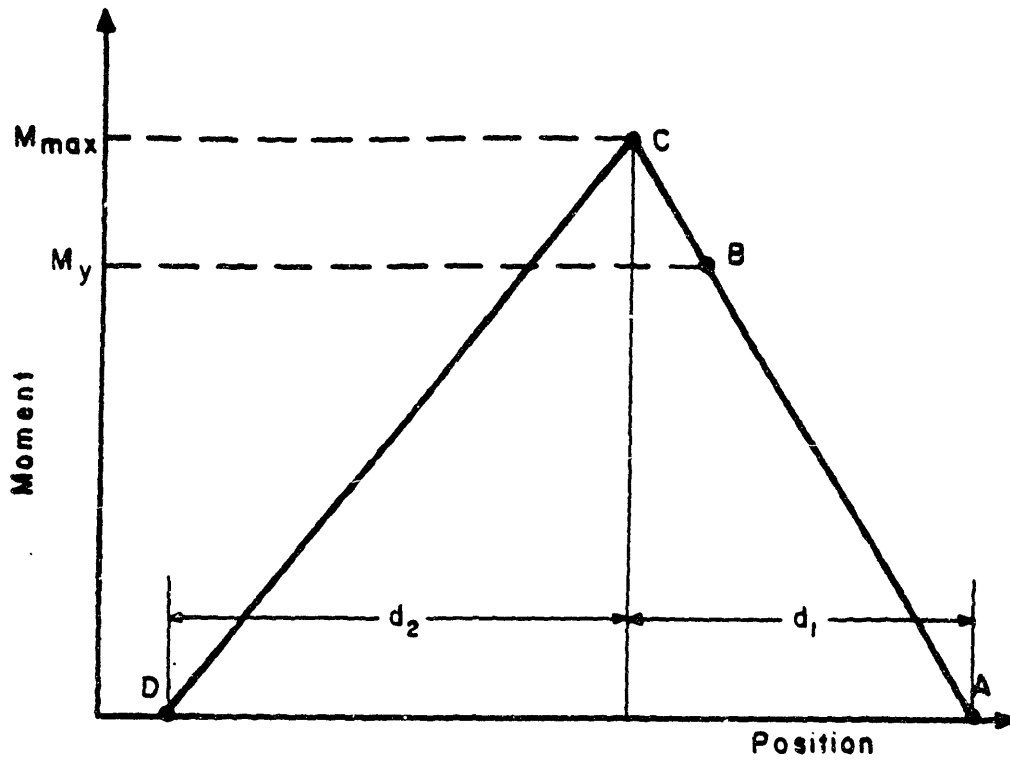
Figure 2.2   Moment - Arc Length Diagram
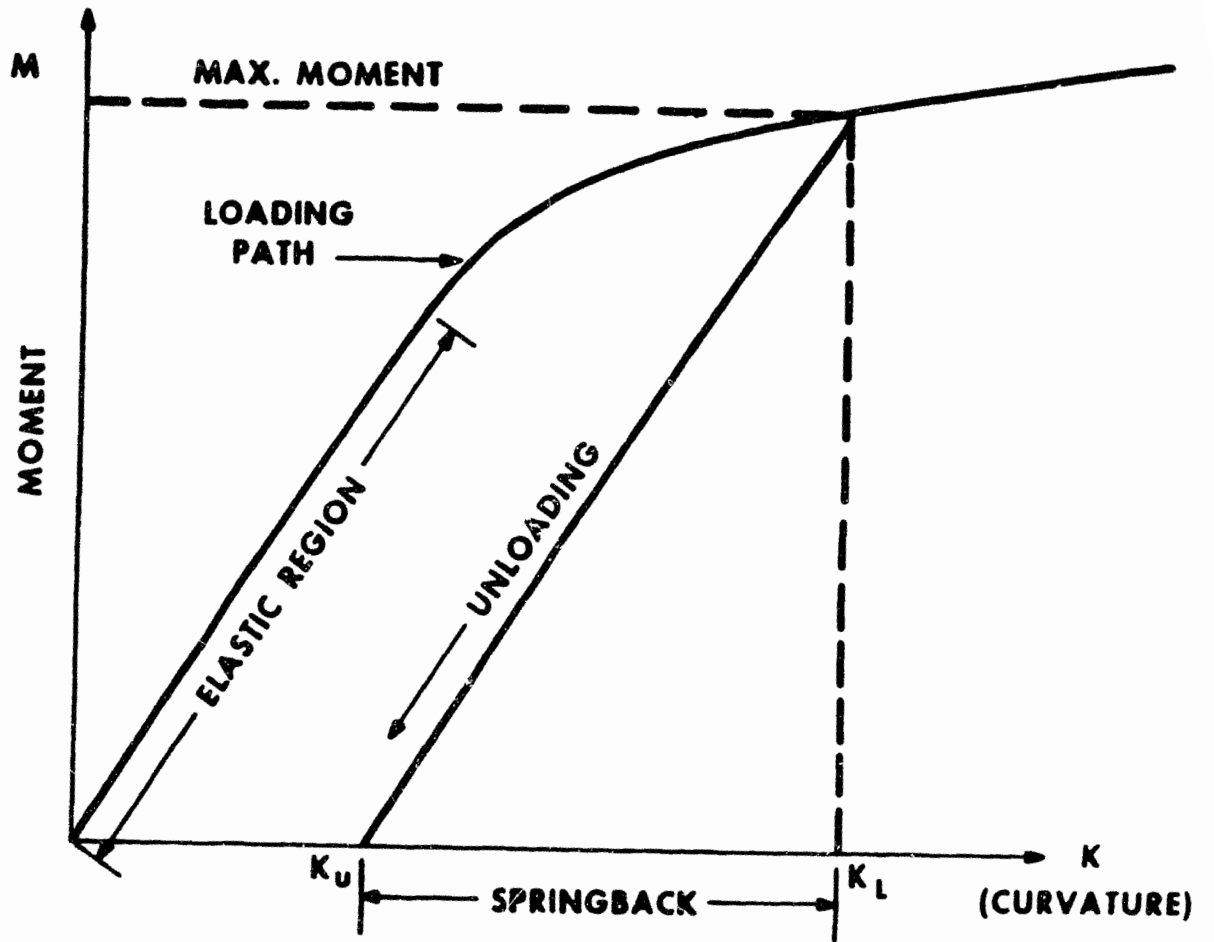
Figure 2.3 Moment - Curvature Diagram

where ΔK is the springback at a location s associated with a maximum moment M(s) at the same point and dM/dK is the slope of the elastic loading line.

Several methods of determining springback are suggested by this moment- curvature (M-K) relationship. In one method, the M-K relationship is defined by a priori measurements such as stress-strain data or force-displacement data during a static bending operation. While this approach completely defines the material constitutive relations during the bending operation, it has a drawback of relying on measurements made prior to the processing of the metal.

An alternative method of determining springback is to directly measure the necessary properties of the workpiece during the process itself. By using the roll forces and displacements, it is possible to construct an approximate M-K diagram that can be used to calculate the springback for process control. This method has been successfully applied to control three-point bending where the M-K information is derived from in-process measurement of die forces and die displacements. However, a major source of error remains in the estimation of sheet curvature because it is not directly measured.

From the above two equations (2.1) and (2.2), the

moment-curvature relationship can be expressed as:

$$K_u = K_L - M / (dM/dK)$$ (2.3)

This equation shows that it is possible to calculate the unloaded curvature of the workpiece while the workpiece is in the loaded condition if the moment and the loaded curvature at the contact point under the center roller are known together with the bending stiffness of the workpiece.

If predictive or open-loop control is applied in this process, the M-K relationship should be precisely known. If K is directly measured at the outlet side of the machine, the data cannot be used to correct the error at that point, but can only be used to eventually maintain a constant final curvature. By contrast, the elastic bending properties of metals are well behaved and can be exploited in a highly accurate closed-loop control scheme. From Equation (2.3), it is apparent that we can indirectly measure the unloaded curvature if we can measure the loaded curvature, maximum moment, and the bending stiffness, as mentioned before. Such a control scheme was performed by Hardt et al. [7] and the block diagram of the closed-loop roll bending control system is shown in Figure 2.4.
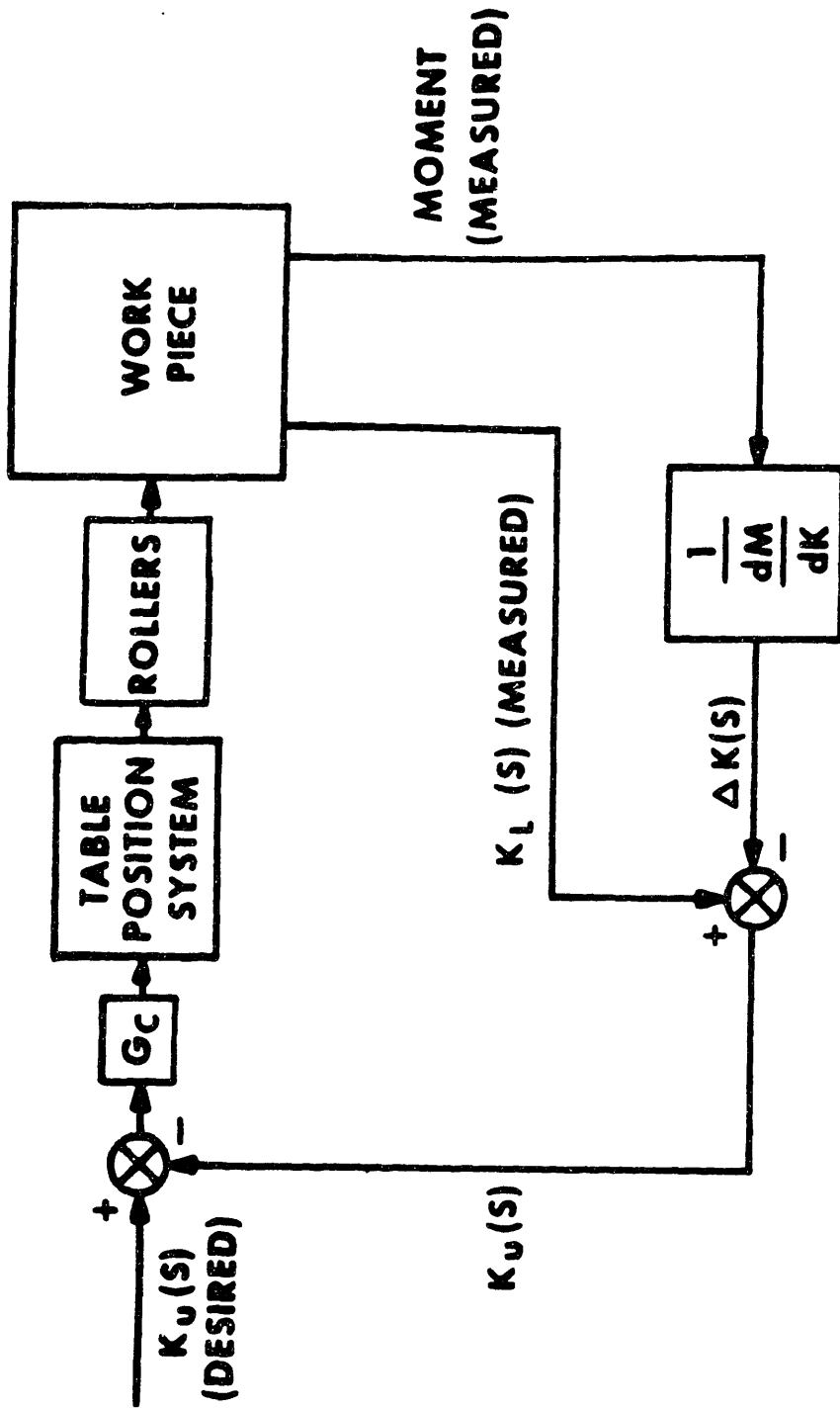
Figure 2.4 Block Diagram of Closed-Loop
Roll-bending Control System

2.3. Curvature-Roll Position Relationship

The **static section** of the workpiece, which is placed between the center and outer rolls, can be modeled as a cantelever beam with the clamp at the center roll contact point as shown in Figure 2.5. The relation between the deflection of the beam at any point x along the beam and the loaded curvature is derived from static analysis:

$$K_L = \frac{d^2y}{dx^2} = \frac{F(\ell - x)}{EI} \qquad (2.4)$$

where EI is the bending stiffness of the workpiece. By integrating Equation (2.4) twice with the boundary conditions:

$$y(0) = 0 \quad \text{and} \quad \frac{dy}{dx}(0) = 0 \qquad (2.5)$$

the deflection, y_x, of the workpiece at any point x along the workpiece can be expressed below:

$$y_x = \frac{F}{EI} \left(\frac{\ell x^2}{2} - \frac{x^3}{6} \right) \qquad (2.6)$$

Since maximum loaded curvature occurs at x=0, it can be obtained from Equation (2.4):

-24-
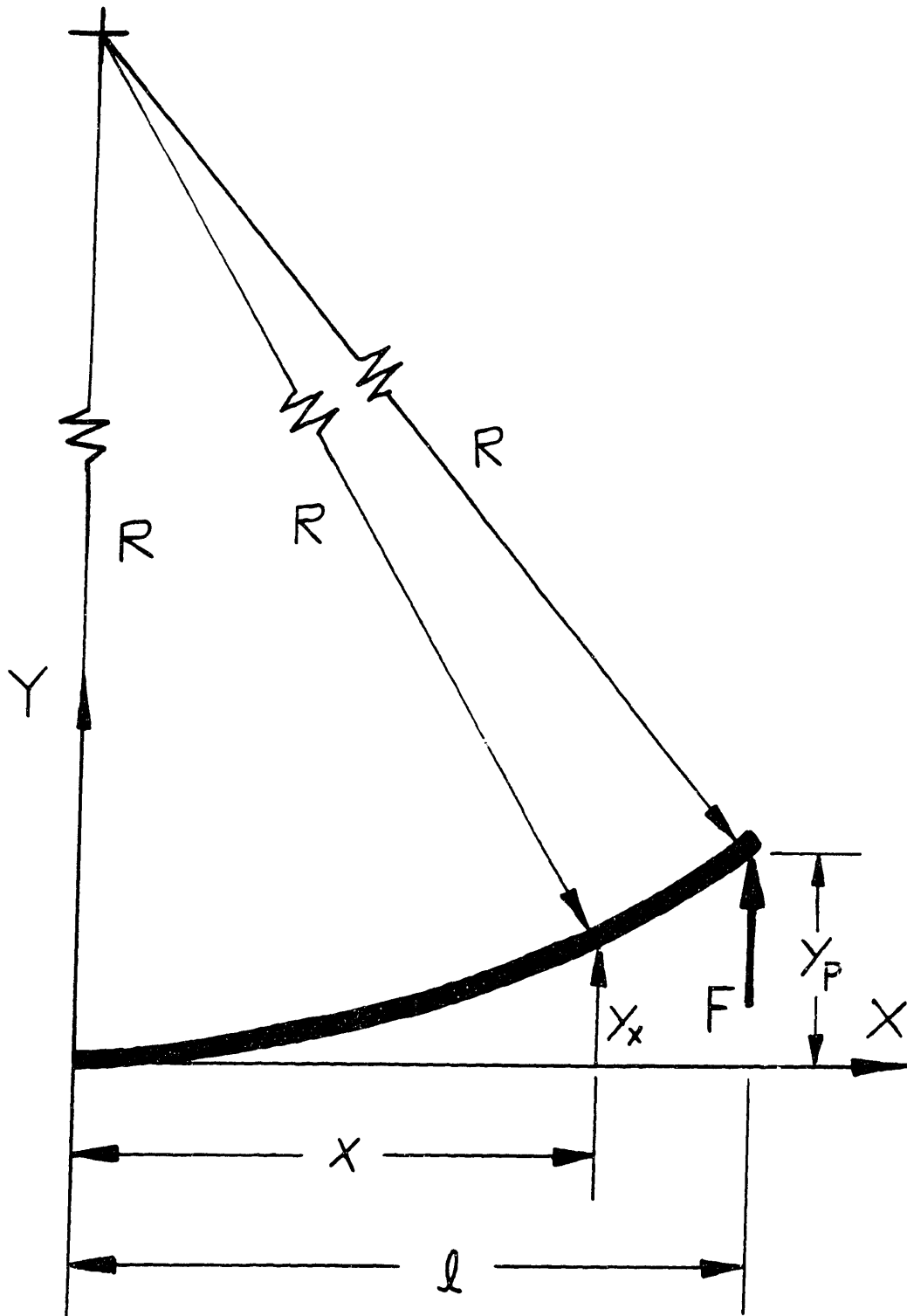
Figure 2.5   Curvature Measurement Scheme

$$K_L = \frac{F\ell}{EI} \tag{2.7}$$

From Equation (2.6), F/EI can be obtained :

$$\frac{F}{EI} = \frac{y_x}{\left(\frac{\ell x^2}{2} - \frac{x^3}{6}\right)} \tag{2.8}$$

Substituting Equation (2.8) into Equation (2.7) gives the relation between the maximum loaded curvature and the deflection of the beam.

$$K_L = \frac{y_x \, \ell}{\left(\frac{\ell x^2}{2} - \frac{x^3}{6}\right)} \tag{2.9}$$

This equation shows that the loaded curvature is a linear function of the displacement of the workpiece at any point x. At the end point of the workpiece, $x = \ell$, the deflection of the workpiece is the displacement of the center roll. Then, the loaded curvature can be expressed as a function of the center roll displacement:

$$K_L = \frac{3\ y_p}{\ell^2} \qquad\qquad (2.10)$$

where y_p is the center roll displacement. This equation shows that the loaded curvature is not dependent on material properties, and thus it is very useful for the static analysis of the workpiece.

2.4. Closed Loop Control

A closed loop control system using a simple proportional controller and proportional-plus-derivative feedback was proposed by Hale [9]. A velocity servo was used to introduce a free integrator to the system for the zero steady-state error. The workpiece model only considers the static relationship with a nonlinearity between the unloaded curvature and the center roll position, as mentioned before.

It is very difficult to measure the rate of change of unloaded curvature. It is possible, however, to obtain a reasonably good approximation of the rate of change of unloaded curvature. Thus the derivative feedback, the rate of change of unloaded curvature, was approximated by the rate of change of the roll velocity, which is the control variable. The estimated derivative feedback was derived from Equation (2.10):

$$\dot{K}_u = \frac{3 \dot{Y}_p}{\ell^2} \qquad (2.11)$$

The form of the controller with the control scheme described above is:

$$U = G1 \left[K_{ud} - K_u - (G2)(\dot{K}_u) \right] \qquad (2.12)$$

where U is the controller output, G1 is the controller gain, and K_u is given by Equation (2.11). Here, G2 is used to determine the location of zero.

Substituting Equation (2.11) into Equation (2.12) gives another form of the controller for $\dot{Y}_p$ instead of K_u.

$$U = G1 \left[K_{ud} - K_u - (G2)\left(\frac{3\dot{Y}_p}{\ell^2}\right) \right] \qquad (2.13)$$

Then the relationship between the roll velocity feedback gain, K_v, and G2 can be obtained:

$$K_v = \frac{3}{\ell^2}(G2) \qquad (2.14)$$

Considering the servo model, static workpiece model, and

closed loop control system with a proportional controller and proportional-plus- velocity feedback using center roll velocity, the system block diagram can be constructed as in Figure 2.6.

In the experiments using the above control scheme [9], the center roll velocity was used for the derivative feedback of unloaded curvature, as proposed before. The unloaded curvature was indirectly obtained, by measuring the loaded curvature and maximum moment, as suggested in [6] and [7]. Figures 2.7 and 2.8 shows the experimental responses at 13 in/sec feedrate, performed by Hale [9], where the input command is a step curvature change of 0.01/in.

The experiments show that the workpiece vibration is a major factor resulting in the system instability. As the controller gain, G1, increases and the roll velocity feedback gain, Kv, or G2 decreases, the system becomes unstable more rapidly. Since the workpiece vibration is the major factor which limits the roll bending system response, it is necessary to study the workpiece dynamics in order to analyze the vibration problem and to stabilize the system.
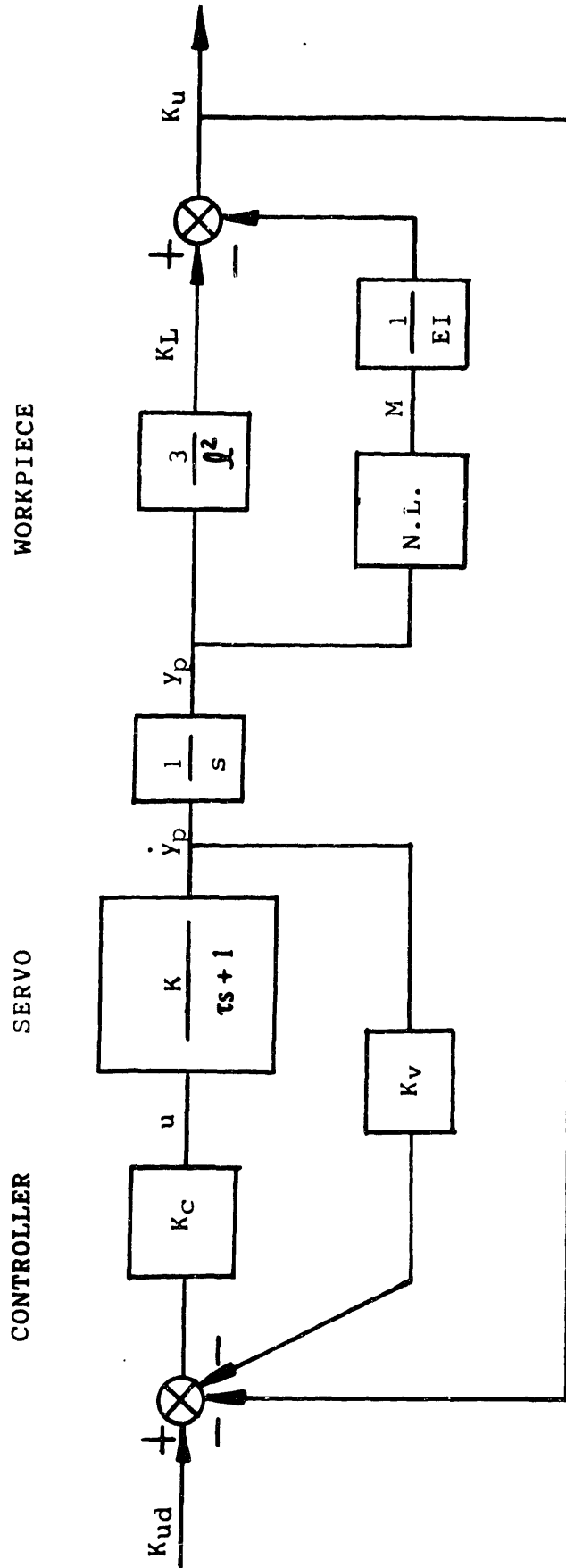
Figure 2.6 Block Diagram of Roll Bending System
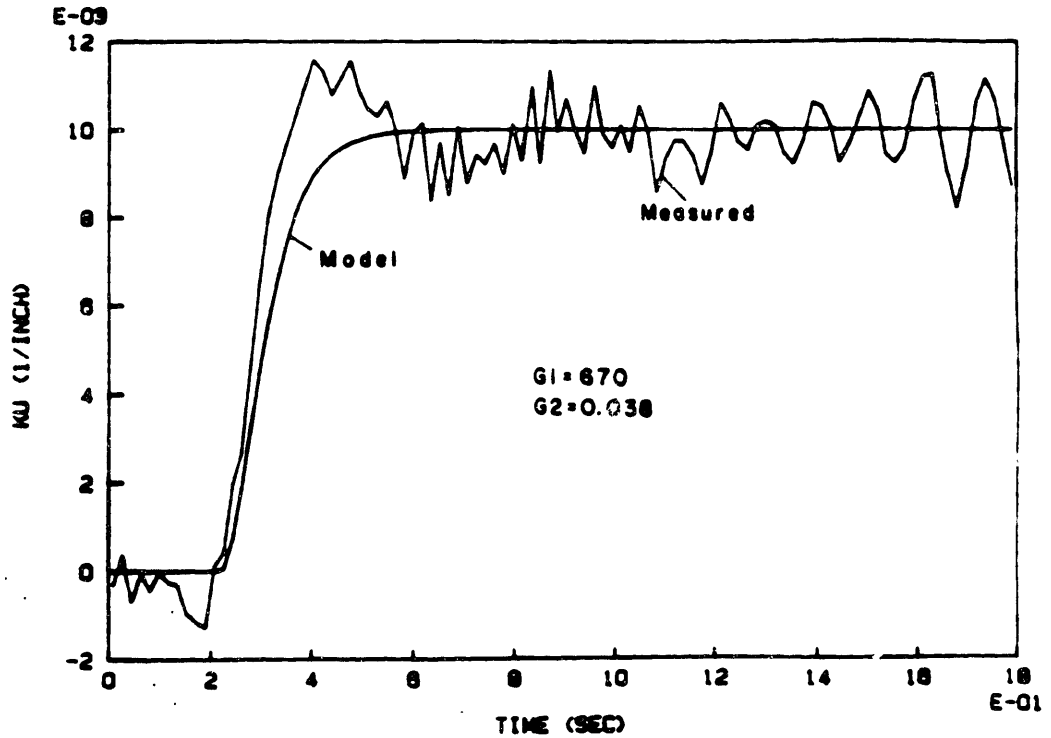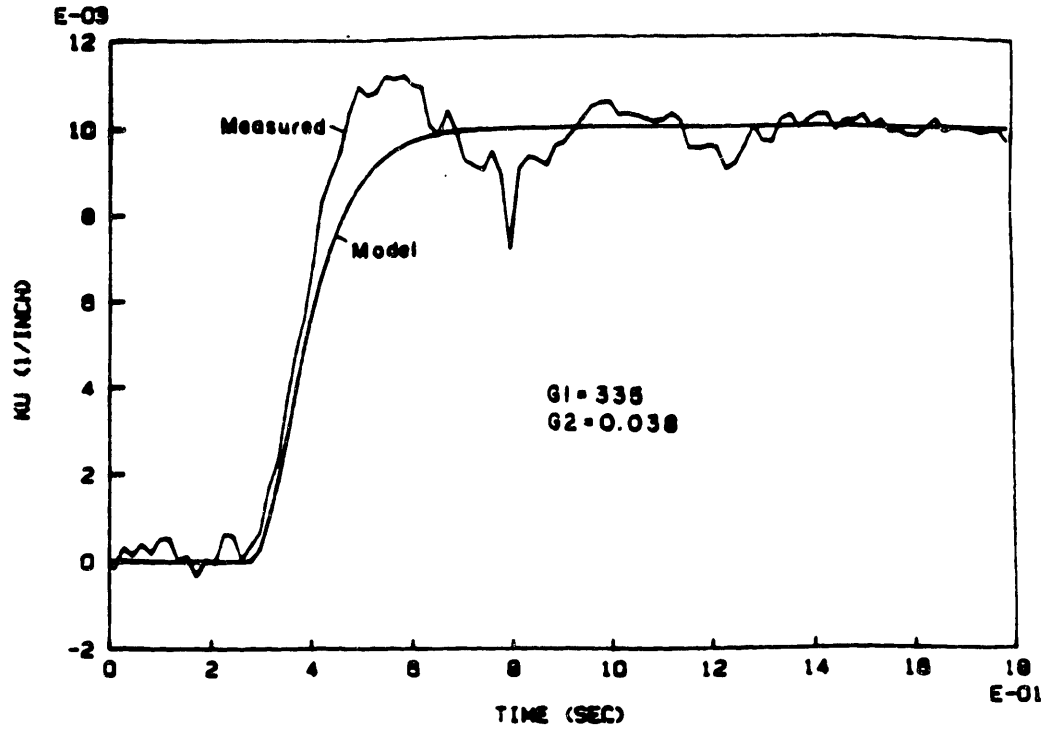
Figure 2.7   Experimental Responses with G2=0.038
              and 15 in/sec Feedrate (From Hale [9])
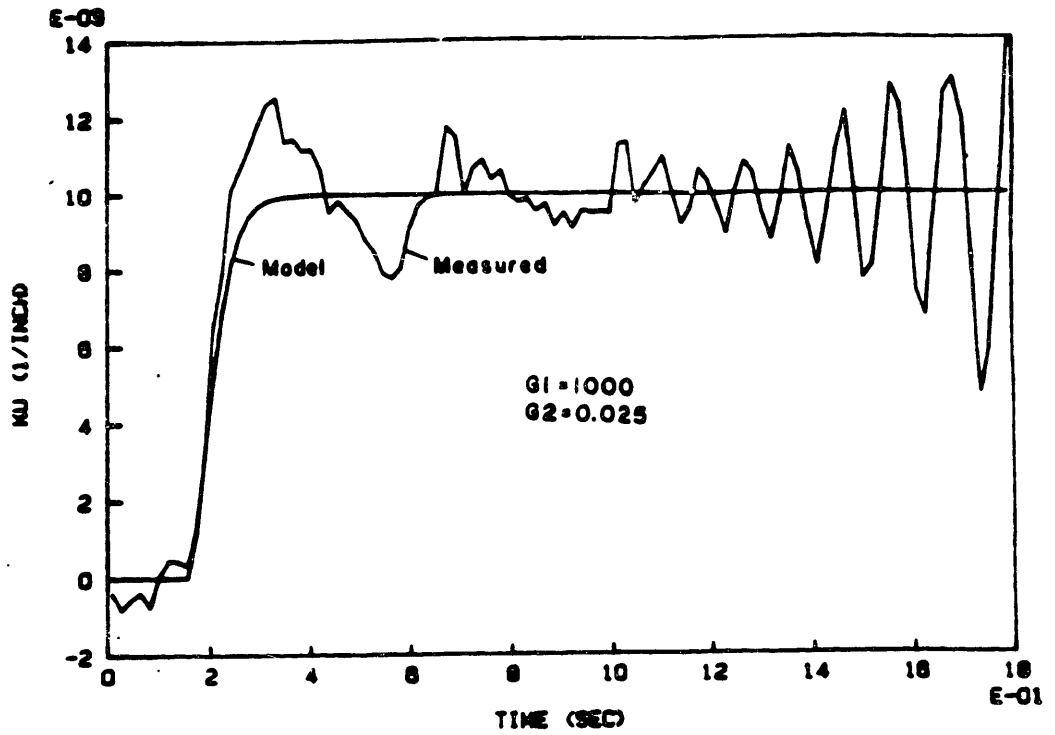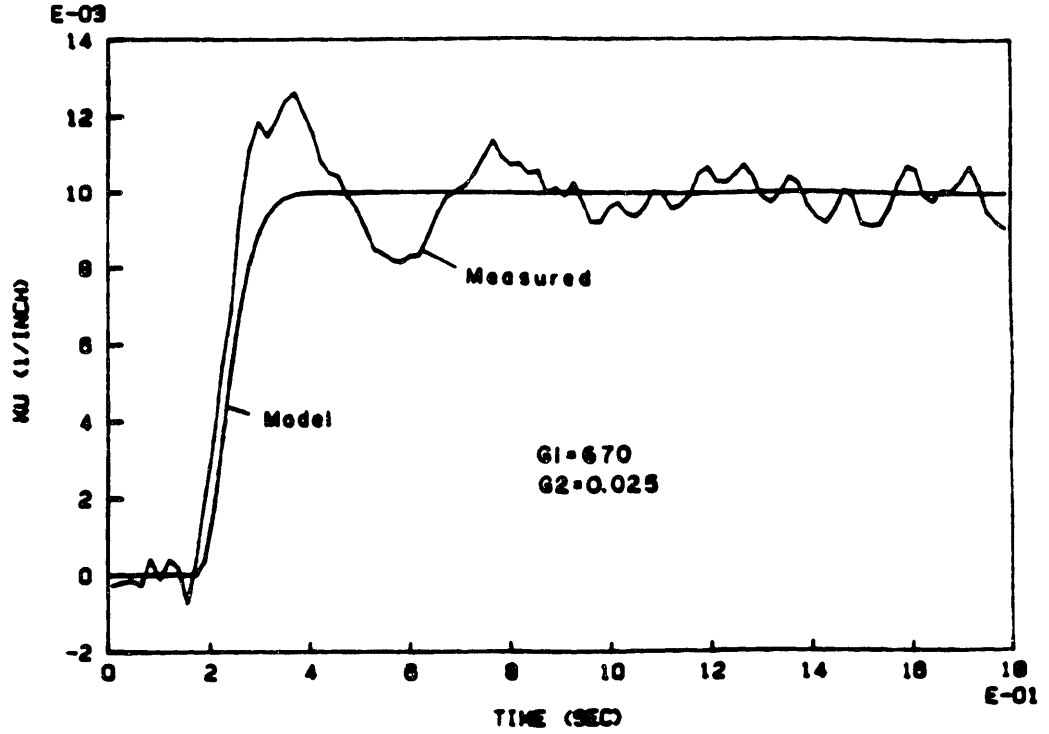
Figure 2.8 Experimental Responses with G2=0.025
and 13 in/sec Feedrate (From Hale [9])

CHAPTER 3

MODELING AND DYNAMIC ANALYSIS

3.1. Workpiece Modeling

3.1.1. Workpiece Model

Workpiece dynamics is related to the stability of the roll bending system. However, a satifactory analysis of the workpiece dynamics is yet to be developed. As the workpiece rolls through the roll bending machine, the workpiece vibration increases and eventually leads to the system instability. Thus it is essential to analyze the dynamics of the roll bending system to model the workpiece and obtain the relationship between the workpiece dynamics and the desired curvature.

Cook et al [5] performed experiments to determine an appropriate model of a three roll bending system. They found that a transfer function relating the center roll position to the loaded curvature was well described by an underdamped second oredr system. They then developed a state variable feedback control system to regulate the sheet curvature and succeeded in obtaining a good response. A model for workpiece dynamics was suggested by Hardt et al [7], to show the effect of workpiece dynamics on the closed loop control of the workpiece shape. The workpiece was modelled as a cantilever beam with a static section and a free section. The analysis of the workpiece dynamics shows that the beam length continuously

increases, and thus the free section clearly dominates the workpiece dynamics as the workpiece rolls through. They then found that the fundamental frequency of the workpiece vibration determined the required system band limit.

General workpiece models have been suggested for the automatic roll bending control system. However, none of the models incorporates the workpiece dynamics related to vibration in the transfer function relating the center roll position to the unloaded curvature. In this chapter a workpiece model including the workpiece dynamics is presented as well as the system control.

It is assumed that each half of the workpiece is modelled as a cantilever beam with a clamp at the center roll contact point, a clamp joint with a point load at the outer roll contact point, and a free section with a lateral beam vibration beyond the outer roll, as shown in Figure 3.1. Such configuration suggests that the workpiece mechanics can be divided into a static section between the center roll and the outer roll, and a dynamic section beyond the outer roll. The maximum moment applied on the center roll contact point results from the static moment due to the point load at the outer roll point and the dynamic moment due to the vibration of the free section.

$$M_b = \ell \times F + M_{bd}$$
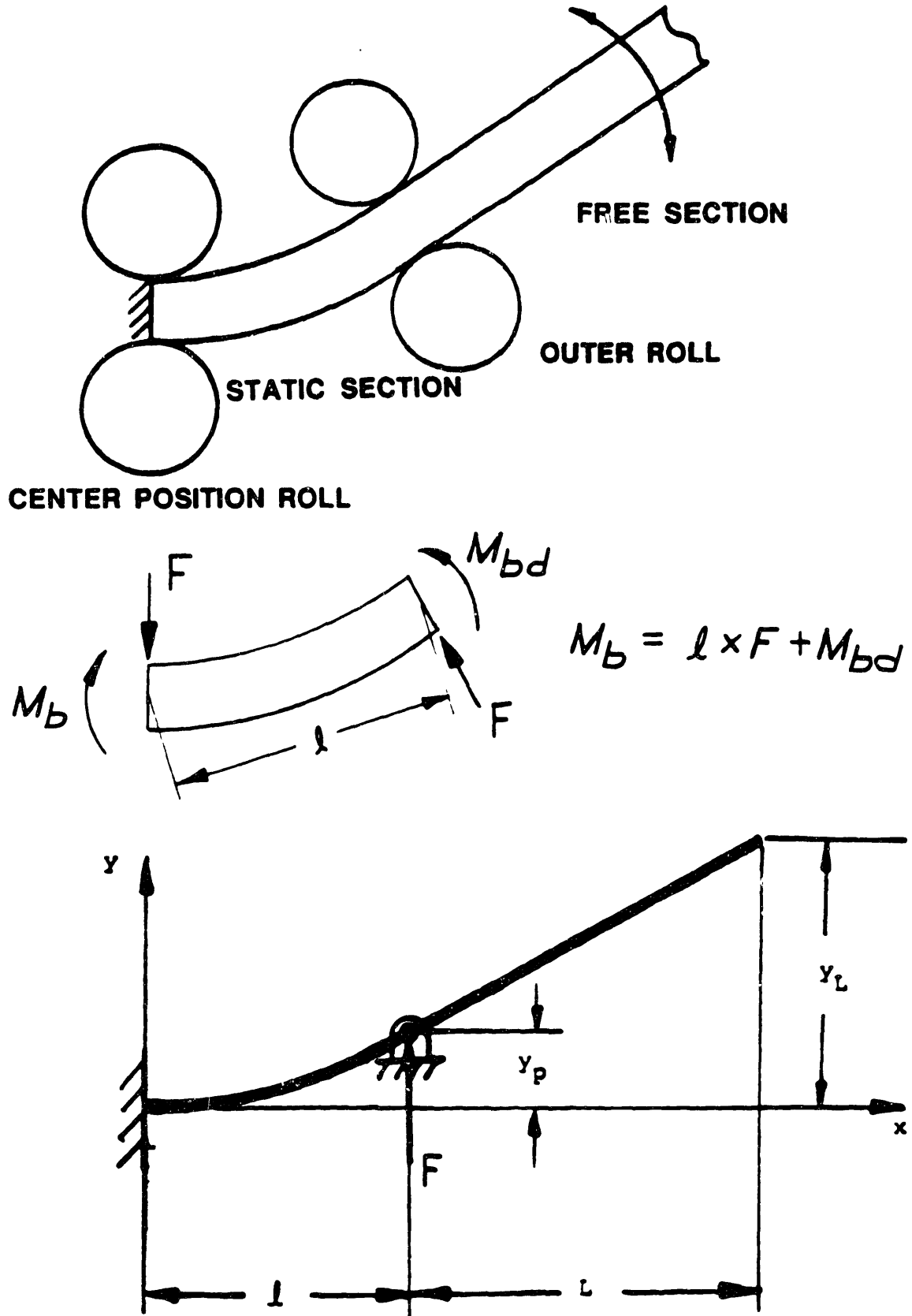
Figure 3.1 Model for Workpiece Dynamics

Since the loaded curvature can be expressed with the center roll position from Equation (2.10), if the relationship between the maximum moment and the center roll position is obtained, the unloaded curvature can be expressed with the center roll position from Equation (2.3). From this, the workpiece model including the workpiece dynamics can be obtained.

3.1.2. Moment-Roll Position Relationship

The static moment can be obtained based on the workpiece characteristics and the mechanics of the roll bending process mentioned in Chapter 2. It is assumed that the workpiece is made of an elastic-perfectly-plastic material with the stress-strain relationship shown in Figure 3.2. Then, assuming that the workpiece has a rectangular cross section which is constant along the length, the relationship between the static moment and loaded curvature can be described as below:

$$M_{bs} = EI \cdot K_L \qquad\qquad K_L < K_y \qquad (3.1)$$

$$M_{bs} = \frac{3}{2} M_y \left(1 - \frac{1}{3}\left(\frac{K_y}{K_L}\right)^2 \right) \qquad K_L \geq K_y \qquad (3.2)$$

where M and K are the moment and loaded curvature at the yield point of the workpiece. This equation means that the static moment increases linearly with the constant beam rigidity as the loaded curvature increases in the elastic
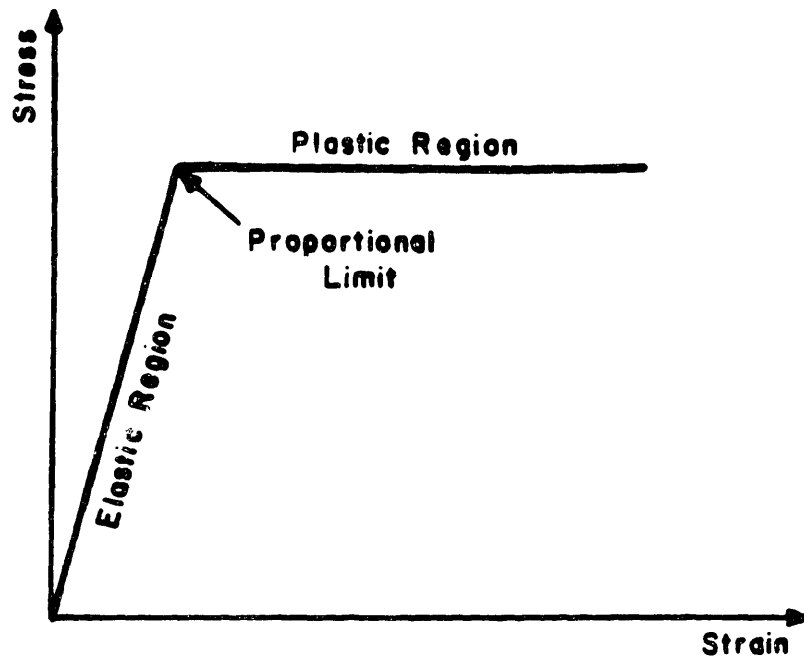
Figure 3.2 Stress-Strain Diagram for an
Elastic-Perfectly-Plastic Material

region, but that the static moment has a nonlinearity with the loaded curvature in the plastic region.

Sustituting Equation (2.8) into Equation (3.1) yields the following relationship between the static moment and center roll position:

$$M_{bs} = \frac{3EIy_p}{\ell^2} \qquad\qquad y < y_y \qquad\qquad (3.3)$$

$$M_{bs} = \frac{9}{2}\frac{EIy_y}{\ell^2}\left(1 - \frac{1}{3}\left(\frac{y_y}{y_p}\right)^2\right) \qquad y \geq y_y \qquad\qquad (3.4)$$

To obtain a transfer function between the center roll position and dynamic moment, it is assumed that the workpiece is a lumped-parameter system with one-degree-of-freedom. Since the first mode of the workpiece vibration dominates the workpiece dynamics, the free section of the workpiece can be modeled as a cantilever beam with the first mode frequency as shown in Figure 3.3.

The end position of workpiece (y_L) related to the center roll position(y_p) is obtained by statics [10]:
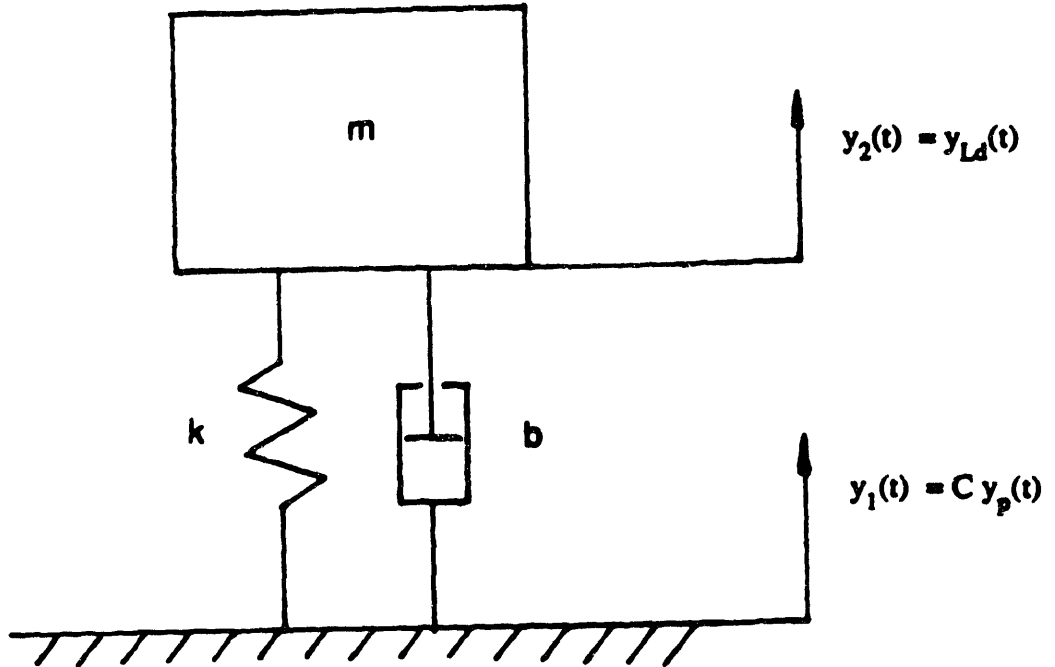
$$\frac{Y_2(s)}{Y_1(s)} = \frac{\omega_n^2}{s^2 + 2\xi\omega_n s + \omega_n^2}$$

where $2\xi\omega_n = b/m$

$$\omega_n^2 = k/m$$

Figure 3.3   Model for Workpiece Free Section Dynamics

$$y_L = \frac{Fl^2}{6EI}\left(3L + 2l\right) \qquad (3.5)$$

and

$$y_p = \frac{Fl^3}{3EI} \qquad (3.6)$$

Therefore,

$$y_L = \frac{3L + 2l}{2l} y_p \qquad (3.7)$$

By the workpiece model shown in Figure 3.3, the dynamic equation between the static end position (y_L) and the dynamic end position (y_{Ld}) can be written as below:

$$m\ddot{y}_{Ld} + b(\dot{y}_{Ld} - \dot{y}_L) + k(y_{Ld} - y_L) = 0 \qquad (3.8)$$

$$m\ddot{y}_{Ld} + b\dot{y}_{Ld} + ky_{Ld} = b\dot{y}_L + ky_L \qquad (3.9)$$

Neglecting the $\dot{y}$ term since $b \ll k$, the transfer function between the static end position and the dynamic end position can be written as below by performing a Laplace transform:

$$\frac{y_{Ld}(s)}{y_L(s)} = \frac{\omega_n^2}{s^2 + 2\xi\omega_n s + \omega_n^2} \tag{3.10}$$

where $2\xi\omega_n = b/m$

$$\omega_n^2 = k/m$$

By the definition of dynamic moment, it can be obtained using the acceleration of the end point of the workpiece:

$$M_{bd} = L \times m\ddot{y}_{Ld} \tag{3.11}$$

By Laplace Transformation,

$$M_{bd}(s) = mLs^2 y_{Ld} \tag{3.12}$$

From the above equations the transfer function between the dynamic moment and the center roll position can be obtained:

$$\frac{M_{bd}(s)}{y_p(s)} = \frac{CmL\omega_n^2 s^2}{s^2 + 2\xi\omega_n s + \omega_n^2} \tag{3.13}$$

where $C = \dfrac{3L + 2\ell}{2\ell}$

3.1.3. Curvature-Roll Position Relationship

As mentioned earlier, the total maximum moment at the center-roll contact point is composed of the static moment and the dynamic moment:

$$M_b = M_{bs} + M_{bd} \qquad (3.14)$$

By springback,

$$K_u = K_L - M_b \, / \, EI \qquad (3.15)$$

Therefore the unloaded curvature can be expressed by the total moment:

$$K_u = K_L - (M_{bs} + M_{bd}) \, / \, EI \qquad (3.16)$$

Using the relationship between moment and center roll position, the unloaded curvature can be expressed with the center roll position:

In the elastic region ($y < y_y$):

$$K_u = 0 \qquad (3.17)$$

In the **plastic** region $(y \geq y_y)$:

$$K_u = \frac{3y}{2}p - \left(\frac{9}{2} \frac{y_y}{\ell^2} \left(1 - \frac{1}{3} \left(\frac{y_y}{y_p} \right)^2 \right) + \frac{1}{EI} M_{bd} \right) \qquad (3.18)$$

3.2. Natural Frequency and Damping Ratio

3.2.1. Calculation of Natural Frequency

Natural frequency of the workpiece is an important factor in the workpiece dynamics, because it affects the band limit of the roll bending system and the system stability. Since the first mode of the vibration is used in the workpiece dynamics, the first mode frequency of a cantilever beam is used as the natural frequency of the workpiece vibration.

Then, the natural frequency can be expressed by the theoretical equation for free vibration of a cantilever beam [11]:

$$\omega_n = 3.52 \left(\frac{EI}{\rho AL^4} \right)^{1/2} \qquad (3.19)$$

where EI = bending stiffness
ρ = material density
A = cross section area
L = length of free section

For 1.0" x 0.25" 2024-T6 aluminum, the natural frequency can

be **expressed** with only the length of the free section of the
workpiece:

$$\omega_n = \frac{4.99 \times 10^4}{L^2} \qquad (3.20)$$

From the above equation, the natural frequency is shown to be
a length-dependent parameter. The graph for the natural
frequency as a function of the workpiece length is shown in
Figure 3.4. The steep slope in the range of the lengths
(4"-10") suggests that the frequency decreases rapidly at
relatively short lengths. This also results in rapid decrease
of the bandwidth of the roll bending system in that range of
lengths.

3.2.2. Measurement of Damping Ratio

Another important factor in the workpiece dynamics is the
damping ratio. This cannot be obtained precisely by a
theoretical calculation, because the values of damping ratio
differ with the equipment and condition of roll bending. By a
signal processing method using a structural dynamic analyzer,
as shown in Figure 3.5, a precise damping ratio can be
measured.

Impulse inputs are given to the material by using a
piezo-electric impulse hammer, and acceleration signal outputs
from the material are measured by an accelerometer. Then, the
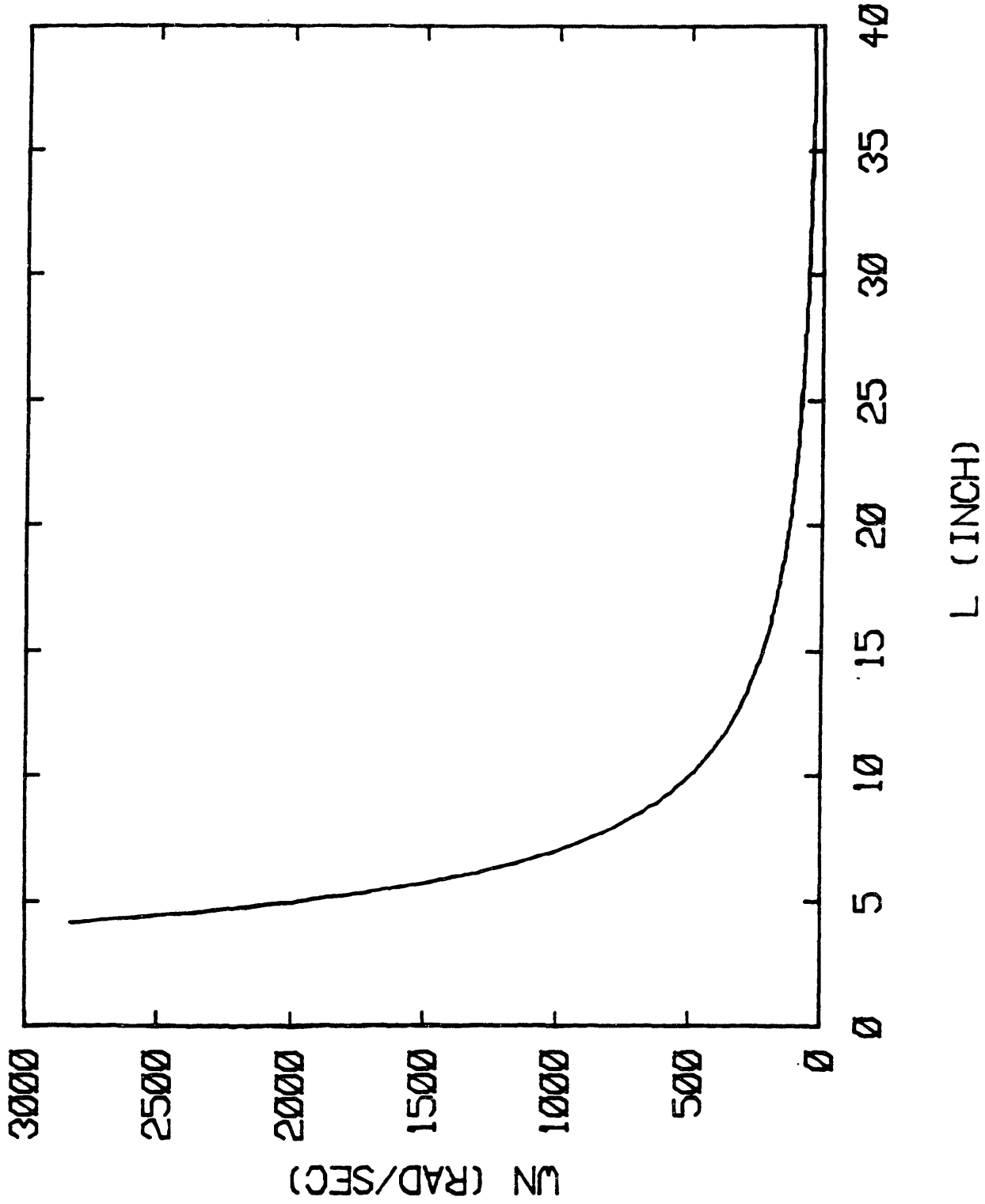
Figure 3.4 Natural Frequency according to
Varying Length of Workpiece
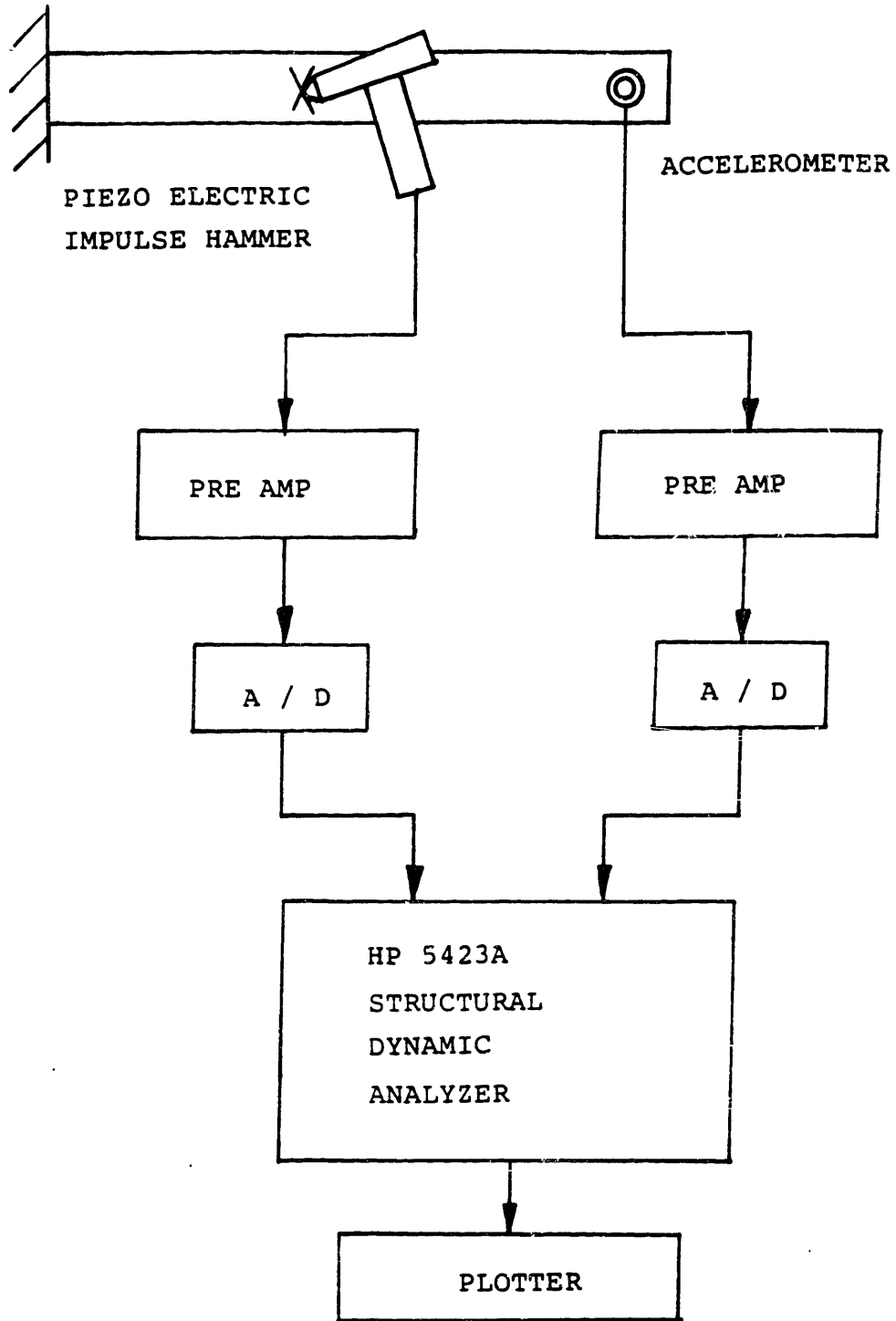
Figure 3.5   Experimental Set-up for Measurement
of Damping Ratio

two signals are sent to a HP 5423A structural dynamic analyzer
through a pre amplifier and an A/D converter respectively. The
frequency spectrum and damping ratio can be obtained
automatically by signal processing in the analyzer.

In this experiment, 2024-T6 aluminum with 1"x0.25"
rectangular cross section was used. The free section length of
the workpiece was 12". To measure the actual damping ratio,
the measurement was made for the same experimental equipment
used in [9], as shown in Figure 3.6. Ten impulses were given
for every test and the average value of the ten measured
outputs was used for the final response. A final response for
the frequency spectrum is shown in Figure 3.7.   Twenty tests
with different impulse positions were performed with the same
exprimental set-up. The average value of the damping ratio of
the aluminum obtained is 0.011.

3.3. Dynamic Analysis and Simulation

3.3.1. System Control

The same control system used in the experiments on roll
bending in [9] is required in order to check the workpiece
dynamics with the simulated responses. Thus, the closed-loop
control system with a proportional controller and a position
and velocity feedback is used, assuming that the velocity of
the center roll can be used instead of the velocity of the
unloaded curvature. Since a linear control theory shows that a
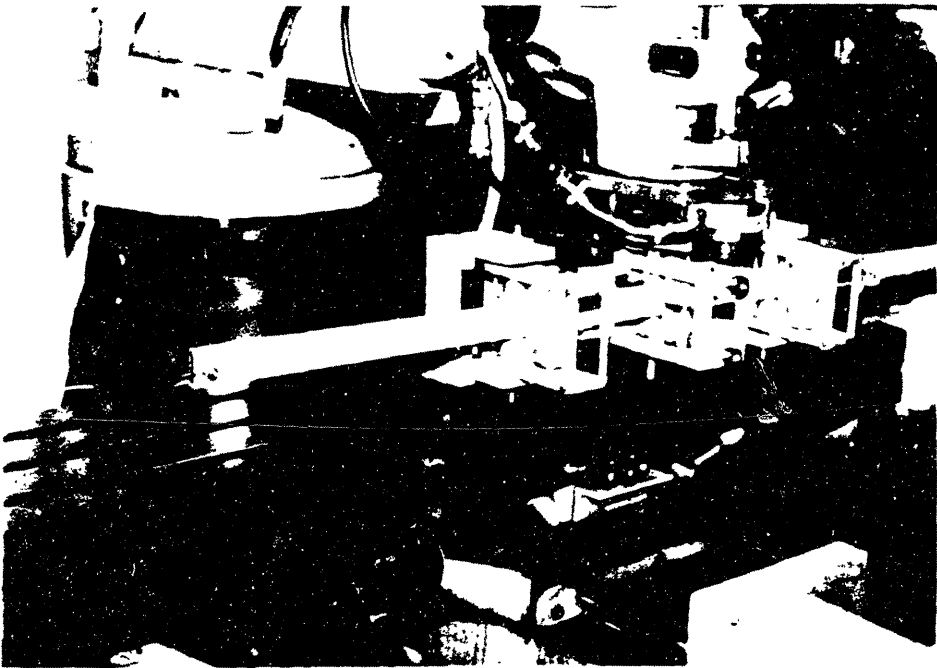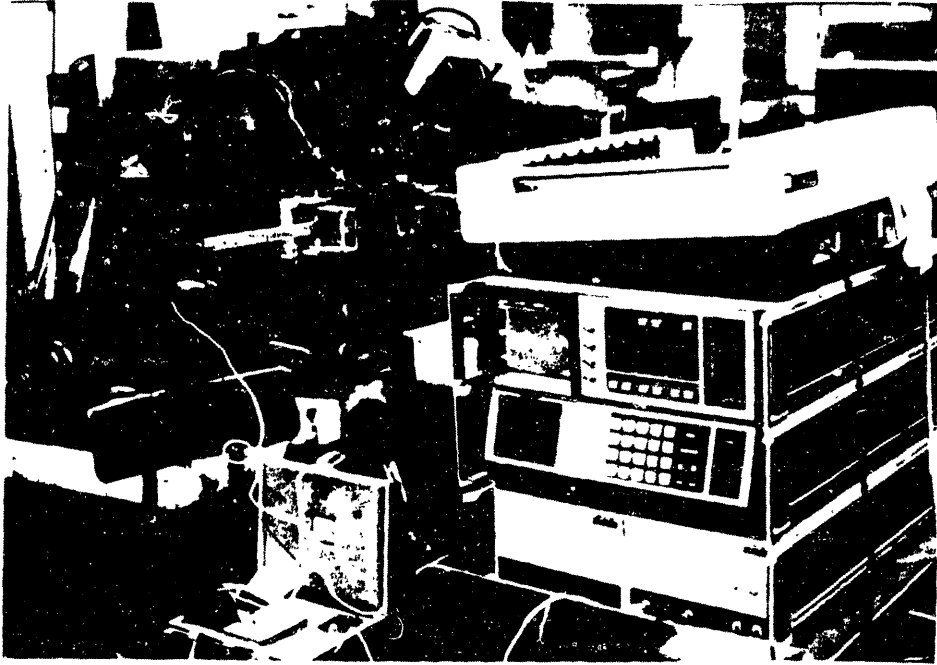
Figure 3.6   Experimental Apparatus for Measurement
of Damping Ratio
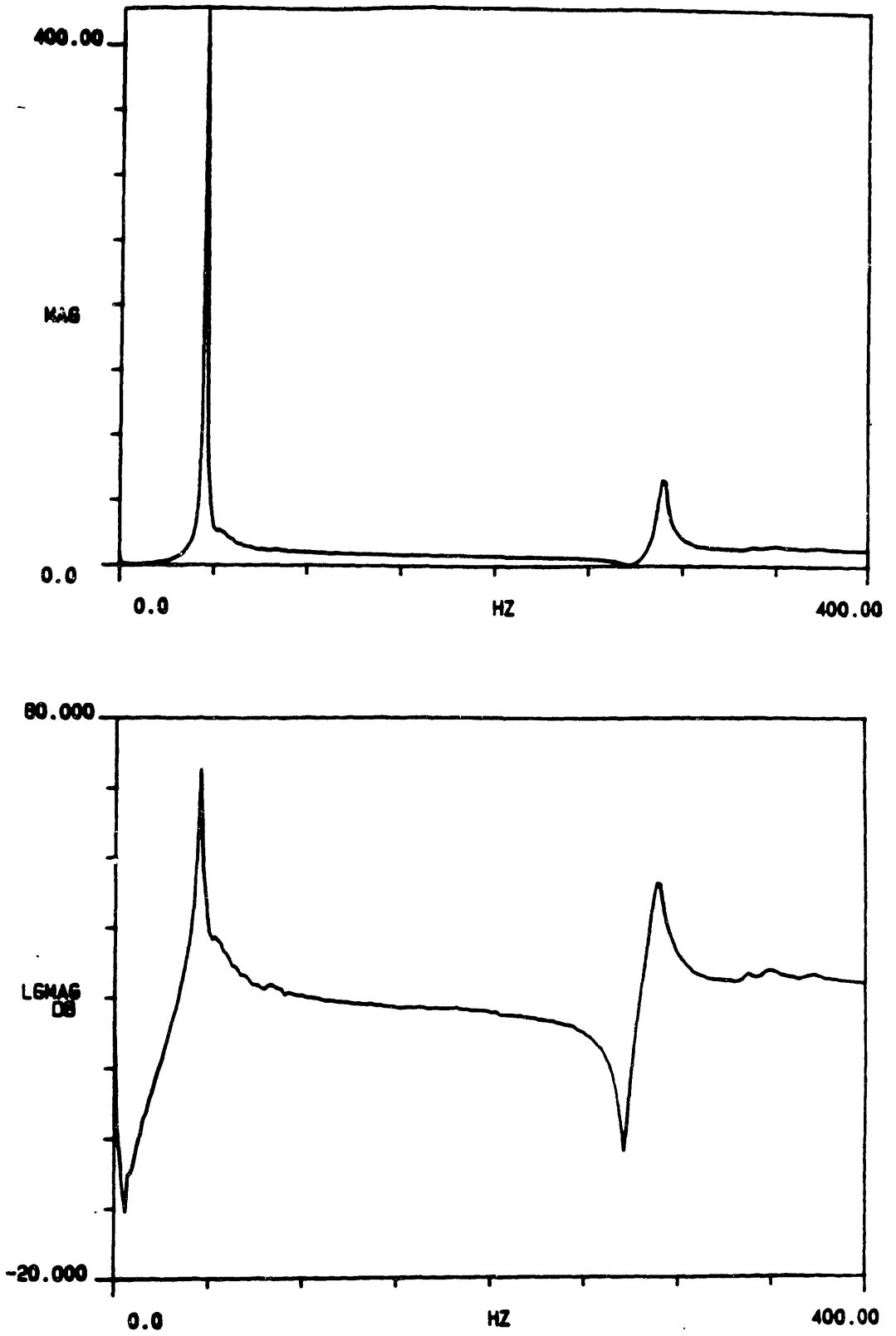
Figure 3.7   Frequency Spectrum

free integrator in the open-loop transfer function of the type 1 system guarantees zero steady-state error to a step input, the velocity-servo model is used to introduce a free integrator to the system. The block diagram for the proposed system is shown in Figure 3.8. The plant of the system is composed of a linear servo model and a nonlinear workpiece model.

The root locus method based on the open loop transfer function is widely used for obtaining the desired poles to get a better response with a proper controller gain in the closed-loop control system [12]. Since this method is valid only for the linear system, the nonlinearity between the center roll position and static moment is neglected in obtaining the transfer function of the system.

Then, the transfer function of the workpiece can be expressed as follows:

$$\frac{K_u}{y_p} = \frac{\left(\dfrac{3}{\ell^2} - \dfrac{CmL\omega_n^2}{EI}\right)s^2 + \dfrac{6\xi\omega_n}{\ell^2}s + \dfrac{3\omega_n^2}{\ell^2}}{s^2 + 2\xi\omega_n s + \omega_n^2} = W(s) \qquad (3.21)$$

Thus, the open-loop transfer funcion of the controller and servo with velocity feedback can be obtained for the controller gain K_c. From the system block diagram shown in Figure 3.8, the transfer function between the center roll velocity and the
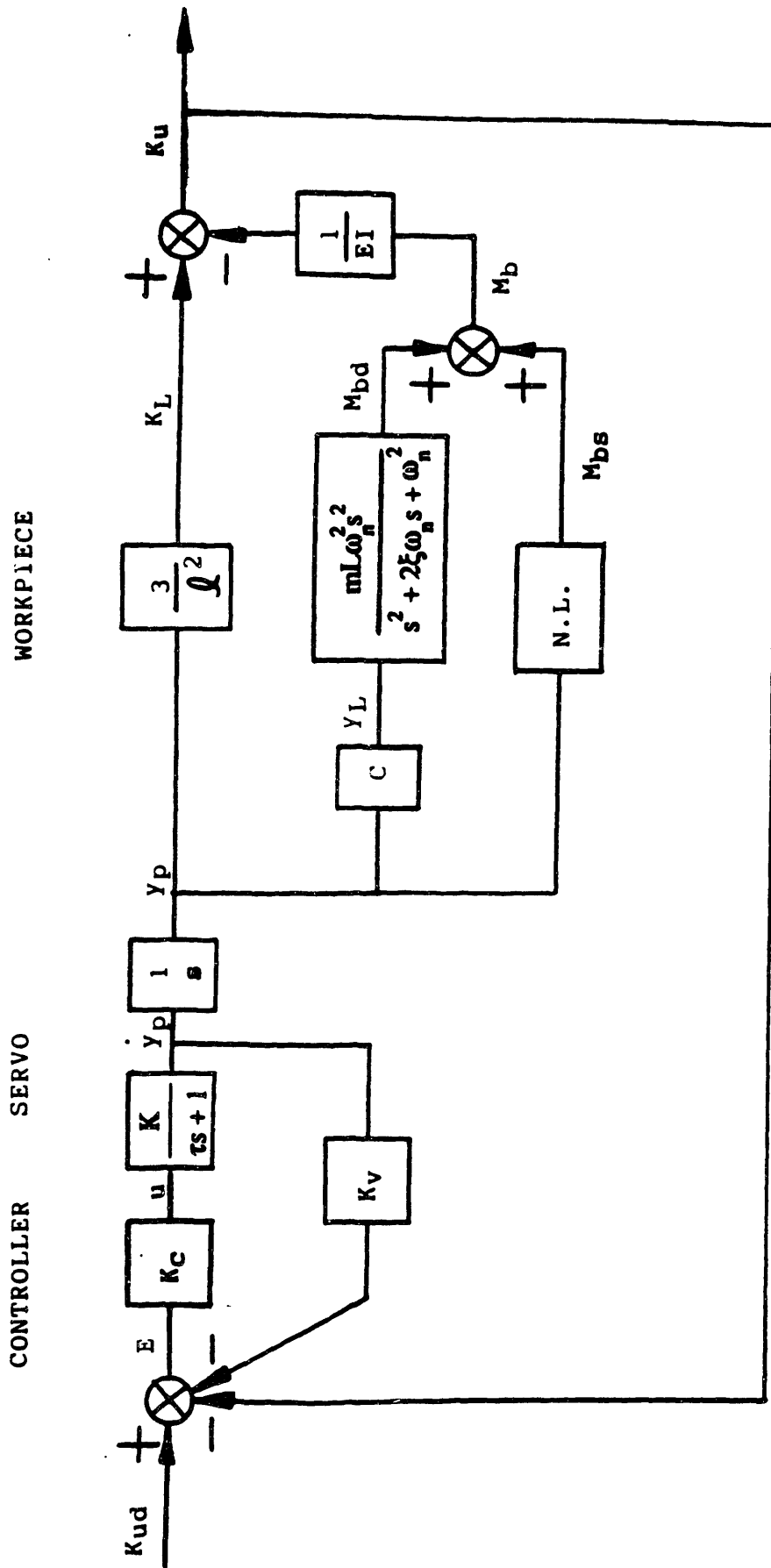
Figure 3.8   Block Diagram of Roll Bending System with Workpiece Model

error can be obtained, considering the velocity feedback:

$$\frac{Y_p(s)}{E(s)} = \frac{G_c}{\tau s + (1 + K_c K_v)}$$ (3.22)

Then, the open loop transfer function can be expressed as

$$GH = \frac{K_c W(s)}{s(\tau s + (1 + K_c K_v))}$$ (3.23)

Thus, the open loop transfer function for the controller gain Kc can be obtained by the following steps:

$$1 + GH = 1 + \frac{K_c W(s)}{s(\tau s + (1 + K_c K_v))} = 0$$ (3.24)

$$\tau s^2 + (1 + K_c K_v) s + K_c W(s) = 0$$ (3.25)

$$\tau s^2 + s + K_c (K_v s + W(s)) = 0$$ (3.26)

$$1 + \frac{K_c (K_v s + W(s))}{\tau s^2 + s} = 0$$ (3.27)

Then,

$$GH = \frac{K_c (K_v s + W(s))}{\tau s^2 + s}$$ (3.28)

Therefore,

$$G(s)\,H(s) = \frac{K_c\left(K_v s^3 + \left(\frac{3}{\ell^2} - \frac{CmL\omega_n^2}{EI} + 2\xi\omega_n K_v\right)s^2 + \left(\frac{6\xi\omega_n}{\ell^2} + K_v\omega_n^2\right)s + \frac{3\omega_n^2}{\ell^2}\right)}{s(\tau s + 1)(s^2 + 2\xi\omega_n s + \omega_n^2)} \qquad (3.29)$$

$$\text{where} \quad K_v = 3G_2/\ell^2$$

$$C = \frac{3L + 2\ell}{2\ell}$$

The values of parameters for 2024-T6 aluminum with 1"x0.25" rectangular cross section are:

$$E = 3.86 \times 10^9 \ \text{lbm/in sec}^2$$

$$I = 0.0013 \ \text{in}^4$$

$$\rho = 0.1 \ \text{lbm/in}^3 \qquad\qquad (3.30)$$

$$A = 0.25 \ \text{in}^2$$

$$\ell = 6 \ \text{in}$$

Since the natural frequency varies with length, the positions of the poles and zeroes of the open loop transfer function for the system change as shown in Figure 3.9. Figure 3.10 shows a root locus at a length of 30 in of the workpiece. As shown Figure 3.9, the system has a non-minimum phase because the zeroes of the workpiece are placed on the right-half plane. This makes the system unstable as the controller gain increses, as shown in Figure 3.10.
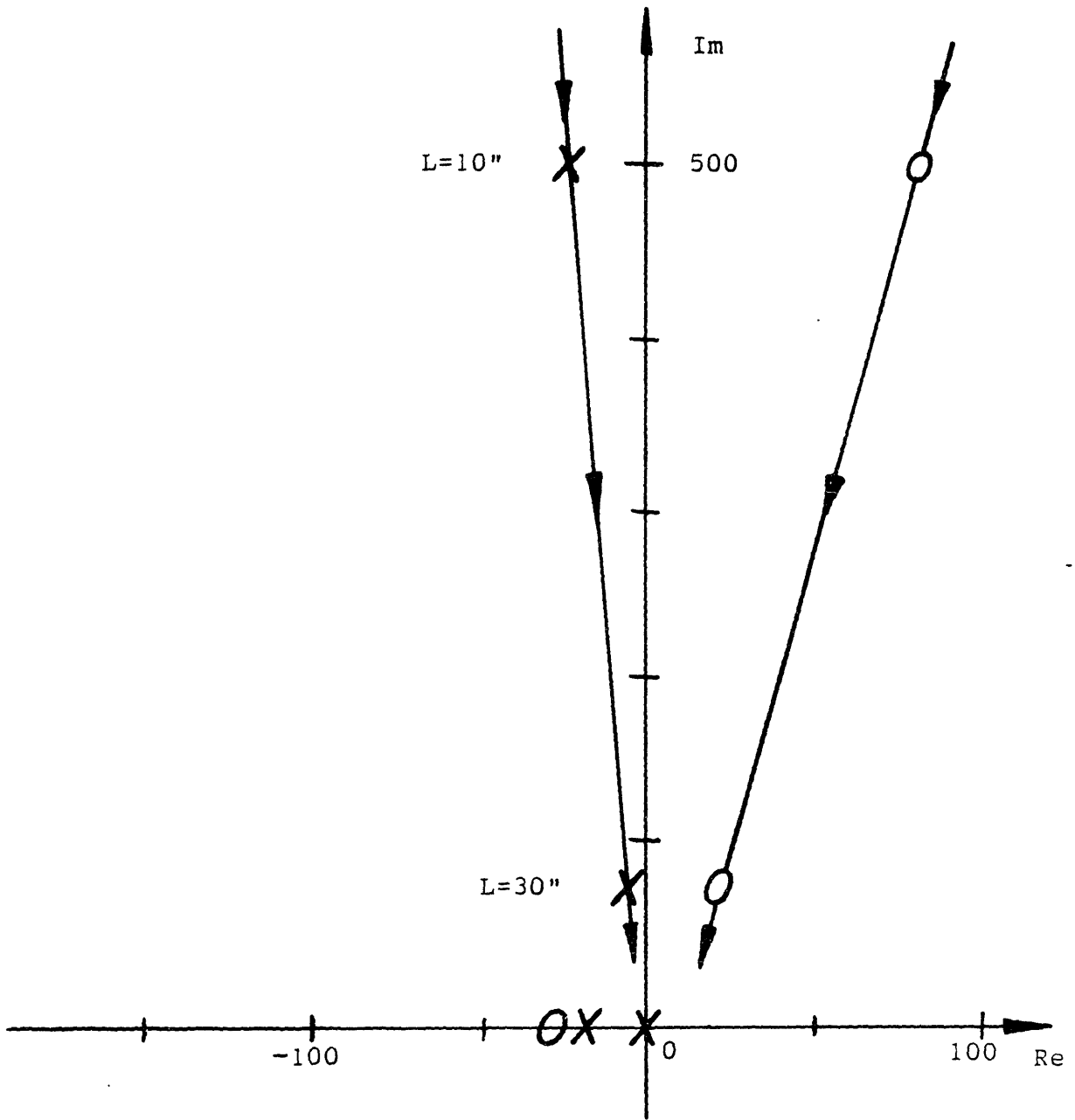
Figure 3.9 Variation of Pole-Zero Positions due to
Varying Length of Workpiece

—54—

Figure 3.10 Root Locus of Roll Bending Control System
with L=30 in

When the workpiece length is short the system is stable for the high gain, but the system becomes unstable even for the low gain as the workpiece length increases, as expected in the workpiece model. This is because the increased workpiece length affects the system stability by shifting the poles of the workpiece close to the instability region due to the decreased natural frequency, as shown in Figure 3.9. The root locus shown in Figure 3.10 represents that the proposed workpiece dynamics is related to the system instability, and therefore the proposed workpiece model may be used to represent the unknown workpiece model.

3.3.2. Simulation and Discussion

The transfer function of the plant should be transformed into the form of state equations for simulation. Since the workpiece has a nonlinear term, as shown in the block diagram (Figure 3.8), two state equations should be considered for the plant. The center roll position is calculated from the servo, and the unloaded curvature is obtained from the workpiece. The transfer functions of the servo and workpiece are transformed to the differential equations, and subsequently to the state equations. The dead-band zone due to springback and the nonlinearity between the center roll position and moment are considered in the simulation.

The same values of the controller gain G1, the feedback gain of $\dot{K}u$, G2 (or the velocity feedback gain Kv), and feedrate as

in the experiments performed in [9] are used so that the unknown workpiece model can be compared to the experimental responses. The simulated responses are shown in Figures 3.11 and 3.12, where the input command is a step curvature change of 0.01/in. Since ℓ = 6 in, the value of Kv is obtained from G2 by Equation (2.14):

$$K_V = \frac{1}{12} \left(G2 \right) \tag{3.31}$$

All the simulated responses have oscillations at high gains as the workpiece length increases with time, as expected from the workpiece model and the root locus analysis. When the value of G2 or Kv is fixed, the system becomes unstable more rapidly as the value of G1 (or Kc) becomes larger. This is because the critical workpiece length for the stability becomes shorter as G1 increases, as mentioned earlier on the root-locus. When the value of G1 is fixed, the critical time for stability becomes slightly shorter as G2 or Kv increases.

In conclusion, the simulated responses for the roll-bending system with the suggested workpiece model agree with the experimental responses shown in Figures 2.7 and 2.8. Therefore, the proposed workpiece model can be used as the unknown workpiece model including the vibration effects which lead to system instability. Based on this workpiece model, an adequate controller to stabilize the system can be designed.
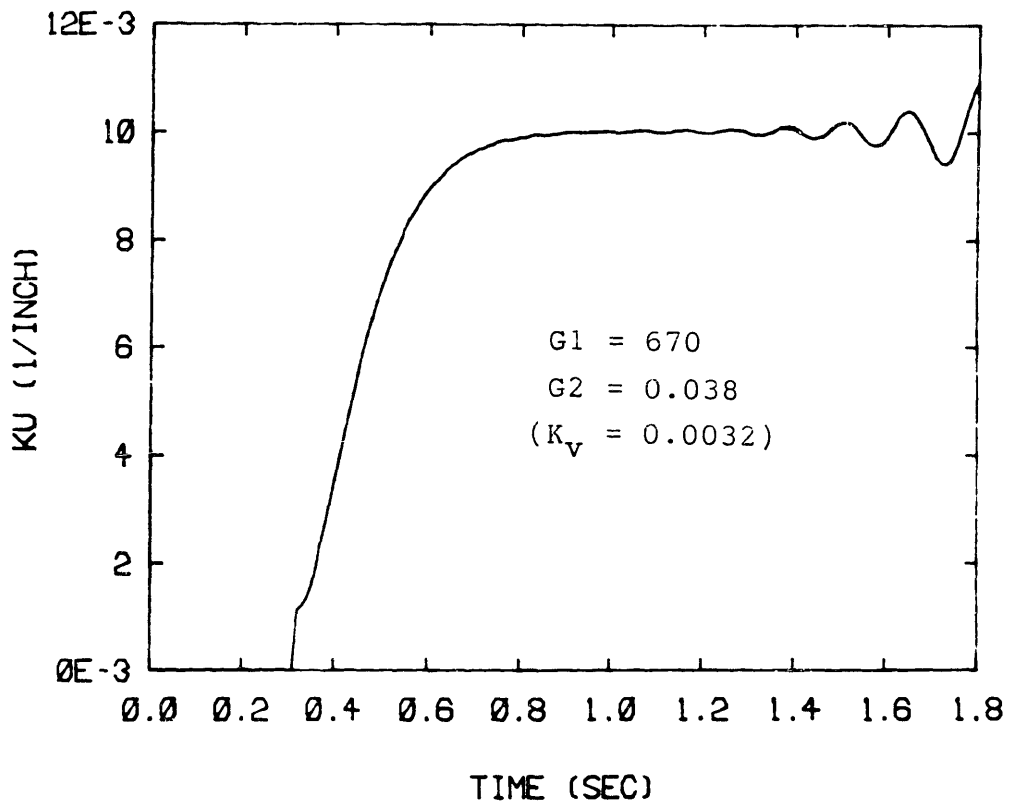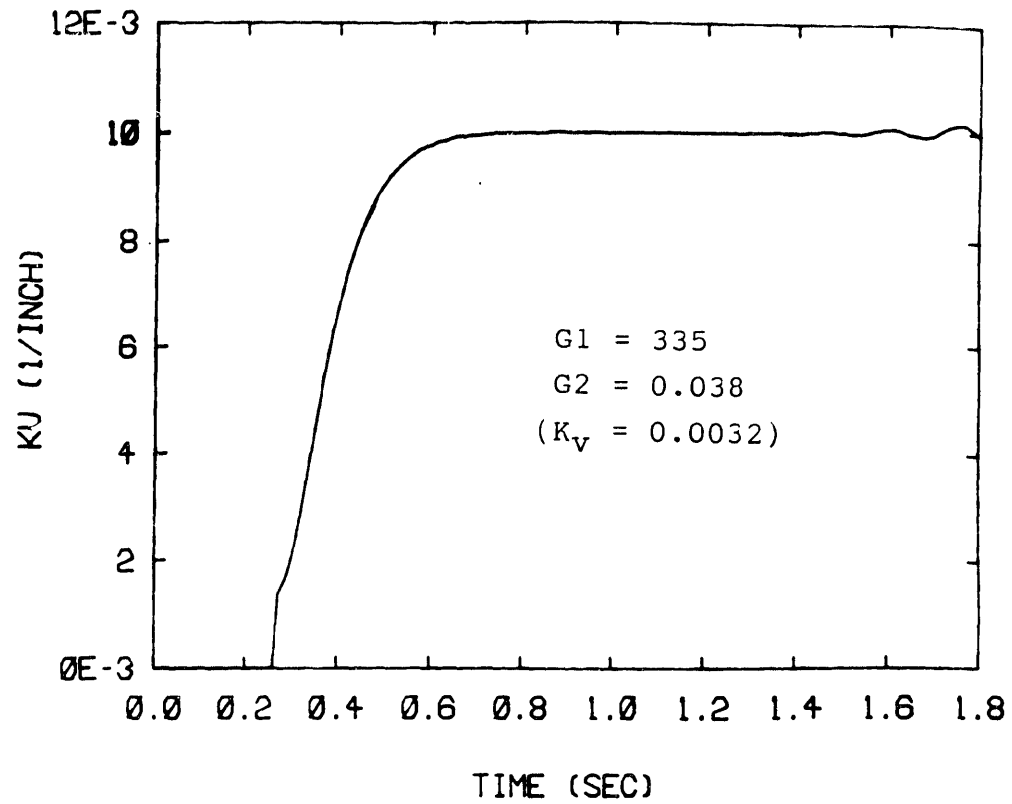
Figure 3.11   Simulated Responses with G2=0.038
and 13 in/sec Feedrate
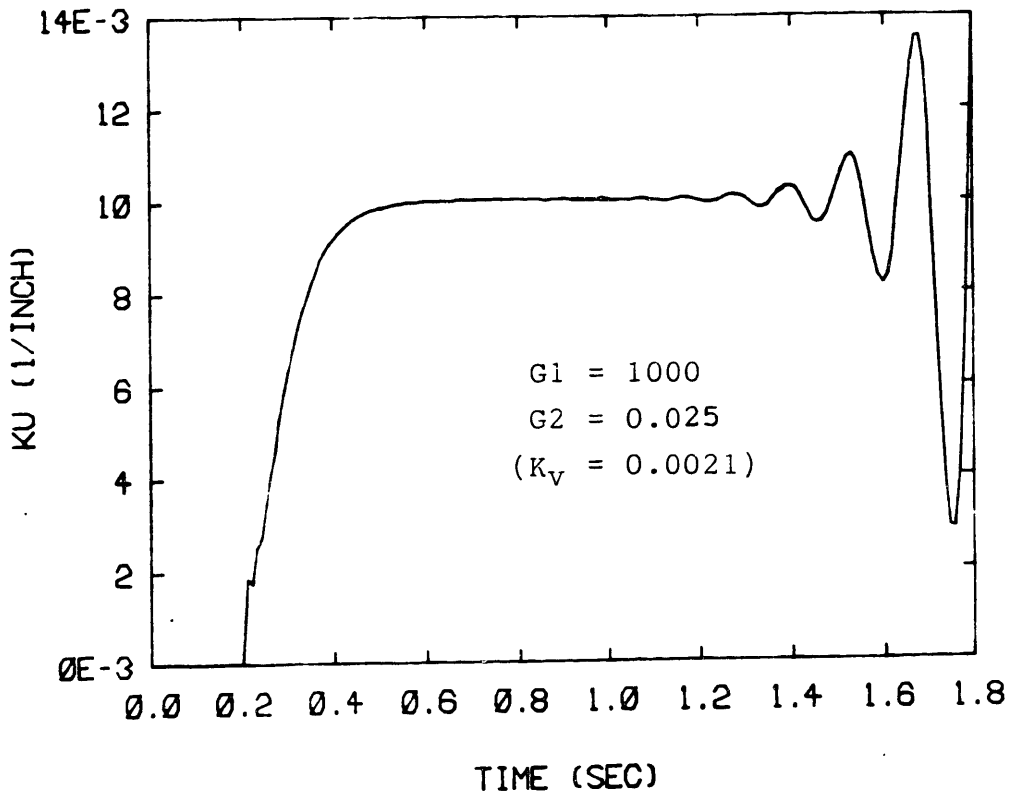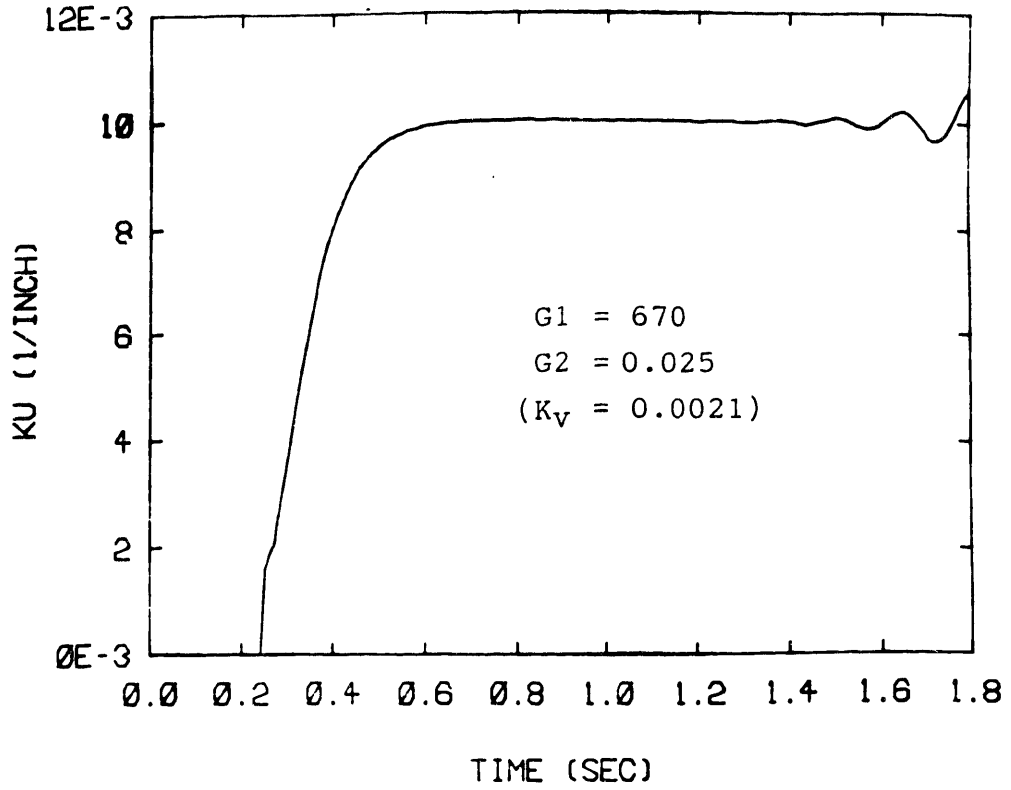
Figure 3.12   Simulated Responses with G2=0.025
and 13 in/sec Feedrate

CHAPTER 4

SCHEDULED GAIN ADAPTIVE CONTROL

4.1. Introduction to Adaptive Control

In general, a control system design is based on the mathematical model of the plant obtained by using physical laws governing its operation and some assumptions. However, the plant model cannot represent exactly the real plant because of inherent uncertainties about the physical plant, the environment, and the plant parameters. In addition, since system nonlinearities and high frequency dynamics are often neglected for the sake of simplicity, the knowledge about the plant dynamics may be poor. Even if the plant dynamics ars known, its parameters are likely to be unknown and/or time-varing due to parameter measurement errors, changes in environment conditions, and changes in operating conditions. The control system should be adequately designed to ensure a satisfactory plant performance despite the presence of uncertainties.

There are several control schemes that can be used to deal with the uncertainties. Among them, adaptive control is the most powerful method for high performance control systems. Landau [13] explains that adaptive control is needed to assure high performance when large and unpredictable variations of the plant dynamic characteristics occur. The popular adaptive -

control techniques are the Self Tuning Control (STC) and the Model Reference Adaptive Control (MRAC). The Scheduled Gain Adaptive Control (SGAC) and the Linear Model Following Control (LMFC) are also used in simple adaptive control applications.

The Self Tuning Control has been developed by Astrom and his colleagues [14, 15, 16]. The STC system has facilities for tuning its own parameters. The parameters of the regulator are adjusted by a recursive parameter estimator and a design calculation. In the MRAC sytem, the parameters of the regulator are adjusted in such a way that the error between the plant output and the model output becomes small. The key problem is to determine the adjustment mechanism so that a stable system, which brings the error to zero, is obtained. The works of Whittaker [17], Monopoli [18], Narendra [19], and Landau [13] have laid the foundation of MRAC algorithm. In this chapter, a continuous-time SGAC and a discrete-time SGAC are presented. The MRAC with a reduced order model will be presented in Chapter 5. Since the STC was not successful in stabilizing the proposed roll bending system with the nonlinearity and nonminimum phase, the result of its application on this system is excluded in this thesis.

4.2. SGAC Scheme

It is somtimes possible to find auxiliary process variables that correlate well with the changes in process dynamics. It is then possible to eliminate the influences of parameter variations by changing the parameters of the regulator as functions of the auxiliary variables. This approach is called Scheduled Gain Adaptive Control because the system was originally used to accommodate changes only in process gain. The SGAC has the advantage that the parameters can be changed quickly in response to process changes. The limiting factors depend on how quickly the auxiliary measurements respond to process changes.

In the proposed roll bending system, the system becomes unstable due to two poles of the workpiece which are located near the imaginary axis in the s plane. The control purpose is to move these poles further to the left side for stability. Since the locations of the workpiece poles are decided by length-dependant natural frequencies, the controller should adapt to the variations. A continuous-time controller with the above control purpose can be designed in s domain by root locus method.

Sometimes an analog-control system is replaced by a computer-control system, simply because the hardware of the latter is cheaper and more realistic. In such a case, it is

natural to look for the method of converting an analog system to a digital system with the same properties. A straightforward way to solve this problem is to use a short sampling interval and to make some discrete-time approximations of the continuous-time controller.

The typical z-transform approximation methods are Euler's method, backward different, and Tustin's approximation. Tustin's approximation has the advantage that the left-half s plane is transformed into the unit circle. With Euler's method, the left-half s plane is transformed into the half-plane Re z < 1. If Euler's method is used, a stable continuous-time system may be approximated by an unstable discrete-time system. But, if Tustin's approximation is used, it will be still stable after the approximation. Therefore, the continuous-time controller designed for the control purpose will be converted to a discrete-time controller by using Tustin's approximation.

4.3. Continuous-time SGAC

The Continuous-time Adaptive Controller on SGAC can be designed for system stability based on the root locus method. As mentioned before, the transfer function of the plant contains two poles from the servo, one zero from the servo-feedback, and two poles and two zeroes from the workpiece. Since the two zeroes in nonminimum phase cannot be

canceled out, the two workpiece poles should be moved to the locations far from the imaginary axis.

Then, two zeroes of the controller are needed to pull the poles. In a digital controller design, the number of poles should be equal to or more than the number of zeroes for up-date control. Thus, considering the hardware capacity of a digital controller, it is recommended to choose two poles in the analog controller design prior to the digital controller design. The two zeroes should be placed near two workpiece poles, with a fixed damping ratio and time-variant natural frequency in order to adapt the two workpiece poles. Then, the system can be stable and those workpiece poles do not become dominant.

The transfer function of the analog controller can be expressed as below:

$$G_c(s) = \frac{K_c(s^2 + 2\xi\omega_{nc}s + \omega_{nc}^2)}{(s + \alpha)^2}$$

(4.1)

Since the zeroes of the controller should be placed near the workpiece poles, the values of damping ratio and natural frequency of the controller were selected as below:

$$\xi_c = 0.35$$

and

(4.2)

$$\omega_{nc} = \omega_n$$

Two poles of the controller are dummy for the real time control, but they affect the movements of the other poles of the root locus. If they are placed near the servo poles, they push strongly the servo poles to enter rapidly the right-half s plane. Considering the hardware capacity of the digital controller, it is reasonable to place the poles at -100 on the real axis. Figure 4.1 shows the root locus for L=30", based on the above controller design scheme. As controller gain increases, the two workpiece poles move to the two controller zeroes but the two poles of servo and controller move to the zeroes of workpiece. This can also make the system unstable but we can choose the value of controller gain in the stable region. Then, the dominant pole gives the fast settling time.

The simulated responses in Figures 4.2 and 4.3 show that the system can be stable up to 20'/sec feedrate with the appropriate controller gain value, and that the system becomes unstable from 30"/sec regardless of controller gains values. The system shows the best performance with Kc=300 and 20"/sec feedrate. Therefore, the roll bending control system can be improved due to the stability and increased feedrate, using the proposed SGAC.
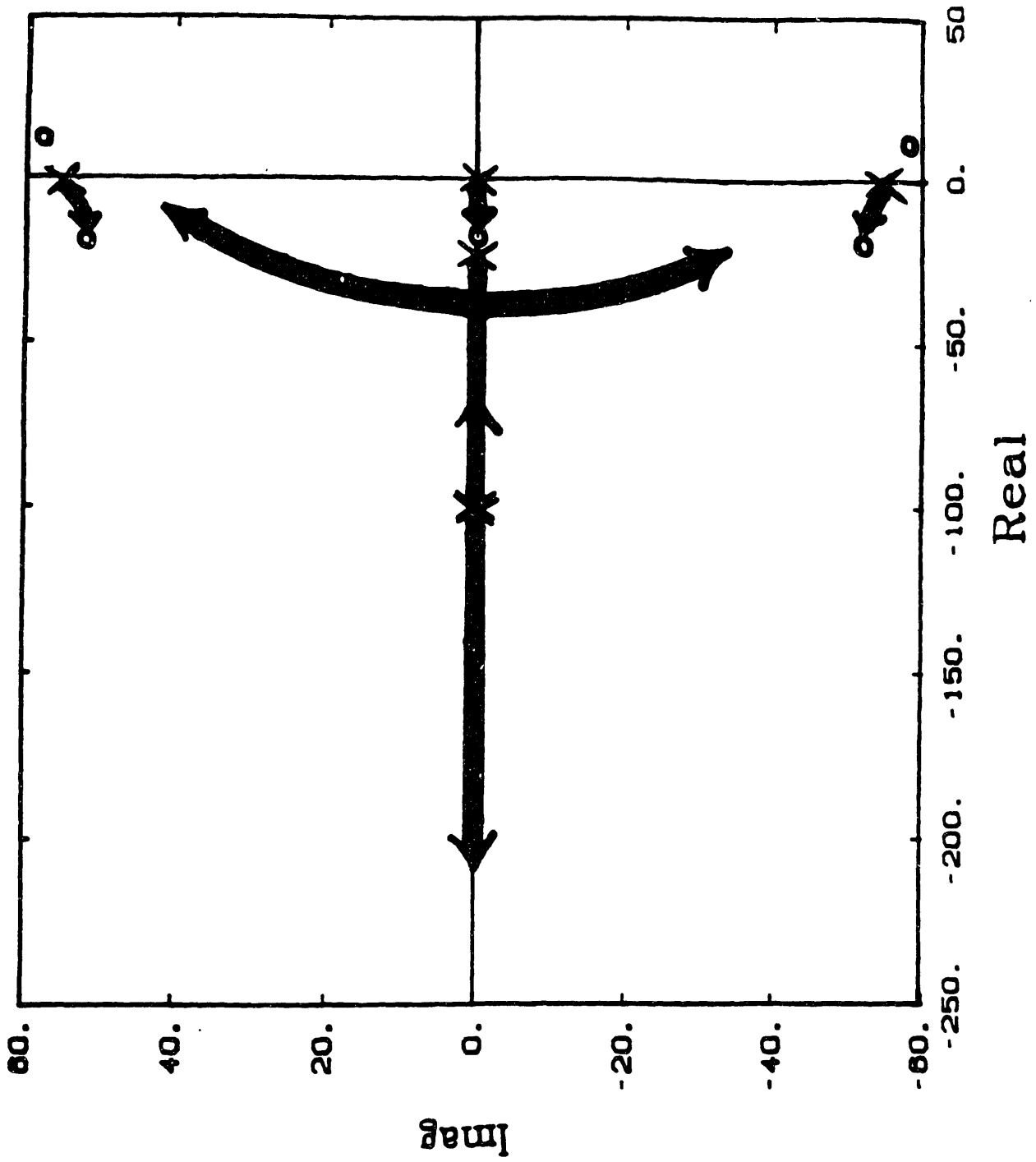
Figure 4.1 Root Locus of Roll Bending System using SGAC
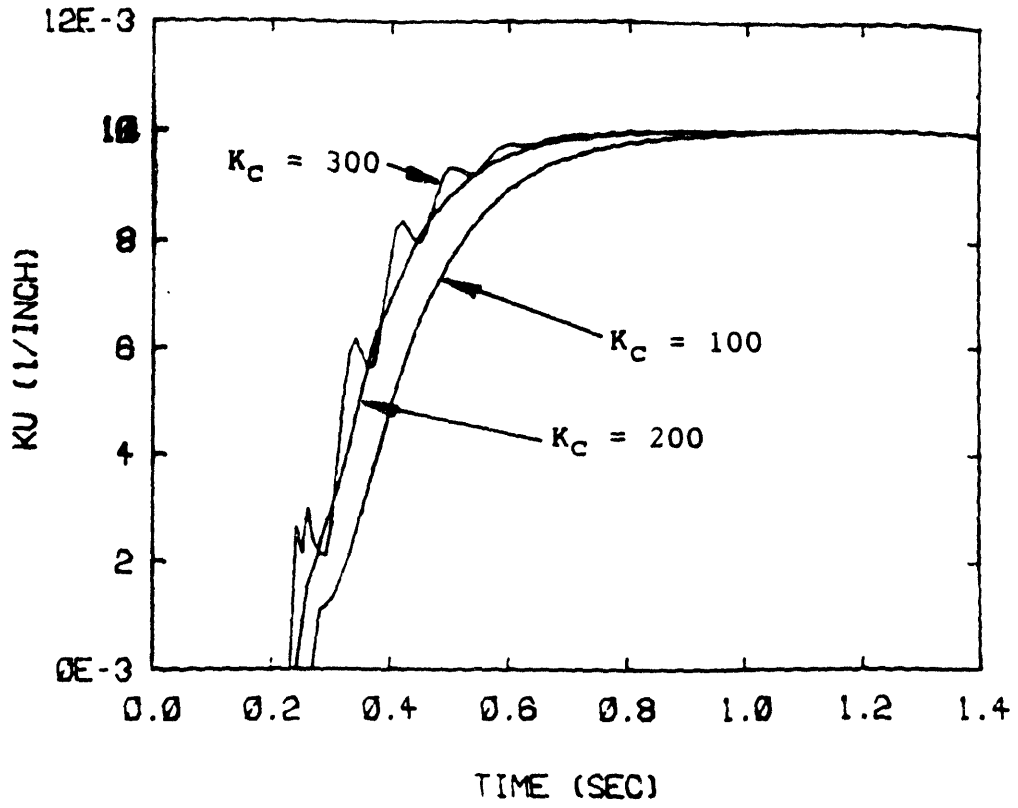
(a) FR = 10 in/sec
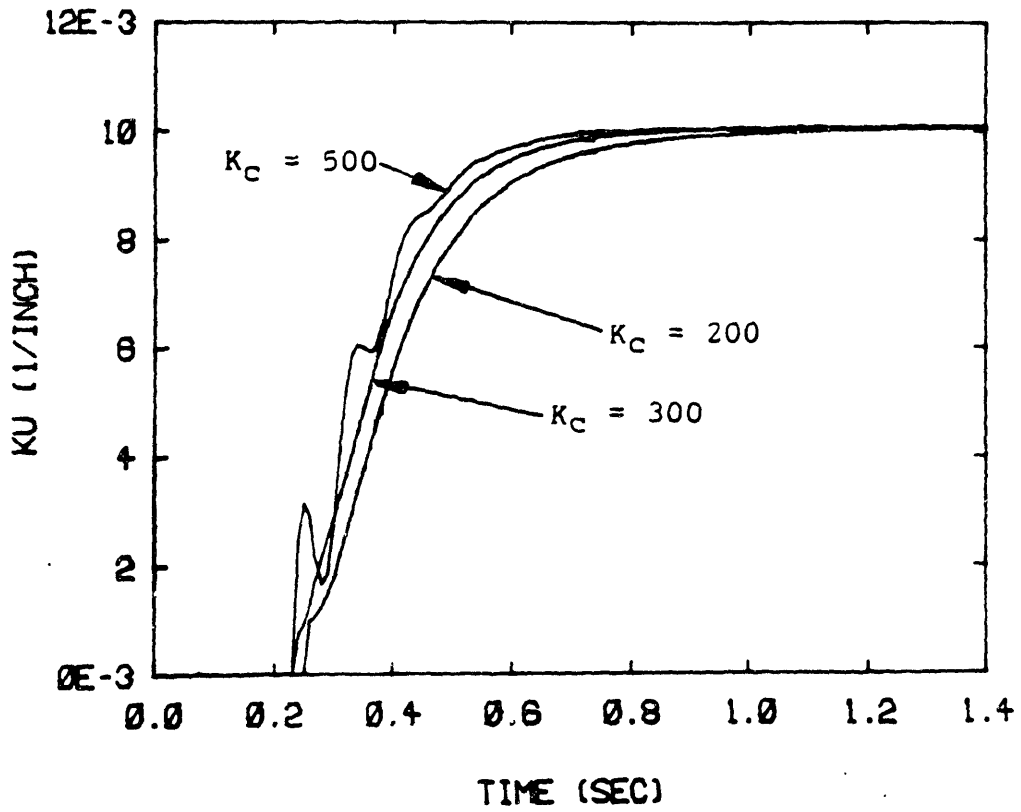
(b) FR = 20 in/sec

Figure 4.2 Simulation of Continuous-time SGAC System
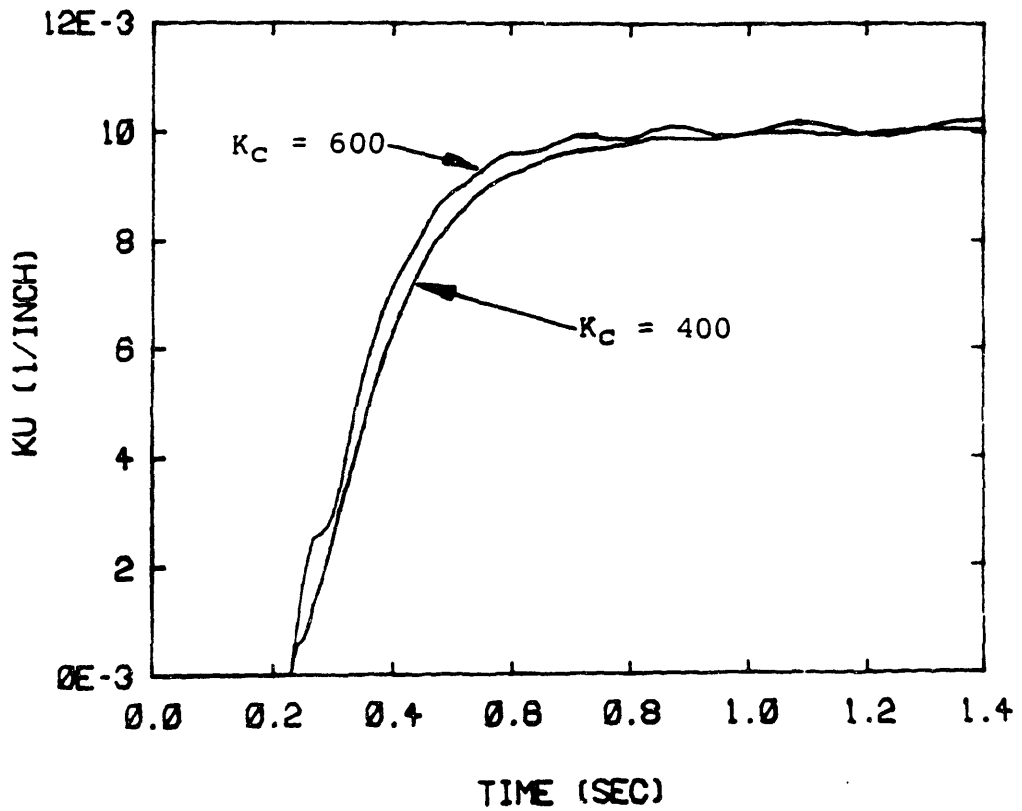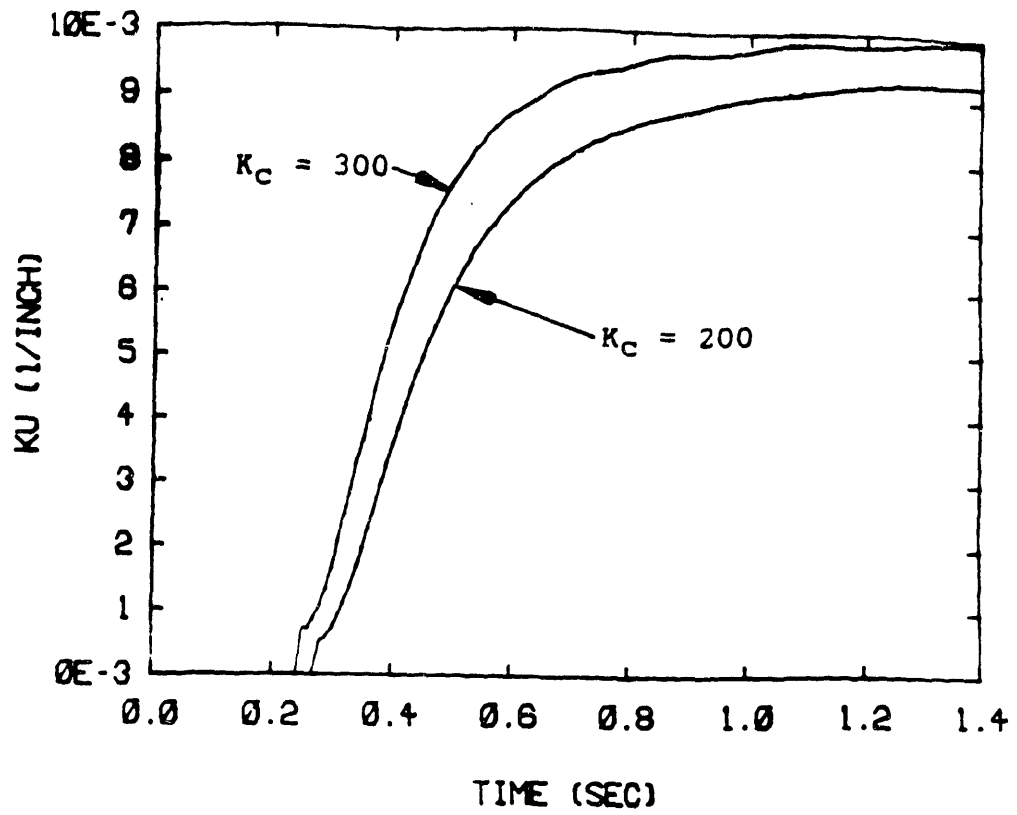
Figure 4.3   Simulation of Continuous-time SGAC System
at 30 in/sec

4.4. Discrete-time SGAC

The **transform** variables z and s are related in some respects by the function z=exp(sT). An approximation, which corresponds to the Trapezoidal method for numerical integration, is:

$$z = e^{sT} \sim \frac{1 + sT/2}{1 - sT/2} \tag{4.3}$$

In digital control context, the approximation in Equation (4.3) is often called the Tustin's approximation method, or bilinear transformation. Then, the pulse transfer function H(z) can be obtained by simply replacing the argument s in G(s) by s' :

$$s' = \frac{2}{T} \frac{z - 1}{z + 1} \tag{4.4}$$

The pulse transfer function of the discrete-time controller can be obtained from the continuous-time controller, using Equation (4.4).

$$H_c(z) = \frac{K_c\left(4(z-1)^2 + 4\xi_c\omega_n T(z-1)(z+1) + \omega_n^2 T^2(z+1)^2\right)}{\left((2+100T)z + (100T-2)\right)^2} \tag{4.5}$$

The controller time step T is selected to be 0.01 sec. Therefore, the pulse transfer function of the controller is

expressed as below:

$$H_c(z) = \frac{K_c\left(4(z^2 - 2z + 1) + 0.04\xi_c\omega_{nc}(z^2 - 1) + 10^{-4}\omega_{nc}^2(z^2 + 2z + 1)\right)}{(3z - 1)^2}$$ (4.6)

In the simulation with the digital controller the hybrid system, which is composed of continuous plant system and discrete-time controller, was used. Figure 4.4 shows the simulated responses at 10"/sec and 20"/sec. The adequate values of Kc result in the system stability, as expected in the analog control system. Figure 4.5 shows the responses for the different values of Kc at 30"/sec. The system becomes unstable as expected. Figure 4.6 indicates that the system can be stable up to Kc=60 at 25"/sec. From the above responses, the system has the best response with Kc=60 at 25"/sec, because of the stability and fast settling time.

As mentioned earlier in this chapter, the plant model cannot be exactly the same as the real plant due to uncertainties. Assuming that the major parameters of the workpiece model, natural frequency, and damping ratio may be different from the real values, it is necessary to check the system responses with the different values. Figures 4.7 shows the simulated responses performed using different natural frequencies and damping ratios from the ones used in Figure 4.6 (a). The system responses are nearly same even if the value of the
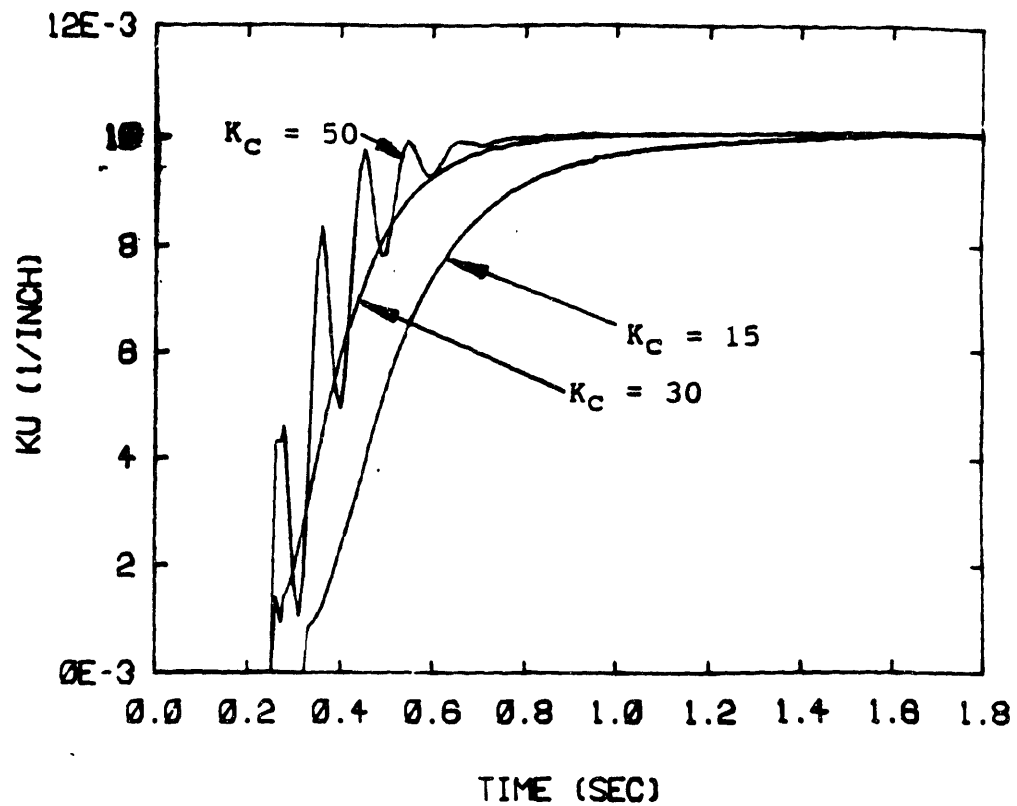
(a) FR = 10 in/sec
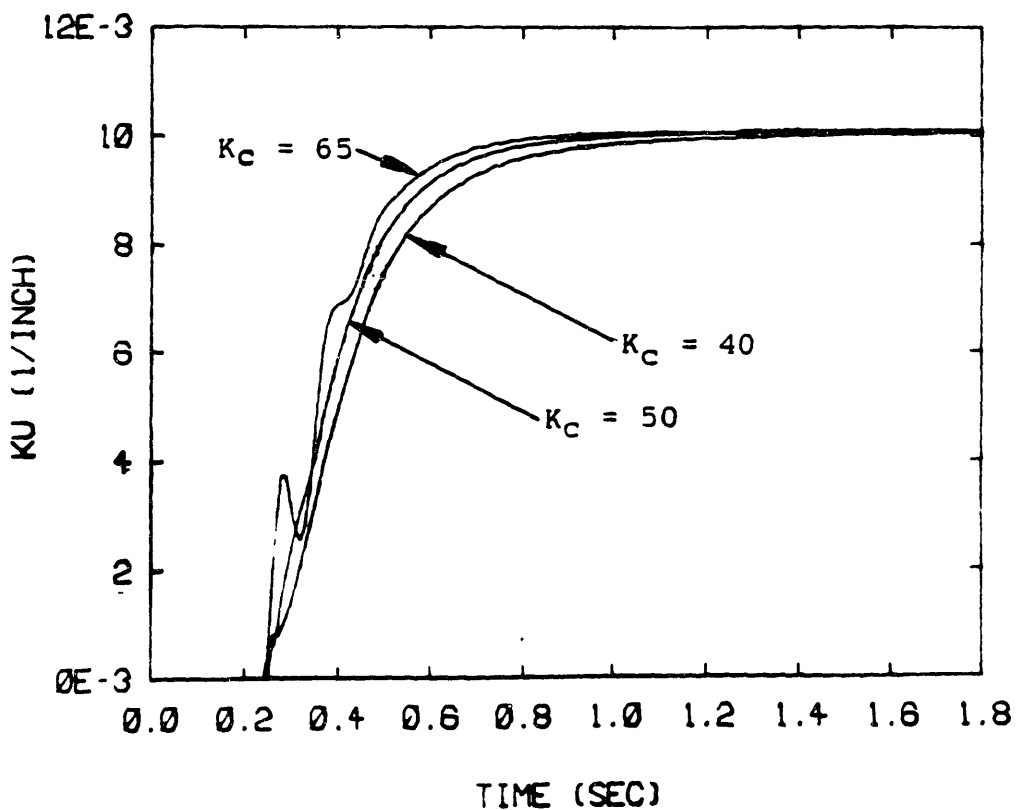
(b) FR = 20 in/sec

Figure 4.4 Simulation of Discrete-time SGAC System
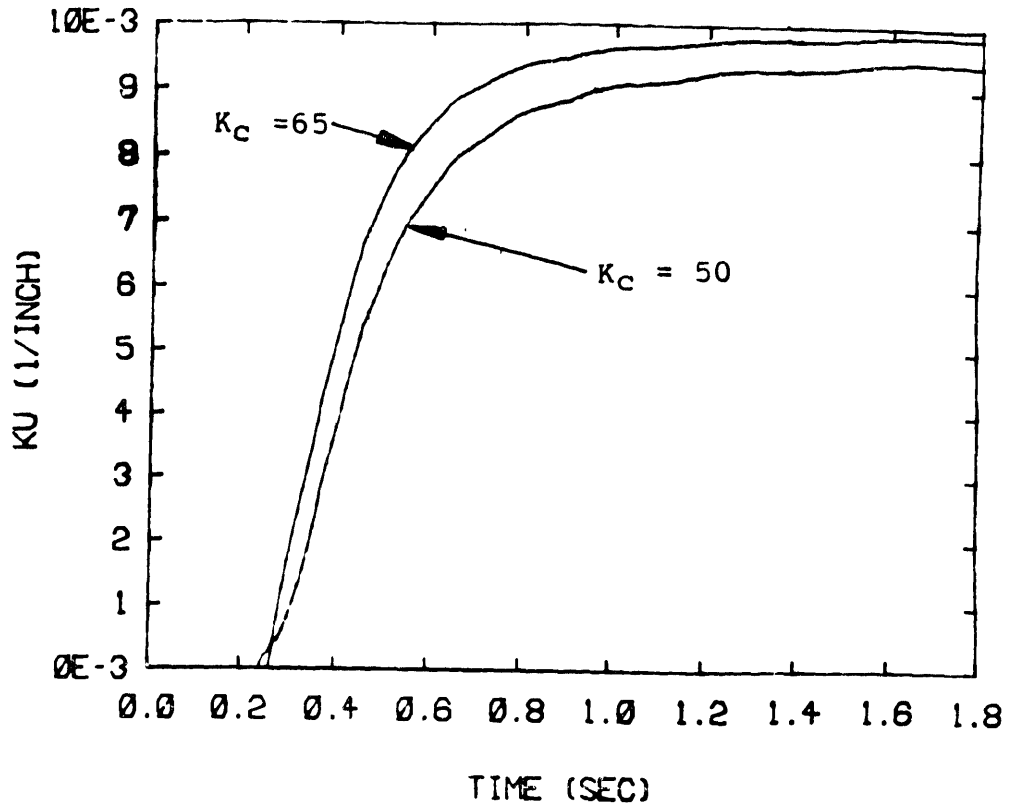
(a)
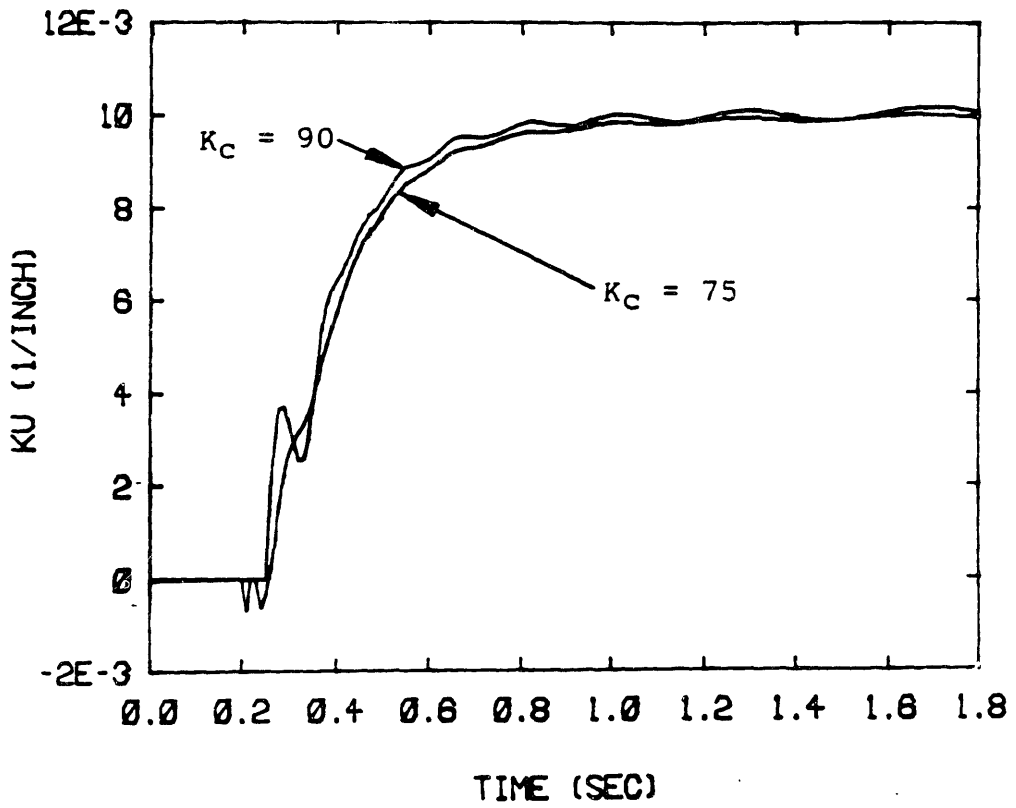
(b)

Figure 4.5   Simulation of Discrete-time SGAC System
at 30 in/sec Feedrate

(a)

(b)
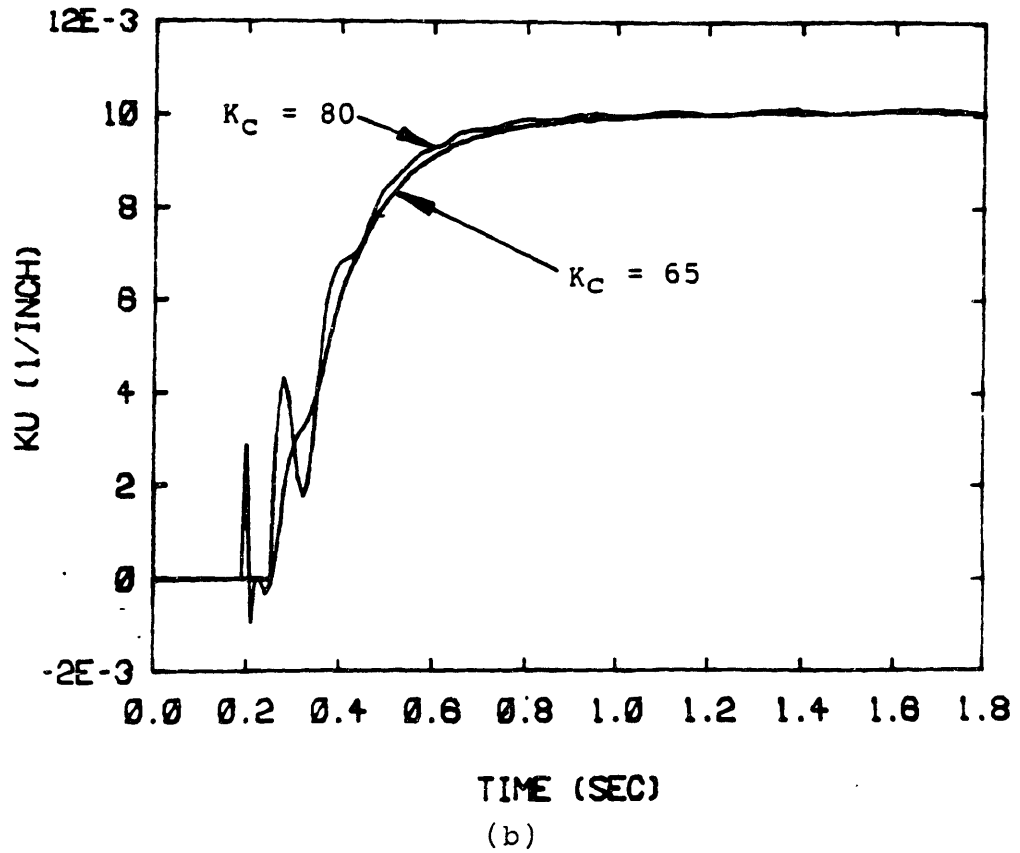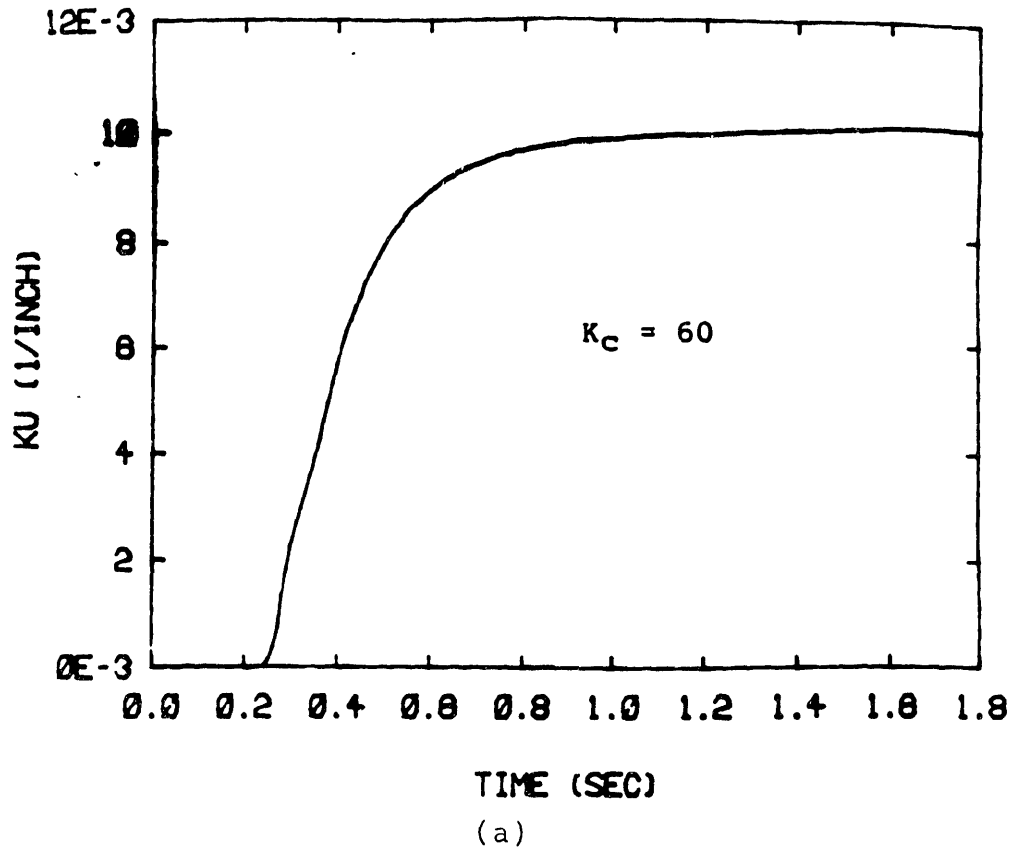
Figure 4.6   Simulation of Discrete-time SGAC System
             at 25 in/sec Feedrate

$$\omega_n = \frac{4.99 \times 10^4}{L^2}$$

(a)

$$\omega_n = \frac{C}{L^2}$$

$$\xi = 0.011$$

(b)
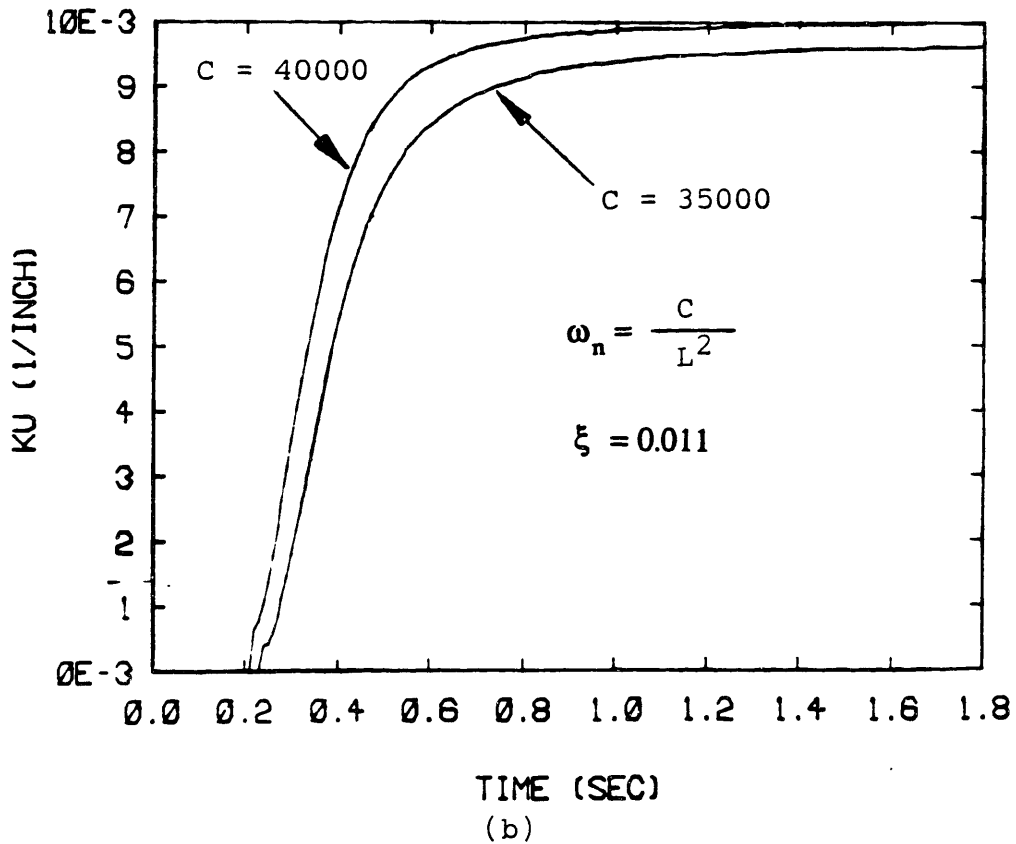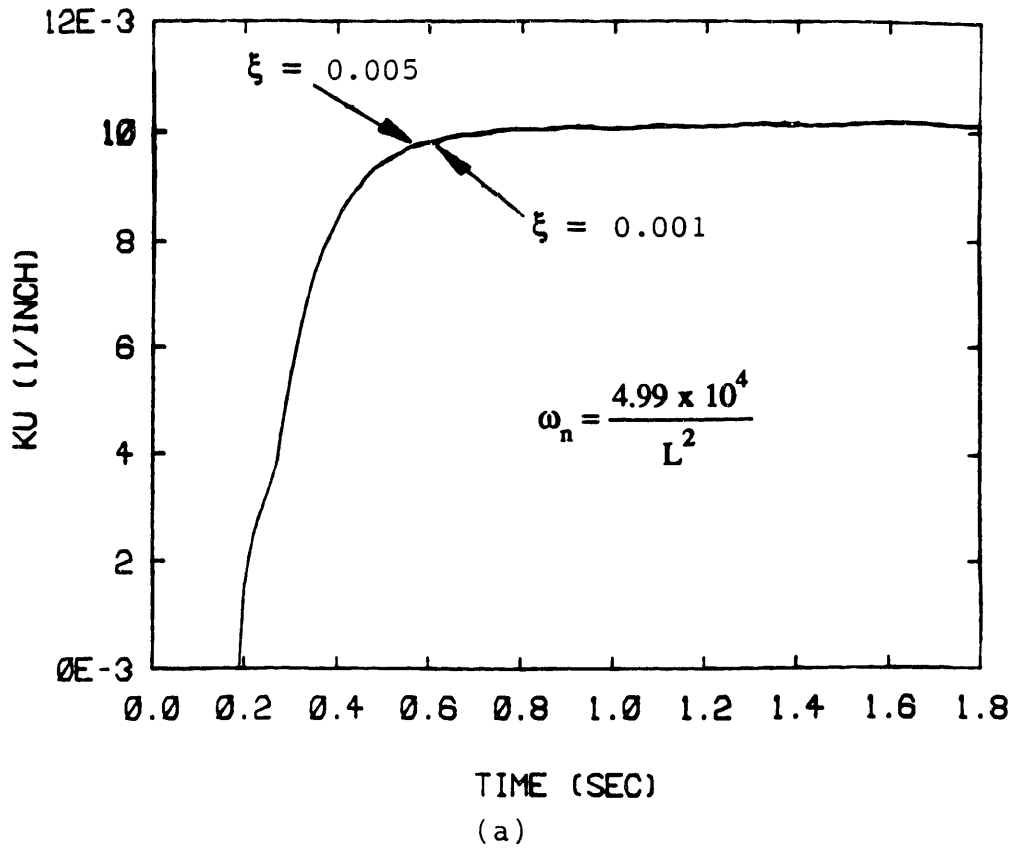
Figure 4.7 Simulation of Discrete-time SGAC System
with Different Natural Frequency
and Damping Ratio

damping ratio decreases up to 0.001. However, if the value of natural frequency are decreases up to 70 %, the system shows a long settling time. It indicates that the proposed SGAC system is not affected by the uncertain damping ratio but it is very sensitive to the uncertain natural frequency. This is because the natural frequency determine the required system band limit. Therefore, if the actual frequencies of the system stay within the range of about 80 % of the calculated natural frequency, the proposed SGAC system will be very useful in constructing a main digital controller to adapt to the variation of the plant parameters.

CHAPTER 5

MODEL REFERENCE ADAPTIVE CONTROL

5.1. Introduction

The MRAC is one of the most popular methods of adaptive control. It reduces the effects of poor knowledge of plant dynamics by using a reference model and assures satisfactory performance in the presence of unpredictable vibrations of plant dynamics by using adaptive mechanism. Since its first introduction by Whittaker [17], MRAC has been a simulating field of research aiming at a variety of important applications. The works of Monopoli [18], Narendra [19, 20], Landau [13], Ioannou [21], and Goodwin et al. [22], have laid the foundation of globally stable algorithms for the deterministic adaptive control algorithm.

The stability proofs of these algorithm require the knowledge of the structure of the plant, which is assumed to be linear. If this assumption holds, one can then measure the parametric error distance through the conditioning of an error signal which is obtained by comparing the plant output to the output of a model with the same structure as the plant. However, this assumption cannot hold in most cases, because it is usually very difficult if not impossible, to model the real plant exactly. Recently much effort has been devoted to the robustness of MRAC algorithms in the presence of unmodelled –

dynamics. The works of Ioannou [21], Rohrs et al. [23, 24], and Papadoulos [25] have shown that if this assumption does not hold, MRAC algorithms may lead to instabilities, making MRAC impractical. Since the proposed plant of the roll bending system has a dead zone nonlinearity, a nonminimum phase, and a high order dynamics with a time-variant parameter whose frequency decreases as the workpiece rolls through, it is more difficult to adapt the plant to the desired model. The works of Orlicki [26] and Ioannou [27] have shown that MRAC with new adaptive laws can adjust a dead zone nonlinearity and a nonminimum phase system to guarantee smaller bounds for the residual tracking error which reduces to zero, when the fixed plant parameters are used. In this chapter, the MRAC systems for the proposed roll bending process are presented.

5.2. MRAC Scheme

The most basic approach to the adaptive algorithm problem has its roots in stability considerations. This is essential because adaptive control systems are highly nonlinear and difficult to analyze. Techniques that ensure global stability are preferable because they remove the burden of stability analysis and allow the designer to concentrate on algorithm parameter selection. In general, it is assumed that the plant is exactly known in terms of its structure and parameters. If the plant does not contain any non-minimum zeroes, it is possible to design a compensator for appropriate pole and zero

placements. However, if the plant parameters are unknown, this will not be possible. By placing the poles and zeroes, we want to achieve a prescribed performance. This can be described by a model which is set in parallel with the closed loop plant. A satisfactory performance is then obtained when the ganeralized error is zero.

For the proposed plant of roll bending system, it is difficult to apply the general concept of MRAC since the system has non-minimum zeroes as mentioned before. It is thus suggested that the adaptive part is located only around the plant and constructed prior to a controller design, as shown in Figure 5.1. A satisfactory performance is obtained when the generalized error e=x-xm is zero. If it is not zero, it is fed into the MRAC adaptation mechanism which adjusts the compensator gains until e is driven to zero. What remains is to design an algorithm that will drive the compensator parameters towards the right direction.

The hyperstability design is one of the stability approaches in MRAC. It relies on the hyperstability theorem developed by Popov and is presented by Landau [13]. In order to use the hyperstability theorem, the error derivative e shoud be known. However, it is very difficult to measure the precise error derivatives in the real case because of the characteristics of the roll bending system. The Narendra, Lin and Valavani (NLV)
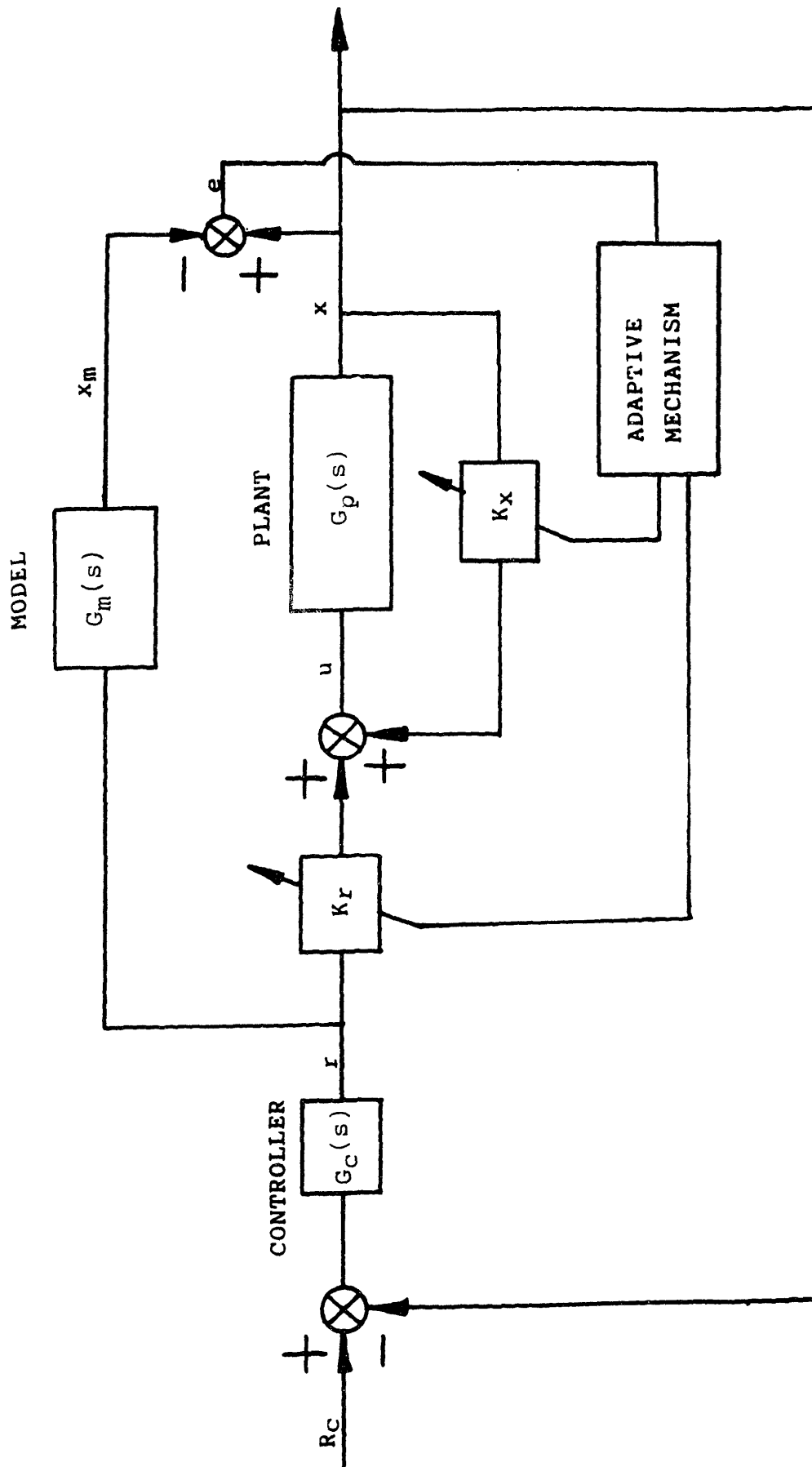
Figure 5.1 Block Diagram of MRAC System

algorithm has been proposed for the stable MRAC system. This is an **improved** globally stable algorithm. The basic difference with Monopoli's algorithm is that in this case auxiliary signals inproving the stability are included. For a first order system, we can present the governing equations:

$$\dot{x} = -ax + bu \tag{5.1}$$

$$\dot{x}_m = -a_m x_m + b_m r \tag{5.2}$$

$$\underline{w}^T = [r, x] \tag{5.3}$$

$$\underline{K}^T = [K_r, K_x] \tag{5.4}$$

$$e = x - x_m \tag{5.5}$$

$$\varepsilon = e + e^* \tag{5.6}$$

$$\dot{e}^* = -a_m e^* - b_m K_e (r^2 + x^2)(e + e^*) \tag{5.7}$$

$$\dot{e}^* = -(a_m + b_m K_e (r^2 + x^2))e^* - b_m K_e (r^2 + x^2)e \tag{5.8}$$

$$u = K_r r + K_x x \tag{5.9}$$

$$\dot{K}_r = K_a r\varepsilon \tag{5.10}$$

$$\dot{K}_x = K_a x\varepsilon \tag{5.11}$$

where $\mathcal{E}$ is the augmented error. First, the MRAC system using NLV algorithm is applied on the plant to check NLV algorithm on the roll bending system. Next, the MRAC system is applied to the plant with the following two cases of the workpiece model. In the first case, it is assumed that the dynamic workpiece model is neglected because in general plants cannot be exactly modelled. In the second case, the dynamic workpiece model is considered but the reference model is made to follow only the servo part. This is because the workpiece model is so complicated that it is difficult to construct an exact reference model for the workpiece.

5.3. MRAC using NLV Algorithm

The purpose of MRAC application to the plant without the workpiece model is to check if the suggested MRAC algorithm works for the nonlinear system such as the proposed roll bending system. The basic MRAC structure is the same as the one shown in Figure 5.1. The simulated responses with Ka=Ke=1, Kro=1, Kxo=0, and a_m =b_m =50 are shown in Figure 5.2. The responses show that the MRAC system using NLV algorithm only for the servo is satisfactory.

Next, the MRAC system is applied to the plant with the servo and static workpiece model in order to check the nonlinearities of the workpiece such as dead zone and the nonlinear relationship between the center roll position and the static
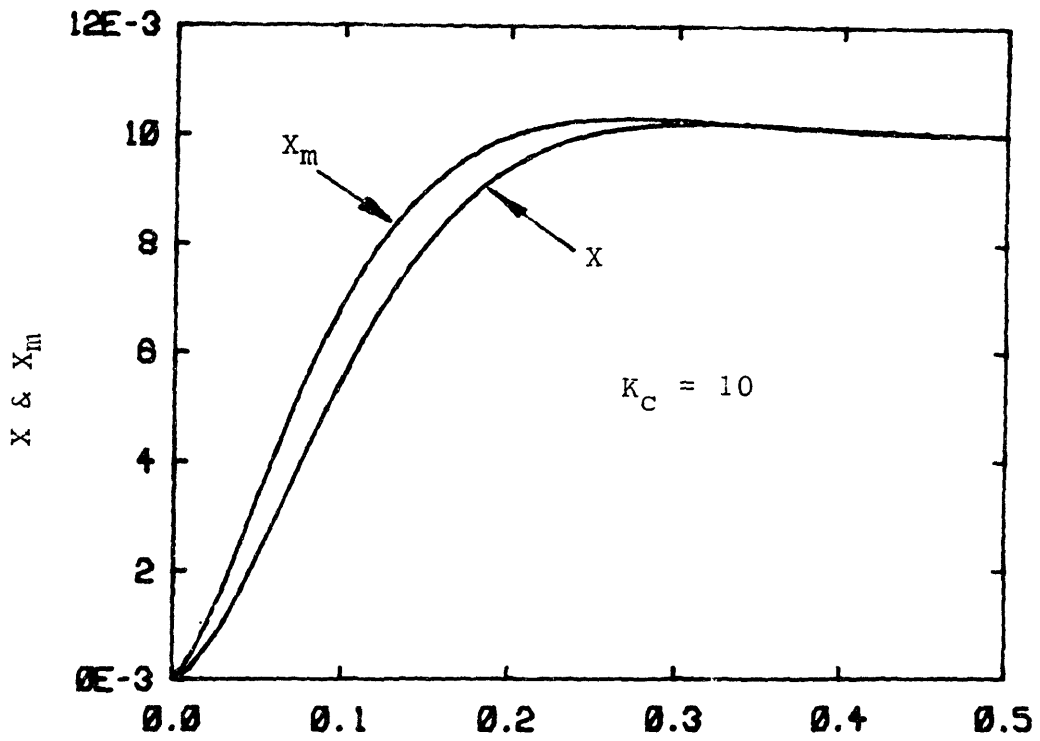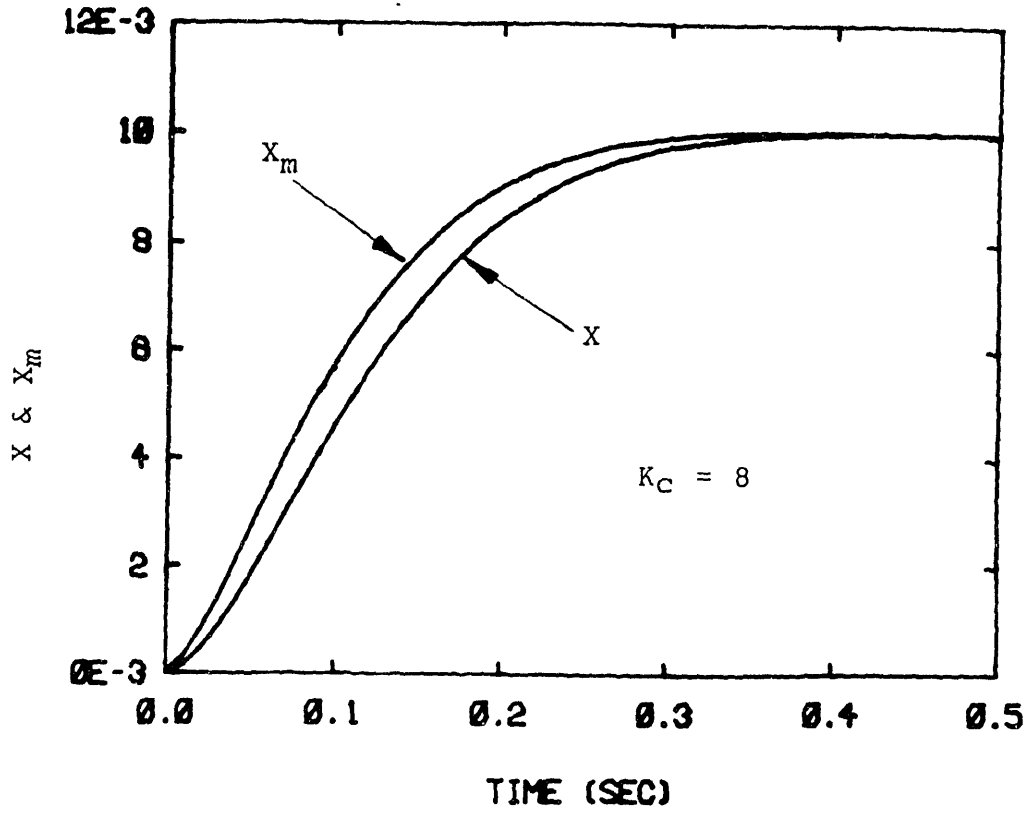
Figure 5.2   Simulation of MRAC System
without Workpiece Model

moment in the plastic region. The nonlinearities due to the material characteristics is neglected in the same structure as the one shown in Figure 5.1., but in the simulation it is considered not only in the plant but also in the model. A proportional controller is used for the second order system. The simulated responses of the system with Ka=Ke=1, Kro=Kxo=1, and $a_m=b_m=50$ are shown in Figure 5.3. The responses show that the MRAC system for the plant with the static workpiece is also satisfactory regardless of the nonlinearities.

Finally, the MRAC system is applied to the complete plant with the dynamic workpiece model. Since the workpiece model is complex and results in the system instability, it is recommended that the plant follows only the second order model to reduce the effects of the workpiece dynamics. The new model is then a reduced order model, compared to the fourth order system of the plant. A proportional controller is used for the control system. Figure 5.4 shows the MRAC system with the reduced order model and NLV algorithm. Figure 5.5 shows the responses of the full-order plant and the reduced-order model to a unit step input with Ka=-1, Ke=1, Kro=-1, Kxo=1, and $a_m=b_m$ =24. The responses show that the error e becomes larger at 10 in/sec feedrate and the system becomes unstable at 20 in/sec as the workpiece length becomes large. This is because the unmodelled workpiece dynamics which causes the instability dominates the system response as the workpiece frequency
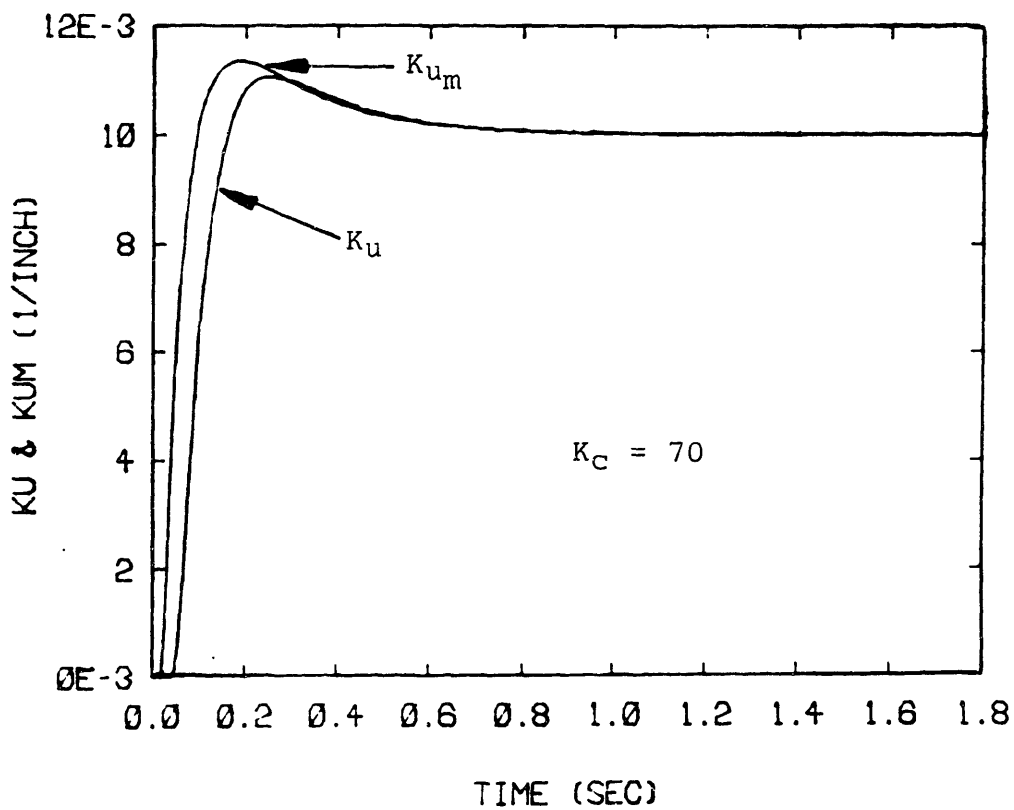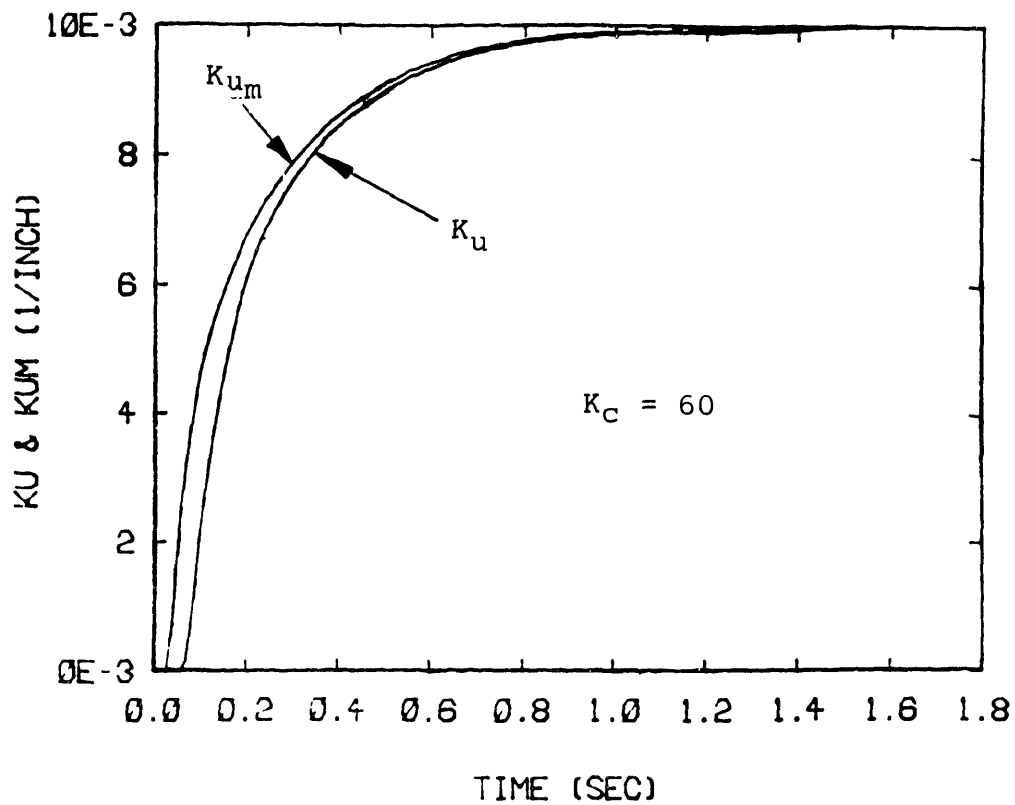
Figure 5.3   Simulation of MRAC System
with Static Workpiece Model
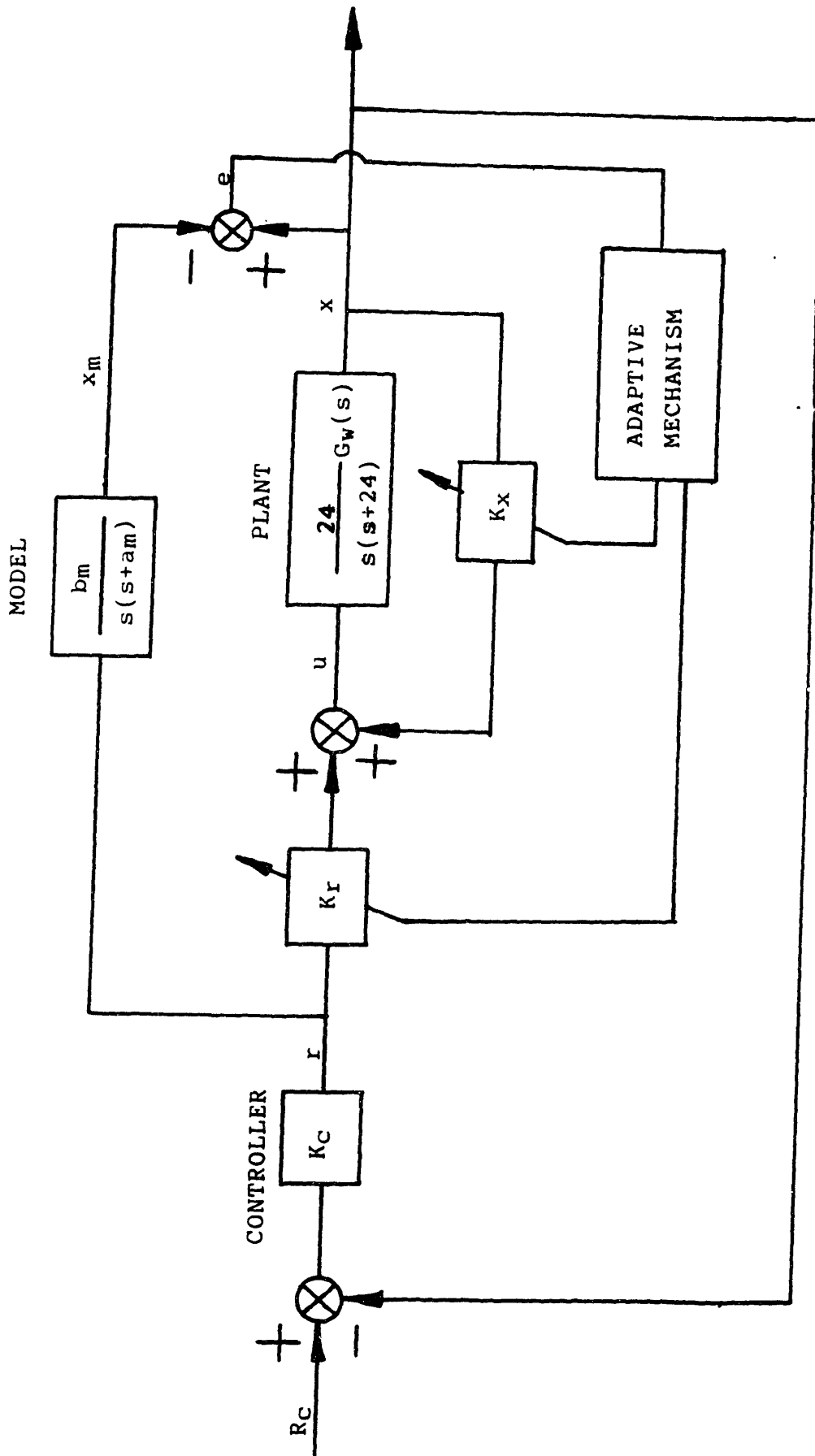
Figure 5.4 Block Diagram of MRAC System
with Workpiece Model
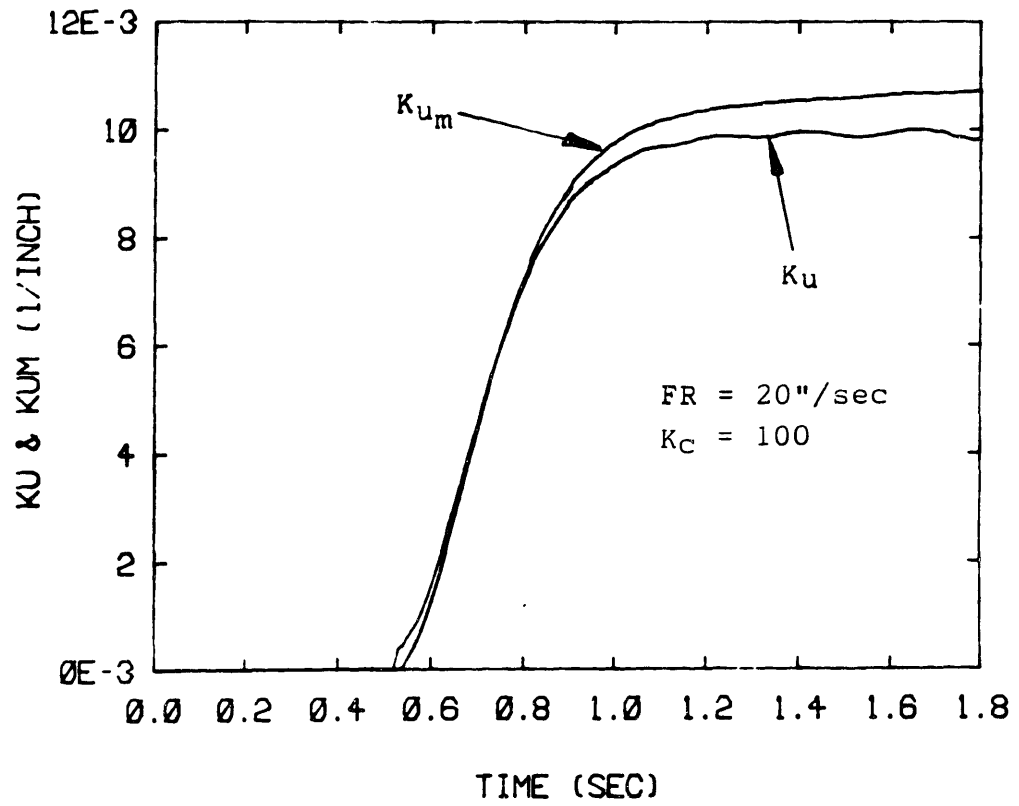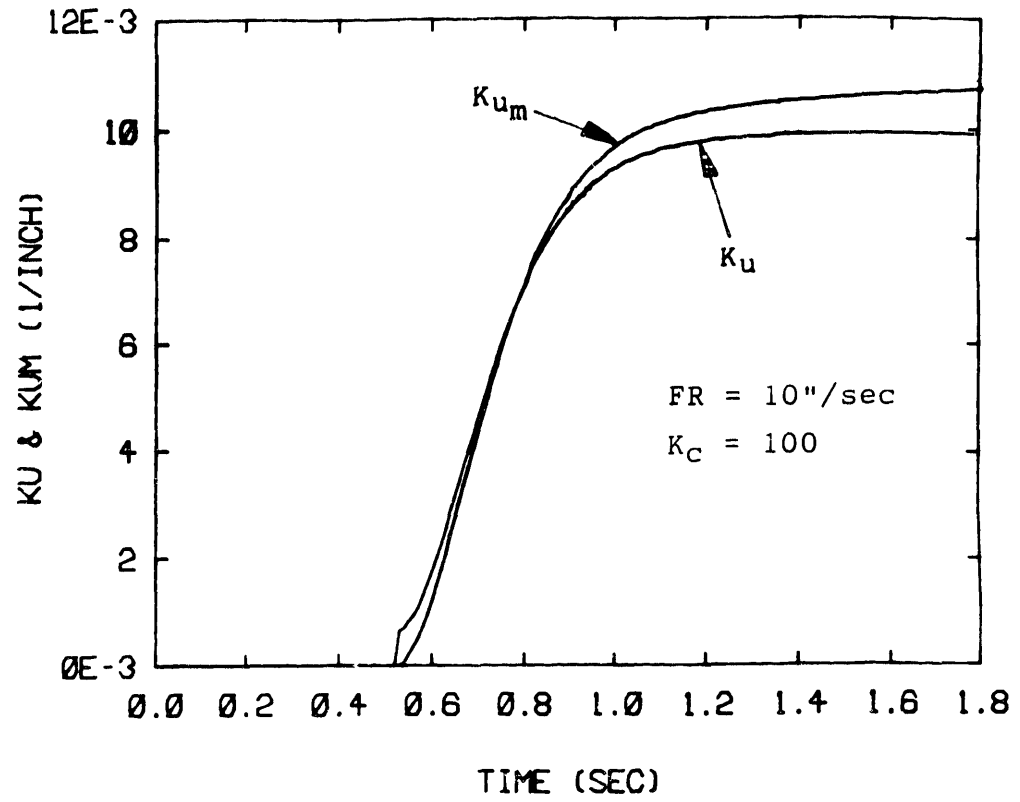
Figure 5.5   Simulation of MRAC System
             with Dynamic Workpiece Model

becomes very low due to the long workpiece length.

1.4. Robust MRAC for Zero Residual Tracking Errors

A new adaptive law for the second order nonminimum phase plant with one dominant and one parasitic mode is suggested by Ioannou [27]. The new adaptive law guarantees smaller bounds for the residual tracking error which reduces to zero when the parasitics disappear. Here, the law is applied to this roll bending system in order to reduce the residual tracking errors which can be seen in Figure 5.5. The new adaptive law using a new auxiliary parameter σ for the adaptive parameter K_x can be expressed as below:

$$u = - K_x \, x + r \qquad\qquad (5.12)$$

$$\dot{K_x} = - \sigma K_x + K_a \mathcal{E} \, x \qquad\qquad (5.13)$$

$$\text{where} \quad \sigma = 0.5 \quad \text{if} \quad \left| K_x \right| \geq K_o$$

$$= 0 \quad \text{otherwise}$$

where Ko is a positive constant. The augmented error is still used. Figure 5.6 shows the simulated responses with Ka=Ke=1, Kxo=-1, Ko=0.01, a_m=b_m=50, and Kc=100. The residual tracking error is evidently reduced to be almost zero with 10 in/sec, but the system still becomes unstable with a feedrate of 20 in/sec. The simulated responses with Kc=150 shown in Figure 5.7 show that the system has a faster rising time but
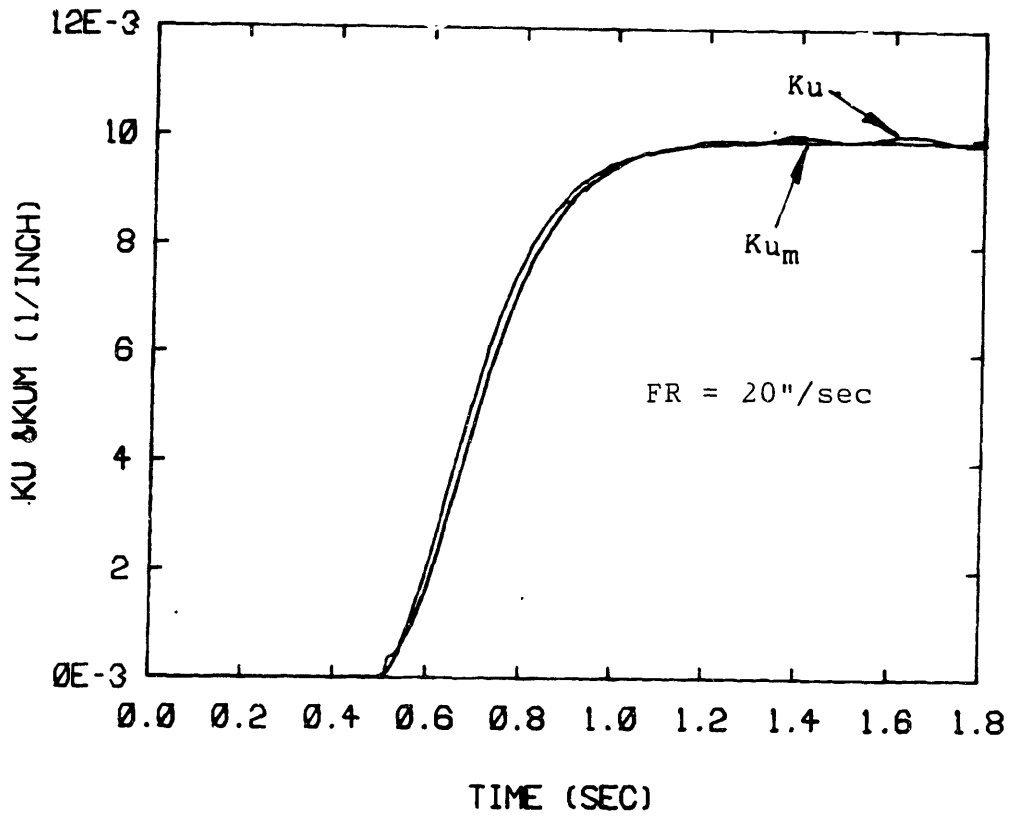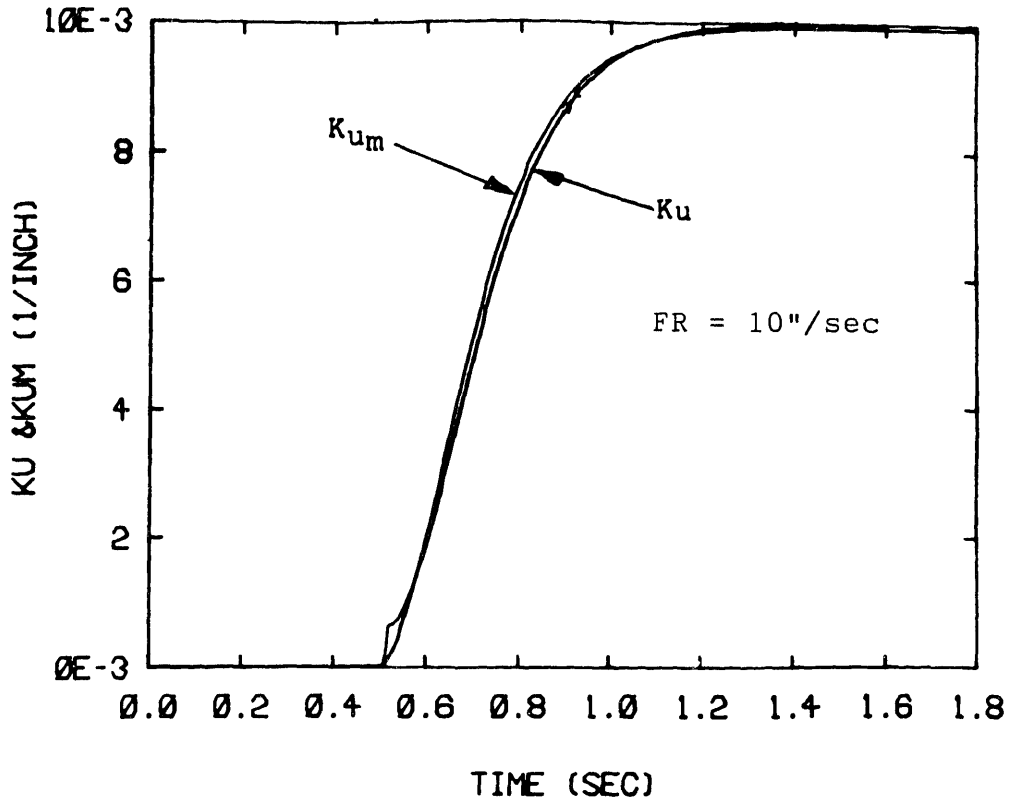
Figure 5.6   Simulation of Robust MRAC System
with Kc=100
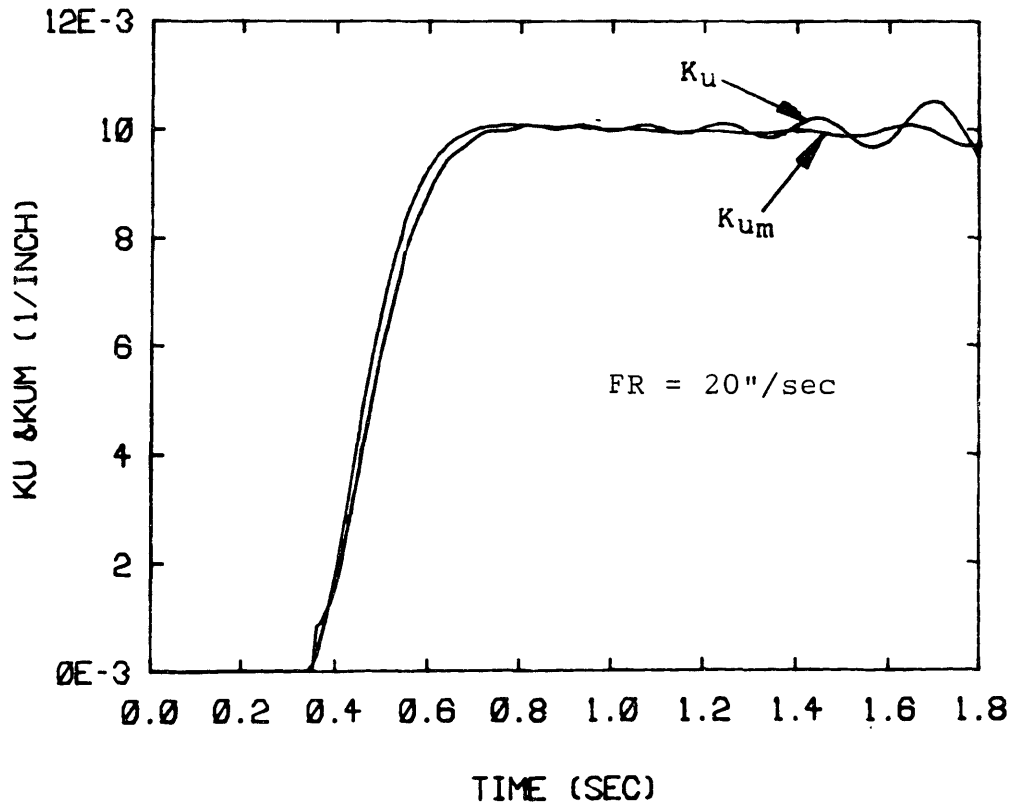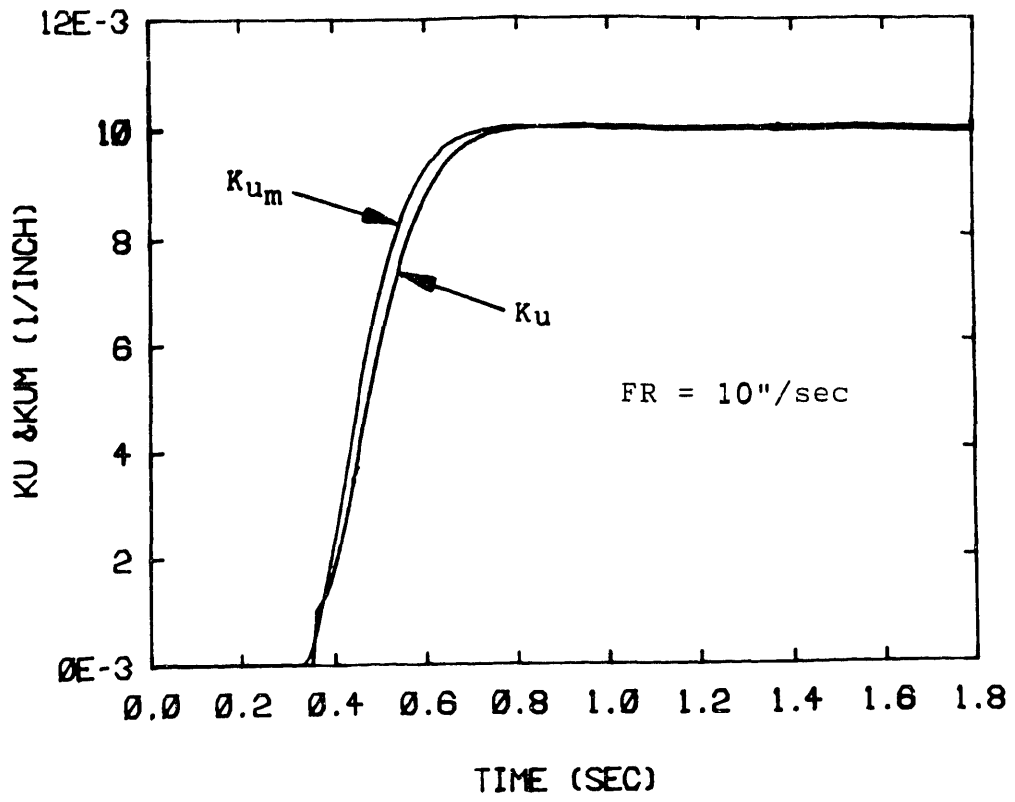
Figure 5.7   Simulation of Robust MRAC System
with Kc=150

becomes unstable more rapidly with a feedrate of 20 in/sec than the responses with Kc=100 in Figure 5.6. This suggests that by using the new adaptive law the error can be reduced but the system still has the instability problem. Figure 5.8 indicates that the system becomes unstable after about 3 seconds even with a feedrate of 10 in/sec. However, if the roll bending process can be completed within 3 seconds with a feedrate of 10 in/sec, the MRAC system using the new adaptive law will be useful for the automation of the roll bending process.
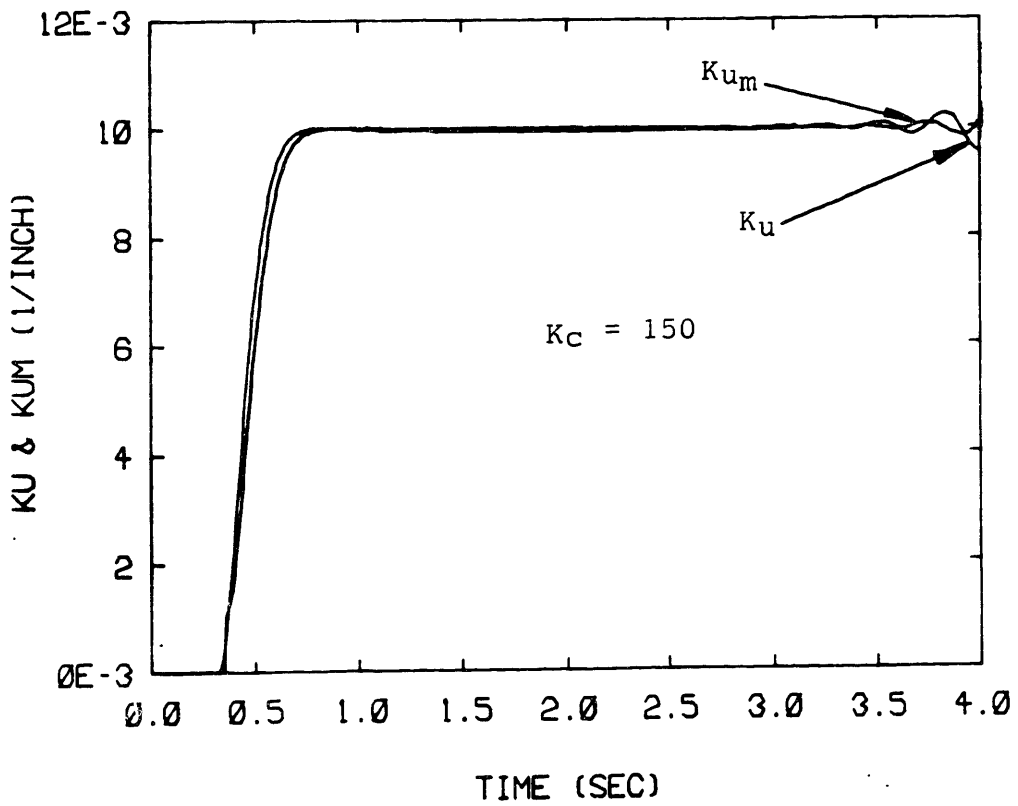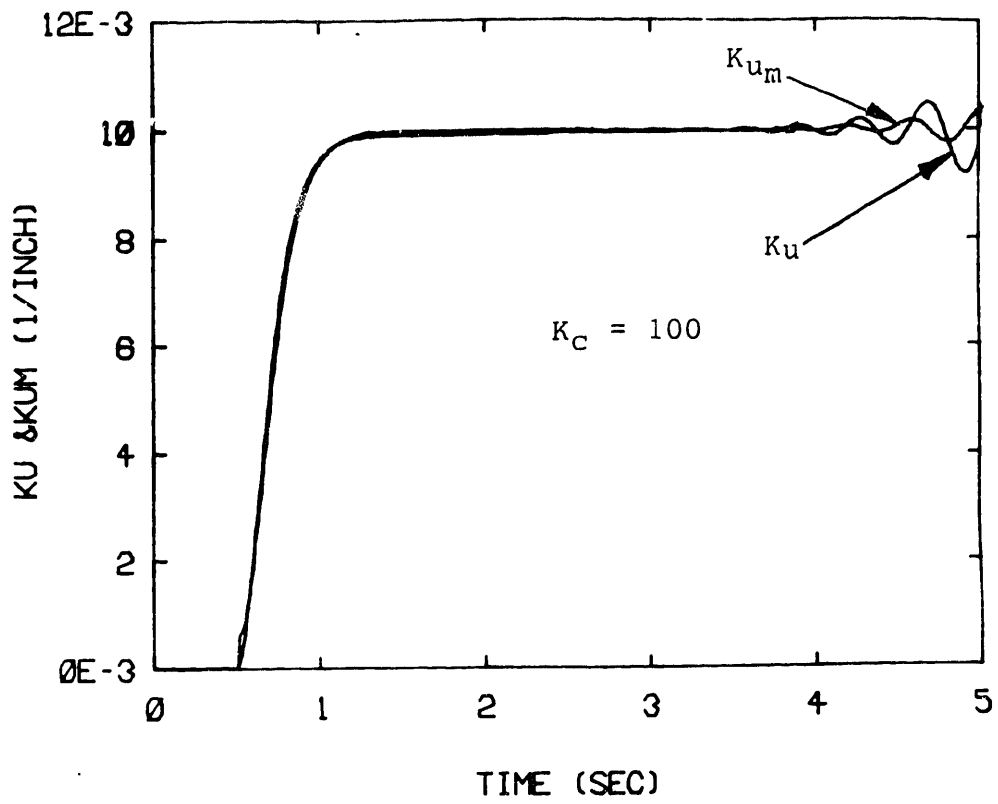
Figure 5.8   Simulation of Robust MRAC System
at 10 in/sec

CHAPTER 6

CONCLUSIONS AND FUTURE RESEARCH

6.1. Conclusions

The simulated responses in Chapter 3 correspond very well to the experimental responses. As the workpiece length continuously increases, the system becomes unstable due to the increased vibration. Although there is a little difference in initial shapes during rising period, the oscillation shapes and frequencies are nearly identical. This indicates that the workpiece model is satisfactory in analyzing the workpiece dynamics and system instability. Therefore, this workpiece model can be used as the unknown workpiece model including vibration, and the model will be very useful in the design of an adaptive control system to stabilyze the system.

Since the plant natural frequency is a time-variant parameter, an adaptive control technique is needed for the system stability and better performance. The typical adaptive control such as the Self Tuning Control(STC) or Model Reference Adaptive Control(MRAC) is not suitable to this system because of the length-variant frequency and nonminimum phase. Thus, a modified Scheduled Gain Adaptive Control was proposed, using root locus method and Tustin's approximation method for the discrete- time control system.

The simulated responses with the SGAC scheme in Chapter 4 show that the system can be stabilized regardless of workpiece vibration. The best performance of the system without oscillation and instability can be obtained with a feedrate of 25"/sec. By using a digital controller and an adaptive control scheme, the simulation becomes more realistic. The simulated responses for a robust MRAC scheme with a new adaptive law in Chapter 5 represent that the residual tracking errors are reduced and the system shows satisfactory performances up to about 3 seconds with a feedrate of 10 in/sec.

Therefore, by using the proposed workpiece model and adaptive control schemes, the quality and productivity of the roll bending system can be improved due to the stability at increased feedrates, and the manufacturing cost can be decreased by the successful automation of the roll bending process.

6.2. Future Research

Roll bending process experiments using the adaptive control systems are needed in order to check the proposed control schemes. The adaptive control system may need further modifications according to the experimental results. Other adaptive control techniques such as STC and MRAC can also be considered with some modifications for the nonminimum phase system. A typical STC with a least square method and

input-output pole-placement method was applied to the roll bending system, but it was not successful because of the workpiece model with dead-zone nonlinearity and nonminimum phase. A modified MRAC with reduced-order model and a new adaptive law for nonminimum phase system was also applied to the system. Then, the system was stable up to about 45" of workpiece length, but became unstable at larger lengths due to the dominant workpiece dynamics at low natural frequencies.

Modelling and Control of three-dimensional roll bending is recommended for the wide applications. Adaptive and closed-loop control of three-dimensional roll bending can lead to on-pass forming of arbitrary workpiece shape. This would not only increase the productivity of the current roll bending process, but also greatly increase the versatility of the process. In addition to three-dimensional roll bending, automation of the roll bending systems for other parts would be studied. This would also increase the versatility and lead to complete automation of roll bending system.

APPENDIX

COMPUTER PROGRAMS

This appendix provides a listing of basic computer programs used in the workpiece modeling, the SGAC scheme, and the MRAC scheme.

The main programs are listed as follows:

1. ROLBEND — Workpiece Modeling

2. ADAPCON — Discrete-Time SGAC

3. NEWMRAC — Robust MRAC

```fortran
          PROGRAM ROLBEND
C
C      *****************************************************
C      * ROLL BENDING MODELING PROGRAM WITH WORKPIECE MODEL *
C      *****************************************************
C
          COMMON /VAR/F(5),Y(5),FF(5),YY(5),M,XKU,COM,DT
          COMMON /CON/XL,WN,Z
          DIMENSION X(10,550),POS(4)
          CHARACTER*40 XLABEL,YLABEL
C
C      PARAMETER
C
          XSL=6.
          Z=0.011
          XYY=0.48
          XKY=0.04
          EI=5020000.
          DT=0.01
          INT=1
          XKU=0.
          Y(1)=0.
          Y(2)=0.
          Y(3)=0.
          Y(4)=0.
          COM=0.
C
          TYPE *, 'ENTER DESIRED UNLOADED CURVATURE ; Kud'
          ACCEPT *, XKUD
          TYPE *, 'ENTER INITIAL W/P LENGTH ; Lo'
          ACCEPT *, XLO
          TYPE *, 'ENTER CONTROLLER GAIN ; G1'
          ACCEPT *, GA
          TYPE *, 'ENTER ZERO PLACEMENT ; Kv=(G2)/12'
          ACCEPT *, GB
          TYPE *, 'ENTER FEEDRATE ; FR'
          ACCEPT *, FR
          TYPE *, 'ENTER TIME INTERATION ; NT=FT/DT (100*FT)'
          ACCEPT *,NT
C
C      INITIALIZE THE DISCRETE CONTROLLER
C
          ERROR=XKUD-XKU-GB*Y(2)
          COM=ERROR*GA
C
C      CALCULATE THE PARAMETERS FOR TIME STEP
C
          ICOUNT=0
          DO 100 IT=1,NT
          ICOUNT=ICOUNT+1
C
C      SERVO MODEL
C
          K=1
          N=2
```

```
C
            DO 10 M=1,4
            CALL STATIC
            CALL DER(N,K)
10          CONTINUE
C
C    WORKPIECE MODEL
C
80          XKL=3.*Y(1)/(XSL**2)
        IF(XKL.GT.XKY) GO TO 30
            XMBS=XKL
        GO TO 40
C
C    STATIC MOMENT
C
30          XMBS=((4.5*XYY)/(XSL**2))*(1.-(((XYY/Y(1))**2)/3.))
C
C    DYNAMIC MOMENT
C
40          XL=XLO+FR*(IT*DT)
            WN=49900./(XL**2)
            K=3
            N=4
            DO 20 M=1,4
            CALL DYNAMIC
            CALL DER(N,K)
20          CONTINUE
            XM=0.025*XL
            XC=(3.*XL+2.*XSL)/(2.*XSL)
            XMBD=(Y(3)+XM*XL*(WN**2)*XC*Y(1))/EI
C
C    TOTAL MOMENT
C
            XMB=XMBS+XMBD
C
C    CALCULATE UNLOADED CURVATURE
C
            XKU=XKL-XMB
C
C    CALCULATE DISCRETE CONTROLLER
C
        IF(Y(1).GT.XYY) GO TO 150
            XKU=0.
150         .IF(ICOUNT.NE.INT) GO TO 50
            ICOUNT=0
            ERROR=XKUD-XKU-GB*Y(2)
            COM=ERROR*GA
C
C    STORE DATA
C
50        DO 60 I=1,2
            X(I,IT)=Y(I)
60        CONTINUE
```

```
              X(5,IT)=XKU
              X(6,IT)=XKL
              X(7,IT)=XMBS
              X(8,IT)=XMBD
              X(9,IT)=XL
              X(10,IT)=IT*DT
100       CONTINUE
          DO 110 I=1,NT
          WRITE(5,90) X(1,I),X(5,I),X(6,I),X(7,I),X(8,I)
90        FORMAT(2X,5F)
110       CONTINUE
C
C     DRAW FIGURES
C
          LABEL=4
          POS(1)=120
          POS(2)=120
          POS(3)=700
          POS(4)=550
          XLABEL='TIME (SEC)'
          YLABEL='KU (1/INCH)'
          CALL QPICTR(X,10,NT,QY(5),QX(10),QMOVE(00),QPOS(POS),
     1              QLABEL(LABEL),QXLAB(XLABEL),QYLAB(YLABEL))
          STOP
          END
```

```
      SUBROUTINE STATIC
C
      COMMON /VAR/F(5),Y(5),FF(5),YY(5),M,XKU,COM,DT
      COMMON /CON/XL,WN,Z
      F(1)=Y(2)
      F(2)=24.*COM-24.*Y(2)
      RETURN
      END



      SUBROUTINE DYNAMIC
C
      COMMON /VAR/F(5),Y(5),FF(5),YY(5),M,XKU,COM,DT
      COMMON /CON/XL,WN,Z
      XM=0.025*XL
      XC=(3.*XL+12.)/12.
      DA=2.*Z*WN
      DB=WN**2
      DC=(4.*(Z**2)-1.)*(XM*XL*(WN**4))
      DD=2.*XM*XL*Z*(WN**3)
      F(3)=Y(4)-DD*Y(1)*XC
      F(4)=DC*Y(1)*XC-DA*Y(4)-DB*Y(3)
      RETURN
      END



      SUBROUTINE DER(N,K)
C
      COMMON /VAR/F(5),Y(5),FF(5),YY(5),M,XKU,COM,DT
      COMMON /CON/XL,WN,Z
      GO TO (10,30,50,70),M
10    DO 20 J=K,N
      YY(J)=Y(J)
      FF(J)=F(J)
      Y(J)=YY(J)+0.5*DT*F(J)
20    CONTINUE
      GO TO 90
30    DO 40 J=K,N
      FF(J)=FF(J)+2.0*F(J)
      Y(J)=YY(J)+0.5*DT*F(J)
40    CONTINUE
      GO TO 90
50    DO 60 J=K,N
      FF(J)=FF(J)+2.0*F(J)
      Y(J)=YY(J)+DT*F(J)
60    CONTINUE
      GO TO 90
70    DO 80 J=K,N
      Y(J)=YY(J)+(FF(J)+F(J))*DT/6.0
80    CONTINUE
90    RETURN
      END
```

```fortran
      PROGRAM ADAPCON
C
C     ************************************
C     * DISCRETE-TIME SGAC SYSTEM PROGRAM *
C     ************************************
C
      COMMON /VAR/F(5),Y(5),FF(5),YY(5),M,XKU,COM,DT
      COMMON /CON/XL,WN,Z
      DIMENSION X(10,550),POS(4),U(1000),E(1000)
      CHARACTER*40 XLABEL,YLABEL
C
C     PARAMETER
C
      XSL=6.
      XYY=0.48
      XKY=0.04
      EI=5020000.
      XKU=0.
      Y(1)=0.
      Y(2)=0.
      Y(3)=0.
      Y(4)=0.
      E(1)=0.
      U(1)=0.
C
      TYPE *, 'ENTER DESIRED UNLOADED CURVATURE ; Kud'
      ACCEPT *, XKUD
      TYPE *, 'ENTER INITIAL W/P LENGTH ; Lo'
      ACCEPT *, XLO
      TYPE *, 'ENTER TIME INTERVAL ; DT'
      ACCEPT *, DT
      TYPE *, 'ENTER TIME STEP ; INT'
      ACCEPT *, INT
      TYPE *, 'ENTER PARAMETERS ; Z, Zc, XWN'
      ACCEPT *, Z, ZC, XWN
      TYPE *, 'ENTER CONTROLLER GAIN ; G1'
      ACCEPT *, GA
      TYPE *, 'ENTER ZERO PLACEMENT ; Kv=(G2)/12'
      ACCEPT *, GB
      TYPE *, 'ENTER FEEDRATE ; FR'
      ACCEPT *, FR
      TYPE *, 'ENTER TIME INTERATION ; NT=FT/DT'
      ACCEPT *,NT
C
C     INITIALIZE THE DISCRETE CONTROLLER
C
      E(1)=XKUD-XKU-GB*Y(2)
      U(1)=E(1)*GA*2.
C
C     CALCULATE THE PARAMETERS FOR TIME STEP
C
      ICOUNT=0
      DO 100 IT=1,NT
      ICOUNT=ICOUNT+1
```

```
C
C       SERVO MODEL
C
        K=1
        N=2
C
        COM=U(IT)
        DO 10 M=1,4
        CALL STATIC
        CALL DER(N,K)
10      CONTINUE
C
C    WORKPIECE MODEL
C
80          XKL=3.*Y(1)/(XSL**2)
        IF(XKL.GT.KYY) GO TO 30
            XMBS=XKL
        GO TO 40
C
C    STATIC MOMENT
C
30          XMBS=((4.5*XYY)/(XSL**2))*(1.-(((XYY/Y(1))**2)/3.))
C
C    DYNAMIC MOMENT
C
40          XL=XLO+FR*(IT*DT)
            WN=XWN/(XL**2)
            K=3
            N=4
            DO 20 M=1,4
            CALL DYNAMIC
            CALL DER(N,K)
20          CONTINUE
            XM=0.025*XL
            XC=(3.*XL+2.*XSL)/(2.*XSL)
            XMBD=(Y(3)+XM*XL*(WN**2)*XC*Y(1))/EI
C
C    TOTAL MOMENT
C
            XMB=XMBS+XMBD
C
C    CALCULATE UNLOADED CURVATURE
C
            XKU=XKL-XMB
C
C    CALCULATE DISCRETE CONTROLLER
C
        IF(Y(1).GT.XYY) GO TO 150
            XKU=0.
C
150         KT=IT+1
        IF(ICOUNT.NE.INT) GO TO 50
            ICOUNT=0
            WN1=0.04*ZC*WN
            WN2=0.0004*WN*WN
```

```fortran
            A1=4.+WN1+WN2
            A2=-8.+2.*WN2
            A3=4.-WN1+WN2
            E(KT)=XKUD-XKU-GB*Y(2)
            U(KT)=(6.*U(KT-1)-U(KT-2)+GA*(A1*E(KT)
     1              +A2*E(KT-1)+A3*E(KT-2)))/9.
C
C     STORE DATA
C
50        DO 60 I=1,2
            X(I,IT)=Y(I)
60        CONTINUE
            X(5,IT)=XKU
            X(6,IT)=XKL
            X(7,IT)=U(IT)
            X(8,IT)=E(IT)
            X(9,IT)=XL
            X(10,IT)=IT*DT
100       CONTINUE
          DO 110 I=1,NT
          WRITE(5,90) X(1,I),X(5,I),X(6,I),X(7,I),X(8,I)
90        FORMAT(2X,5F)
110       CONTINUE
C
C     DRAW FIGURES
C
          LABEL=4
          POS(1)=120
          POS(2)=120
          POS(3)=700
          POS(4)=550
          XLABEL='TIME (SEC)'
          YLABEL='KU (1/INCH)'
          CALL QPICTR(X,10,NT,QY(5),QX(10),QMOVE(00),QPOS(POS),
     1              QLABEL(LABEL),QXLAB(XLABEL),QYLAB(YLABEL))
          STOP
          END
```

```
        PROGRAM NEWMRAC
C
C       ************************************************
C       * ROBUST MRAC PROGRAM WITH NEW ADAPTIVE LAW *
C       ************************************************
C
        COMMON /VAR/F(10),Y(10),FF(10),YY(10),M,XKU,COM,DT
        COMMON /CON/XL,WN,Z,ZC
        DIMENSION X(10,550),POS(4)
        CHARACTER*40 XLABEL,YLABEL
C
C       PARAMETER
C
        DATA XSL/6./Z/0.011/XYY/0.48/XKY/0.04/EI/5020000./
     1      INT/1/XKU/0./COM/0./UA/0./
     2      Y(1),Y(2),Y(3),Y(4),Y(5),Y(6)/6*0./
C
        TYPE *, 'ENTER DESIRED UNLOADED CURVATURE ; Kud'
        ACCEPT *, XKUD
        TYPE *, 'ENTER TIME INTERVAL ; DT'
        ACCEPT *, DT
        TYPE *, 'ENTER INITIAL W/P LENGTH ; Lo'
        ACCEPT *, XLO
        TYPE *, 'ENTER CONTROLLER GAIN ; Kc'
        ACCEPT *, GA
        TYPE *, 'ENTER MODEL GAIN ; Am, Bm'
        ACCEPT *, AM, BM
        TYPE *, 'ENTER ADAPTIVE MECH. GAIN ; Ka, Ke'
        ACCEPT *, XKA, XKE
        TYPE *, 'ENTER INITIAL Kx, Ko, Co'
        ACCEPT *, Y(9), XKO, XCO
        TYPE *, 'ENTER FEEDRATE ; FR'
        ACCEPT *, FR
        TYPE *, 'ENTER TIME INTERATION ; NT=FT/DT'
        ACCEPT *, NT
C
C       CALCULATE THE PARAMETERS FOR TIME STEP
C
        ICOUNT=0
        DO 100 IT=1,NT
        ICOUNT=ICOUNT+1
C
C       --------------------
C        CONTROLLER DESIGN
C       --------------------
C
        K=6
        N=6
        DO 250 M=1,4
        F(6)=GA*(XKUD-XKU)
        CALL CONDER(N,K)
250     CONTINUE
        UA=Y(6)-XKU*Y(9)
```

```
C
C       ------------------------------
C         CONTINUOUS PROCESS SYSTEM
C       ------------------------------
C
C       SERVO MODEL
C
        K=1
        N=1
C
        DO 10 M=1,4
        F(1)=24.*UA-24.*Y(1)
        CALL CONDER(N,K)
10      CONTINUE
C
C       WORKPIECE MODEL
C
80      XKL=3.*Y(1)/(XSL**2)
        IF(Y(1).GT.XYY) GO TO 30
          XMBS=XKL
          XKUP=3.*F(1)/(XSL**2)
        GO TO 40
C
C       STATIC MOMENT
C
30      XMBS=((4.5*XYY)/(XSL**2))*(1.-(((XYY/Y(1))**2)/3.))
        XKUP=3.*F(1)*(1.-(XYY/Y(1))**3)/(XSL**2)
C
C       DYNAMIC MOMENT
C
40      XL=XLO+FR*(IT*DT)
        WN=49900./(XL**2)
        K=3
        N=4
        DO 20 M=1,4
        CALL MODYNA
        CALL CONDER(N,K)
20      CONTINUE
        XM=0.025*XL
        XC=(3.*XL+2.*XSL)/(2.*XSL)
        XMBD=(Y(3)+XM*XL*(WN**2)*XC*Y(1))/EI
C
C       TOTAL MOMENT
C
        XMB=XMBS+XMBD
C
C       CALCULATE UNLOADED CURVATURE
C
        XKU=XKL-XMB
C
C       NON-LINEARITY BY SPRINGBACK
C
```

```fortran
      IF(Y(1).GT.XYY) GO TO 300
          XKU=0.
C         XKUP=0.
C
C     ------------------
C      REFERENCE MODEL
C     ------------------
C
300       K=5
          N=5
          DO 200 M=1,4
          F(5)=-AM*Y(5)+BM*Y(6)
          CALL CONDER(N,K)
200       CONTINUE
          XKLM=3.*Y(5)/(XSL**2)
          IF(Y(5).GT.XYY) GO TO 210
          XMBM=XKLM
C          XKUMP=3.*F(5)/(XSL**2)
          GO TO 150
210       XMBM=((4.5*XYY)/(XSL**2))*(1.-(((XYY/Y(5))**2)/3.))
150       XKM=XKLM-XMBM
C
C     ----------------------------------------------
C      PARAMETER ADJUSTMENT: NEW ADAPTIVE LAW
C     ----------------------------------------------
C
          E=XKU-XKM
C
          K=2
          N=2
          DO 550 M=1,4
          AB=XKE*((XKU*XKU)+Y(6)*Y(6))
          AA=AM+BM*AB
          BB=BM*AB
          F(2)=-AA*Y(2)-BB*E
          CALL CONDER(N,K)
550       CONTINUE
C
          EPS=E+Y(2)
C
          IF(ABS(Y(9)).GE.XKO) GO TO 600
              C=0.
          GO TO 650
600           C=XCO
C
650       K=9
          N=9
          DO 350 M=1,4
          F(9)=XKA*EPS*XKU-C*Y(9)
          CALL CONDER(N,K)
350       CONTINUE
```

```
C
C       --------------
C        STORE DATA
C       --------------
C
50              X(1,IT)=Y(1)
                X(2,IT)=Y(5)
                X(3,IT)=EPS
                X(4,IT)=XKM
                X(5,IT)=XKU
                X(6,IT)=XKL
                X(7,IT)=Y(6)
                X(8,IT)=Y(9)
                X(10,IT)=IT*DT
100     CONTINUE
C
        DO 110 I=1,NT
        WRITE(5,90) X(1,I),X(10,I),X(3,I),X(4,I),X(5,I),X(8,I)
90      FORMAT(2X,6F)
110     CONTINUE
C
C       ------------------
C        DRAW FIGURES
C       ------------------
C
        LABEL=4
        POS(1)=120
        POS(2)=120
        POS(3)=700
        POS(4)=550
        XLABEL='TIME (SEC)'
        YLABEL='KU &KUM (1/INCH)'
        CALL QPICTR(X,10,NT,QY(4,5),QX(10),QMOVE(00),QPOS(POS),
     1              QLABEL(LABEL),QXLAB(XLABEL),QYLAB(YLABEL))
        STOP
        END
```

```
        SUBROUTINE MODYNA
C
        COMMON /VAR/F(10),Y(10),FF(10),YY(10),M,XKU,COM,DT
        COMMON /CON/XL,WN,Z,ZC
        XM=0.025*XL
        XC=(3.*XL+12.)/12.
        DA=2.*Z*WN
        DB=WN**2
        DC=(4.*(Z**2)-1.)*(XM*XL*(WN**4))
        DD=2.*XM*XL*Z*(WN**3)
        F(3)=Y(4)-DD*Y(1)*XC
        F(4)=DC*Y(1)*XC-DA*Y(4)-DB*Y(3)
        RETURN
        END




        SUBROUTINE CONDER(N,K)
C
        COMMON /VAR/F(10),Y(10),FF(10),YY(10),M,XKU,COM,DT
        COMMON /CON/XL,WN,Z,ZC
        GO TO (10,30,50,70),M
10      DO 20 J=K,N
        YY(J)=Y(J)
        FF(J)=F(J)
        Y(J)=YY(J)+0.5*DT*F(J)
20      CONTINUE
        GO TO 90
30      DO 40 J=K,N
        FF(J)=FF(J)+2.0*F(J)
        Y(J)=YY(J)+0.5*DT*F(J)
40      CONTINUE
        GO TO 90
50      DO 60 J=K,N
        FF(J)=FF(J)+2.0*F(J)
        Y(J)=YY(J)+DT*F(J)
60      CONTINUE
        GO TO 90
70      DO 80 J=K,N
        Y(J)=YY(J)+(FF(J)+F(J))*DT/6.0
80      CONTINUE
90      RETURN
        END
```

REFERENCES

1. Hardt, D.E., "Shape Control in Metal Bending Processes: The Model Measurement Tradeoff", editor, D.E. Hardt, <u>Information Control Problems in Manufacturing Technology</u>, 1982, Fourth IFAC/IFIP Symposium, pp. 35-40.

2. Allison, B.T. and Gossord, D.C., "Adaptive Breakforming", <u>Proc. 8th North American Manufacturing Research Conference</u> May 1980, pp. 252-256.

3. Stelson, K.A., "The Adaptive Control of Breakforming using In-process Measurement for the Identification of Workpiece Material Characteristics", Ph.D. Thesis, MIT., Oct., 1981

4. Hansen, N.E. and Jannerup, O.E., "Modelling of Elastic-Plastic Bending of Beams using a Roller Bending Machine", <u>Trans. of ASME</u>, <u>Journal of Engineering for Industry</u>, Vol. 101, No. 3, August 1979, pp. 304-310.

5. Cook, G., Hansen, N.E., and Trostmann, E., "General Scheme for Automatic Control of Continuous Bending of Beams", <u>Trans. of ASME</u>, <u>Journal of Dynamic Systems, Measurement and Control</u>, Vol. 104, No. 2, June 1982, pp. 173-179.

6. Roberts, M.A., "Experimental Investigation of Material Adaptive Springback Compensation in Roller Bending", M.S. Thesis, MIT., August 1981.

7. Hardt, D.E., Roberts, M.A., and Stelson, K.A., "Closed-Loop Shape Control of a Roll-Bending Process", <u>Trans. of ASME</u>, <u>Journal of Dynamic System, Measurement and Control</u>, December 1982, Vol. 104, No. 4, pp. 317-322.

8. Hardt, D.E. and Hale, M.B., "Closed Loop Control of a Roll Straightening Process", <u>Annals. of the CIRP</u>, Vol. 33, No. 1, August 1984, pp. 137-140.

9. Hale, M.B., "Dynamic Analysis and Control of a Roll Bending Process", M.S. Thesis, MIT., June 1985.

10. Crandall, S.H., Dahl, N.C., and Lardner, T.J., editors, <u>An Introduction to the Mechanics of Solids</u>, 2ed, McGraw-Hill, New York, 1959.

11. Crandall, S.H., Karnopp, D.C., et al, <u>Dynamics of Mechanical and Electromechanical Systems</u>, McGraw-Hill, New York, 1968.

12. Ogata, K., <u>Modern Control Engineering</u>, Prentice-Hall, Englewood Cliffs, N.J., 1970.

13. Landau, Y.D., _Adaptive Control: The Model Reference Approach_, Marcel Dekker, New York, 1979.

14. Astrom, K.J., Borissou, L.L., and Wittenmark, B., "Theory and Applications of Self-Tuning Regulators", _Autometica_, Vol. 13, 1977, pp. 457-476.

15. Astrom, K.J. and Wittenmark, B., "Self-Tuning Controllers based on Pole-Zero Placement", _IEEE Proc._, Vol. 127, No.3, May 1980, pp. 120-130.

16. Astrom, K.J. and Wittenmark, _Computer Controlled Systems: Theory and Design_, Prentice-Hall, Eaglewood Cliffs, 1984

17. Whittaker, H.P., Yamron, J., and Keezer, A., "Design of Model Reference Control System for Aircraft", _MIT Instrument Lab Report_, R-164, 1959.

18. Monopoli, P.V., "Model Reference Adaptive Control with an Augumented Error Signal", _IEEE Trans. Automatic Control_, AC-19, October 1974.

19. Narendra, K.S. and Valavani, L.S., "Stable Adaptive Controller Design-Direct Control", _IEEE Transactions on Adaptive Control_, Vol. AC-23, 1978.

20. Narendra, K.S., Liu, Y.H., and Valavani, L.S., "Stable Adaptive Controller Design, Part II: Proof of Stability", _IEEE Transaction on Adaptive Control_, Vol. AC-25, 1980.

21. Ioannou, P.A. and Kokotovic, P.V., "Singular Perturbation and Robust Redesign of Adaptive Control", _Proc. 21st IEEE Conference on Decision and Control_, Orlando, 1980.

22. Goodwin, G.C., Ramadge, P.L., and Caines, P.E., "Discrete Time Multivariable Adaptive Control", _IEEE Transaction on Adaptive Control_, Vol. AC-25, 1980.

23. Rohrs, C.E., Valavani, L.S., and Athans, M., "Robustness of Adaptive Control Algorithm in the Presence of Unmodelled Dynamics", _Proc. 21st IEEE conference on Decision and Control_, 1982, pp. 3-11.

24. Rohrs, C.E., _Adaptive Control in the Presence of Unmodelled Dynamics_, Ph.D. Thesis, MIT., Sep. 1982

25. Papadoulos, E.G., _An Investigation of MRAC Algorithm for Manufacturing Processes: Problems and Potentials_, S.M. Thesis, M.I.T., 1983.

26. Orlicki, D.M., _Model REference Adaptive Control System_

using a Dead Zone Non-linearity, Ph.D. Thesis, MIT., April 1985.

27. Ioannou, P., "Robust Adaptive Controller with Zero Residual Tracking Errors", Proc. of 24st Conference on Decision and Control, December 1985, pp. 135-140.